

Differentiation Potential of the Human Adipose Stem Cells
in Response to Regulation of ROCK, FAK and MEK-ERK
Signaling Pathways

Laura Hyväri
Master's Thesis
University of Tampere
BioMediTech
May 2015

ACKNOWLEDGEMENTS

This study was carried out in Adult stem cell research group, BioMediTech, University of Tampere. First and foremost I would like to express my deepest gratefulness to our group leader, Docent Susanna Miettinen, PhD, and my supervisor Dr. Sari Vanhatupa, PhD, for having this opportunity to execute my master's thesis project in the fascinating field of stem cell research. I couldn't have hoped for a better group to work in. I am greatly thankful to Sari for supporting me throughout my thesis with expertise, patience and encouragement. The conversations with her have been both educational and intriguing. Sari always had the time and interest for my project.

Secondly, I offer my sincerest gratitude to all the "Mese group" members for interesting discussions and helpful answers for my numerable of questions. This project could not have been accomplished without the technical support from my group members. I want to thank especially Miia Juntunen, Anna-Maija Honkala, Sari Kalliokoski and Miina Ojansivu for invaluable advice and guidance in the laboratory. In addition, I would like to give special thanks to Reija Autio for tips with statistical analyses and to Heli Koivisto for computer support.

Finally, I would like to offer my gratitude to my family. Lauri, I cannot tell you enough how grateful I am to have you by my side. You have encouraged me to accomplish my goals with your example. I would like to thank my mum, dad, sister and grandparents for all the love and support you have given me during my studies, above all during the last months of the writing process. Special thanks belongs to my beloved friends and fellow classmates, who have become very important to me. You all helped me to keep my spirits up during the challenging times. Last but not least, my thanks go to our furry friend Manta, who tried her best to assist with the writing of this thesis.

This work was financially supported by three month funding from Pirkanmaa Hospital District, Tampere, Finland.

Laura Hyväri,
Tampere 15.5.2015

PRO GRADU -TUTKIELMA

Paikka: TAMPEREEN YLIOPISTO
BioMediTech
Tekijä: HYVÄRI, LAURA EMILIA
Otsikko: ROCK, FAK ja MEK-ERK signalointireittien säätelyn vaikutus ihmisen rasvan kantasolujen erilaistumispotentiaaliin
Sivumäärä: 80s. + liitteet 6s.
Ohjaaja: FT Sari Vanhatupa
Tarkastajat: Professori Markku Kulomaa ja FT Sari Vanhatupa
Päiväys: Toukokuu 2015

TIIVISTELMÄ

Tausta ja tavoitteet

Rasvakudoksesta peräisin olevat rasvan kantasolut ovat lupaava solulähde luun kudosteknologisiin sovelluksiin. Rasvan kantasolut kasvavat ja jakautuvat soluviljelmässä, ja niiden tiedetään pystyvän erilaistumaan useiksi solutyypeiksi, kuten rasva-, luu- ja rustosoluiksi. Solujen kiinnittyminen ympäristöönsä ja solujen morfologia ovat tekijöitä, jotka säätelevät mesenkymaalisten kantasolujen erilaistumisprosessia. Näiden solunsisäisten mekanismien yksityiskohdat ovat kuitenkin yhä pitkälti tuntemattomia. Tämän tutkimuksen tavoitteena oli saada lisätietoa signalointireiteistä, jotka ovat osana kiinnittymis- tai morfologiavälitteistä erilaistumista ihmisen rasvan kantasoluissa. Tutkimuksessa analysoitiin ROCK (Rho kinaasi), FAK (Fokaaliadheesiokinaasi) ja MEK-ERK (Mitogeneeniaktivoituva proteiinikinaasi) -välitteisen signaloinnin merkitystä rasvan kantasolujen luu- ja rasvaerilaistumispotentiaaliin.

Menetelmät

ROCK, FAK ja MEK-ERK signaloinnin merkitystä rasvan kantasolujen erilaistumisessa tutkittiin inhiboimalla näitä signaalireittejä spesifeillä inhibiittorimolekyyleillä: ROCK1 inhibiittori Y-27632 2HCl, FAK inhibiittori PF-562271 ja MEK inhibiittori PD98059. Inhibiittorien vaikutusta solujen elinkykyyn ja jakautumiseen arvioitiin LIVE/DEAD[®]- ja CyQUANT[®]-analyysillä. Kantasolujen rasvaerilaistumista tutkittiin Oil Red O värjäyksellä, ja luuerilaistumista analysoitiin kvantitatiivisella alkalisella fosfataasin (ALP) määrittämisellä, sekä kvalitatiivisella että kvantitatiivisella Alizarin Red värjäyksellä. Solunsisäistä proteiiniaktivaatiota tutkittiin WesternBlot -analyysimenetelmällä.

Tulokset

Tulokset osoittivat, että rasvan kantasolujen kiinnittyminen kasvualustaan ja soluväliaineeseen on edellytyksenä niiden elinkyvylle, kasvuille ja luuerilaistumiselle. Solujen kiinnittymisen häiritseminen FAK- tai ROCK -inhibiittoreilla heikensi luuerilaistumista. Solujen morfologia ohjasi rasvan kantasolujen erilaistumislinjan valintaa: levittäytynyt solutukiranka lisäsi luuerilaistumista, kun taas solun pyörästynyt muoto suosi erilaistumista rasvakudoksen suuntaan. ROCK toimi luuerilaistumisen positiivisena säätelijänä, ja tämän signaalireitin inhibitio lisäsi rasvaerilaistumista tutkituilla solulinjoilla. Myös toiminnallisen MEK-ERK signaloinnin havaittiin olevan edellytyksenä solunjakautumista ja -erilaistumista sääteleville solumekanismeille.

Johtopäätökset

Tämän tutkimuksen perusteella solujen adheesiokyky on olennainen osa tai jopa edellytys erilaistumista tukeville solunsisäisille toiminnoille rasvan kantasoluissa. Kiinnittymistä ja morfologiaa säätelevät ROCK, FAK ja MEK-ERK signalointikaskadit olivat tutkimuksen perusteella osallisina rasvan kantasolujen luuerilaistumisessa. Aktiivinen ROCK proteiini toimi rasvaerilaistumisen negatiivisena säätelijänä, kertoen solujen muodon vaikutuksesta rasvan kantasolujen erilaistumispotentiaaliin. Tulokset osoittavat, että solujen kiinnittymistä vahvistamalla sekä solumorfologiaa säätelemällä voitaisiin tukea rasvan kantasolujen erilaistumismekanismeja.

MASTER'S THESIS

Place: UNIVERSITY OF TAMPERE
BioMediTech
Author: HYVÄRI, LAURA EMILIA
Title: Differentiation Potential of the Human Adipose Stem Cells in Response to Regulation of ROCK, FAK and MEK-ERK Signaling Pathways
Pages: 80pp. + appendices 6pp.
Supervisor: Dr. Sari Vanhatupa, PhD
Reviewers: Professor Markku Kulomaa and Dr. Sari Vanhatupa
Date: May 2015

ABSTRACT

Background and aims

Adipose stem cells (ASCs), obtained from adipose tissue, are a promising cell source for bone tissue engineering applications. ASCs exhibit stable growth and proliferation *in vitro* and they possess multi-lineage differentiation capacity into various cell lineages including adipocytes, osteoblasts and chondrocytes. The differentiation process of mesenchymal stem cells (MSC) is known to be regulated through cell attachment and morphology, however, the intracellular details of the regulation remain unidentified. The aim of this study was to enlighten the signaling events in cell attachment or morphology -mediated differentiation in hASCs. The significance of Rho-kinase (ROCK), Focal adhesion kinase (FAK) and Mitogen-activated protein kinase/Extracellular signal-regulated kinase (MEK-ERK) signaling to hASC differentiation potential towards osteoblasts and adipocytes were analyzed.

Methods

To assess the significance of ROCK, FAK and MEK-ERK signaling pathways to hASC differentiation, specific inhibitor molecules targeted to these cascades were used: ROCK1 inhibitor Y-27632 2HCl, FAK inhibitor PF-562271 and MEK inhibitor PD98059. The inhibitor effect on cell viability and proliferation were assessed with LIVE/DEAD[®] assay and CyQUANT[®] assay, respectively. The hASC adipogenic differentiation was determined by Oil Red O staining, and the osteogenic differentiation was assessed by quantitative alkaline phosphatase assay (qALP), and qualitative and quantitative Alizarin Red staining. The intracellular protein activation was evaluated with Western Blot analysis method.

Results

The results indicated that cell attachment to the culture platform and to the extracellular matrix (ECM) is critical for cell viability, proliferation and induction of the osteogenic differentiation of hASCs. Disruption of the cell adhesion with FAK or ROCK inhibition suppressed the osteogenic differentiation. Cell morphology guided hASC lineage commitment: spread cytoskeleton induced osteogenesis while rounded shape favoured commitment to adipogenesis. ROCK was found to be a positive regulator of osteogenesis and the inhibition of ROCK enhanced adipogenesis in the hASC lines studied. Also functional MEK-ERK pathway was required for various intracellular processes regulating cell proliferation and differentiation in hASCs.

Conclusions

Taken together, the cell adhesion is an essential part and a prerequisite of many intracellular functions in hASC differentiation. Based on this study, ROCK, FAK and MEK-ERK signaling cascades were involved in the osteogenic differentiation of hASCs. An active ROCK protein worked as a negative regulator of adipogenesis, representing the influence of cell morphology to the differentiation potential of hASCs. The results indicate, that the differentiation mechanisms of hASCs could be supported by enhancing the cell adhesion and regulating the morphology of the cells.

TABLE OF CONTENTS

1. INTRODUCTION	1
2. REVIEW OF THE LITERATURE.....	3
2.1 Stem cells	3
2.1.1 Mesenchymal stem cells	4
2.1.2 Adipose stem cells	6
2.1.3 Isolation and characterization of the adipose stem cells	7
2.2 Differentiation potential of the ASCs.....	8
2.2.1 Signaling events in the osteogenic differentiation	9
2.2.2 Signaling events in the adipogenic differentiation.....	10
2.3 Cell attachment.....	12
2.3.1 Integrins	12
2.3.2 Focal adhesions	13
2.3.3 Cell attachment mediated signaling in the cell differentiation	14
2.4 Cell morphology as a regulator of cell differentiation	20
2.4.1 ROCK signaling pathway	21
2.4.2 Mechanotransduction	23
3. AIMS OF THE PRESENT STUDY	25
4. MATERIALS AND METHODS	26
4.1 The hASC culture	26
4.2 Flow cytometric surface marker expression analysis	28
4.3 Culture conditions of the hASCs in the experiments	28
4.4 Cell attachment and viability.....	29
4.5 CyQUANT® cell proliferation assay	30
4.6 Oil Red O fat vacuole staining	31
4.7 Alkaline phosphatase activity.....	31
4.8 Mineralization	32
4.9 Western Blot analysis	32
4.10 Microscopy, photography and image editing	34
4.11 Statistical analysis.....	34
5. RESULTS	35
5.1 Flow cytometric surface marker expression analysis	35
5.2 Inhibitor effect on the cell viability and attachment.....	36
5.3 Cell morphology.....	37
5.4 Effect of FAK, ROCK and MEK kinase inhibition on the cell proliferation.....	39
5.5 The effect of FAK, ROCK and MEK-ERK inhibition on differentiation potential of the hASCs.....	41

5.5.1	Adipogenic differentiation	41
5.5.2	Early osteogenic differentiation	44
5.5.3	Mineralization	48
5.6	Western Blot analysis of the inhibitor functionality	50
6.	DISCUSSION	52
6.1	The cell attachment and proliferation are interfered with the inhibitors.....	52
6.2	The hASC morphology changes as a result of the inhibitor treatments.....	53
6.3	ROCK works as a molecular switch between osteogenesis and adipogenesis in hASC differentiation	54
6.4	FAK mediated attachment is required for the hASC osteogenic differentiation	56
6.5	Functional MEK-ERK signaling is required in the hASC differentiation	58
6.6	Cross-talk between ROCK, FAK and MEK-ERK cascades	59
6.7	Donor variation.....	60
7.	CONCLUSIONS.....	62
8.	REFERENCES.....	63
9.	APPENDICES	73

ABBREVIATIONS

ADSC	adipose-derived stem cell
AF	amniotic fluid
ALP	alkaline phosphatase
AM	adipogenic medium
aP2	fatty acid-binding protein
ASC	adipose stem cell
BM	basic medium
BMP	bone morphogenetic protein
BMPR	BMP-receptor
BMSC	bone marrow stem cell
C/EBP	enhancer binding protein
Cbfa1	core-binding factor alpha 1
DEX	dexamethasone
DMEM	Dulbecco's Modified Eagle Medium
DMSO	dimethyl sulfoxide
ECL	enhanced chemiluminescence
ECM	extracellular matrix
ERK	extracellular signal-regulated kinase
ERM	ezrin-radixin-moesin
ESC	embryonic stem cell
EthD-1	ethidium homodimer-1
FA	focal adhesion
FACS	fluorescence activated cell sorting
FAK	focal adhesion kinase
FAS	fatty acid synthase
FAT	focal adhesion targeting domain
FATP-1	fatty acid transport protein-1
FSC	fetal stem cell
GEF	guanine nucleotide exchange factor
Grb	growth receptor -bound protein
hASC	human adipose stem cell
hBMSC	human bone marrow stem cell
HFSC	human fat stem cell
hMSC	human mesenchymal stem cell
HRP	horseradish peroxidase
HS	human serum
HSC	hematopoietic stem cell
IBMX	3-isobutyl-1-methylxanthine/isobutylmethylxanthine
IgG	immunoglobulin G
iPSC	induced pluripotent stem cell
ISCT	International Society for Cellular Therapy
JNK	c-Jun N-terminal kinase
KLF5	Krüppel-like transcription factor 5
LPL	lipoprotein lipase
MAPK	mitogen-activated protein kinase
MAPKK	MAPK kinase
MAPKKK	MAPKK kinase
MEK	mitogen-activated protein kinase

MLC	myosin light chain
MSC	mesenchymal stem cell
OM	osteogenic medium
OCN	osteocalcin
p38	p38-activating kinase
PBS	phosphate-buffered saline
PFA	paraformaldehyde
PH	pleckstrin homology
PLA	processed lipoaspirate
PPAR γ	peroxisome proliferator-activated receptor
pref-1	pre-adipocyte factor-1
PTK	protein tyrosine kinase
PVDF	polyvinylidene fluoride membrane
ROCK	Rho-associated coiled-coil kinase
RT	room temperature
Runx2	runt-related transcription factor 2
SD	standard deviation
SDS-PAGE	sodium dodecyl sulphate polyacrylamide gel electrophoresis
SEM	standard error of the mean
SH2/3	SRF homology domains 2 and 3
SVF	stromal vascular fraction
TAG	triacylglycerol
TPPP1	tubulin polymerization promoting protein 1
UCB	umbilical cord blood
WB	Western Blot

1. INTRODUCTION

The current clinical standard for the treatment of large bone defects is an autologous bone graft (Zhang et al. 2014). Another option is the usage of allogenic bone substitute such as a demineralized bone matrix (Levi, Longaker 2011). However, these methods have disadvantages, such as low availability of the bone substitutes, donor site morbidity and the immunoreactions arising from the use of allografts (Ng et al. 2005). Due to these challenges, regeneration via autologous stem cell transplantation has become a promising approach to the osseous restoration of large-size bone defects (Tirkkonen et al. 2013, Zhang et al. 2014). Cranio-maxillofacial defects have already been repaired with autologous adipose stem cells combined with biomaterials (Tirkkonen et al. 2013). In tissue engineering applications, immune reactions can be avoided using the patient's own multipotent mesenchymal stem cells (MSC) as a stem cell source (Mathieu, Lobo 2012). The cells can be isolated, expanded *ex vivo*, and transplanted to the defect site using a biomaterial scaffold as a carrier (Tirkkonen et al. 2013).

In addition to bone tissue engineering, also soft tissue engineering benefits from techniques to use autologous stem cells. Soft tissue substitutes are needed in reconstructive and corrective surgery after trauma, tumor resection or the correction of congenital deficiency, and in cosmetic surgery (Vermette et al. 2007). Current fat tissue transplants are not sufficiently long-lasting and the transpositioned fat undergoes unpredictable resorption (Niemelä et al. 2007, Vermette et al. 2007). In addition, the adipocytes are brittle and obtaining a sufficient vascularization of the graft has been challenging (Vermette et al. 2007).

Adipose tissue possesses several advantageous properties as a MSC source. Large quantities of adipose stem cells (ASC) can be harvested from adipose tissue (Zuk et al. 2002, Kern et al. 2006) and isolated from liposuction aspirates or excised fat samples (Vermette et al. 2007, Wosnitza et al. 2007). Additionally, the ASCs possess multilineage differentiation potential (Lindroos, Suuronen & Miettinen 2011). Human ASCs are also intriguing cells due to their therapeutic capacity. hASCs can stimulate tissue recovery, since they can work in paracrine manner by secreting growth factors and promote stem cell differentiation into cell lines needed (Bonfield, Caplan 2010, Galateanu et al. 2012).

Cell attachment and morphology have been found to be key regulatory factors determining hASC differentiation. Cell attachment to the extracellular matrix (ECM) is mediated primarily through integrins and focal adhesions (FA). Osteogenesis of MSCs has been shown to be more prevalent with spread actin cytoskeleton (Treiser et al. 2010) and greater number of focal adhesions while adipogenesis is encouraged by preventing cell attachment (Mathieu, Lobo 2012). Especially

actomyosin contractility promotes osteogenesis in MSCs (McBeath et al. 2004, Kilian et al. 2010). However, the specific details of the underlying intracellular mechanisms that initiate hASC differentiation are not fully understood. Increased knowledge of the mechanisms regulating the adhesion and morphology of hASCs would provide us tools to develop improved stem cell -based bone and soft tissue engineering applications. The biomaterials used as a scaffold for the cells create an additional challenge regarding cell adhesion. The material should provide a good platform to the cells to adhere, proliferate and differentiate (Giannitelli et al. 2015). Thus, the identification of central mechanisms in cell-biomaterial contacts is essential.

The aim of my thesis was to enlighten the signaling events controlling the hASC differentiation into osteogenic and adipogenic lineages. The present study was conducted to investigate the significance of Rho-kinase (ROCK), Focal adhesion kinase (FAK) and Mitogen-activated protein kinase/Extracellular signal-regulated kinase (MEK-ERK) signaling to hASC differentiation potential towards osteoblasts and adipocytes. These three signaling pathways chosen for the study are known to be involved in cell attachment or morphology -mediated differentiation of MSCs based on the existing literature. To assess the significance of these pathways to hASC differentiation, the signal transduction was inhibited with small specific inhibitor molecules. The following methods were used in the present study: LIVE/DEAD[®] assay, CyQUANT[®] cell proliferation assay, Oil Red O staining, quantitative alkaline phosphatase assay (qALP), qualitative and quantitative Alizarin Red staining and Western Blot analysis.

2. REVIEW OF THE LITERATURE

2.1 Stem cells

Stem cells are defined as self-renewing progenitor cells that possess long-term viability and have the ability for multilineage differentiation (Zuk et al. 2002, Passier, Mummery 2003, Choumerianou, Dimitriou & Kalmanti 2008). Stem cells are typically classified into three groups based on their differentiation capacity. Differentiation potential of stem cells has been presented by Brignier and Gewirtz, 2010. Totipotent stem cells have the potential to develop into any type of cell forming the complete embryo. Totipotency appears with the fertilization of the egg and disappears by the time the embryo reaches the 4- to 8-cell stage. Stem cells are pluripotent when they have lost the ability to generate an entire organism, but they still have the potential of differentiating into the cells of three embryonic layers (ectoderm, mesoderm and endoderm). Stem cells that have restricted differentiation ability are called multipotent. These cells are situated in the various tissues and organs of an adult organism. Multipotent stem cells are capable of differentiating into a limited number of cell types. (Brignier, Gewirtz 2010)

Stem cells are divided into embryonic, fetal or adult stem cells according to their origin. The classification is based on the stage of ontogenesis (the development of an organism) in which the stem cells appear (Zuk et al. 2002, Passier, Mummery 2003, Pappa, Anagnou 2009). Different types of stem cells are shortly presented in the following chapters. The main focus of this review is on adult stem cells, primarily in adipose stem cells.

Embryonic stem cells (ESC) are derived from the totipotent cells of the early mammalian embryo. They are characterized by prolonged, undifferentiated proliferation *in vitro*, immortality, and pluripotency having stable developmental potential to form all three embryonic germ layers even after prolonged culture (Thomson et al. 1998, Zuk et al. 2002, Brignier, Gewirtz 2010). Despite the enormous potential of ESCs, their usage elicits ethical and political issues (Zuk et al. 2002). ESCs have been comprehensively reviewed by Wobus and Boheler (Wobus, Boheler 2005).

Fetal stem cells obtain pluripotential or multipotential features (proliferation rates and plasticity features). They can be derived either from the fetus itself or from the extra-embryonic structures such as umbilical cord blood (UCB), amniotic fluid (AF), Wharton's jelly, the amniotic membrane and the placenta. The extra-embryonic structures lack the ethical reservations associated with ESCs making them an attractive stem cell source. (Pappa, Anagnou 2009)

Another type of stem cells, induced pluripotent stem (iPS) cells, was introduced by Yamanaka and co-workers in 2006 (Takahashi, Yamanaka 2006). The iPS cells were generated for clinical applications to avoid tissue rejection following ESC transplantation in patients since it is possible to

create patient-specific iPSCs (Brignier, Gewirtz 2010). However, at the moment iPS cells are most widely used in stem cell research, especially in the field of drug development. iPS cells are produced by reprogramming somatic cells to ESC-like cells (Yamanaka 2009). iPS cells can be generated from differentiated cells by using retroviral-mediated introduction of transcription factors that are required for the maintenance of pluripotency and proliferation of ESCs (Yamanaka 2009, Brignier, Gewirtz 2010) They can give rise to cells derived from all three germ layers *in vitro* and *in vivo* (Brignier, Gewirtz 2010).

Despite the attractive qualities of ESCs, FSCs and iPS cells, such as nearly unlimited proliferation and differentiation potential *in vitro* and *in vivo*, the use of these cells in clinical applications is challenging due to the legal, ethical and political issues they elicit. Also the safety of these cells must be concerned since the unlimited proliferation of ESCs and iPS cells may cause an increased risk of teratoma formation (Thomson et al. 1998, Yamanaka 2009). To overcome the problems related to pluripotent stem cells, alternative sources of stem cells have been under investigation.

Stem cells can be found in the most specialized tissues of the body. These adult stem cells are responsible for maintaining the tissue homeostasis by the regeneration of the tissue specific cells after trauma, cell turnover or disease (Pittenger et al. 1999, Brignier, Gewirtz 2010). Adult stem cells are multipotent being able to differentiate only to tissue specific cell types (Hipp, Atala 2008). Multiple sources of adult stem cells have been found including bone marrow, brain, liver, skin and gastrointestinal tract (Brignier, Gewirtz 2010), as well as skeletal muscle, pancreas, eye, blood and dental pulp (Hipp, Atala 2008). The yield of stem cells from differentiated tissues is quite low and often the cells are difficult to isolate (Hipp, Atala 2008, Brignier, Gewirtz 2010). Adult stem cells can be classified based on the embryonic germ layer (ectoderm, mesoderm and endoderm) they stem from. Hematopoietic stem cells (HSC) and mesenchymal stromal cells (MSC) originated from mesoderm have been vastly studied for decades (Choumerianou, Dimitriou & Kalmanti 2008). HSCs can be harvested from bone marrow or umbilical cord blood (Brignier, Gewirtz 2010). These cells are capable of producing myeloid and lymphoid lineages in blood (Hipp, Atala 2008), but are also shown to be able of nonhematopoietic differentiation *in vitro* (Brignier, Gewirtz 2010). Mesenchymal stem cells are presented in detail in Chapter 2.1.1.

2.1.1 Mesenchymal stem cells

The genesis of mesodermal tissues in either embryos or adult organisms is referred to a mesengenic process (Figure 1) (Caplan 1994). The process is involved in the continual turnover of the mesenchymal tissues and the rapid repair of tissue injuries. Mesenchymal stem cells are a pivotal part

of the mesengenic process by being responsible for regenerating mesenchymal tissues (Caplan 1994, Pittenger et al. 1999). MSCs are undifferentiated cells with high proliferative capacity (Pittenger et al. 1999, Kern et al. 2006). They are characterized by their capacity to adhere to the surface of culture flasks, in other words, their plastic-adherency (Dominici et al. 2006, Sivasubramanian et al. 2012). MSCs have also been named as multipotent mesenchymal stromal cells, as stated by the International Society for Cellular Therapy (ISCT), because the majority of MSCs lack the complete stemness property being multipotent instead of pluripotent (Horwitz et al. 2005, Brignier, Gewirtz 2010). A distinguishing feature of MSCs is the formation fibroblast-like colonies with well-spread cells *in vitro* (Pittenger et al. 1999, Kern et al. 2006, Sivasubramanian et al. 2012).

Bone marrow was the first reported source of MSCs with stem cell -like characteristics (Pittenger et al. 1999, Kern et al. 2006, Weinzierl, Hemprich & Frerich 2006, Hipp, Atala 2008). Human MSCs were first isolated by Caplan and colleagues from bone marrow samples in the late 1980s (Caplan, Bruder 2001). It is currently known that MSCs can be obtained from several tissues (Kern et al. 2006). Brignier and Gewirtz (2010) state that MSCs are most conveniently isolated from bone marrow and umbilical cord blood (UCB). Galateanu et al. (2012), on the contrary, claim subcutaneous adipose tissue to be advantageous over other MSC sources.

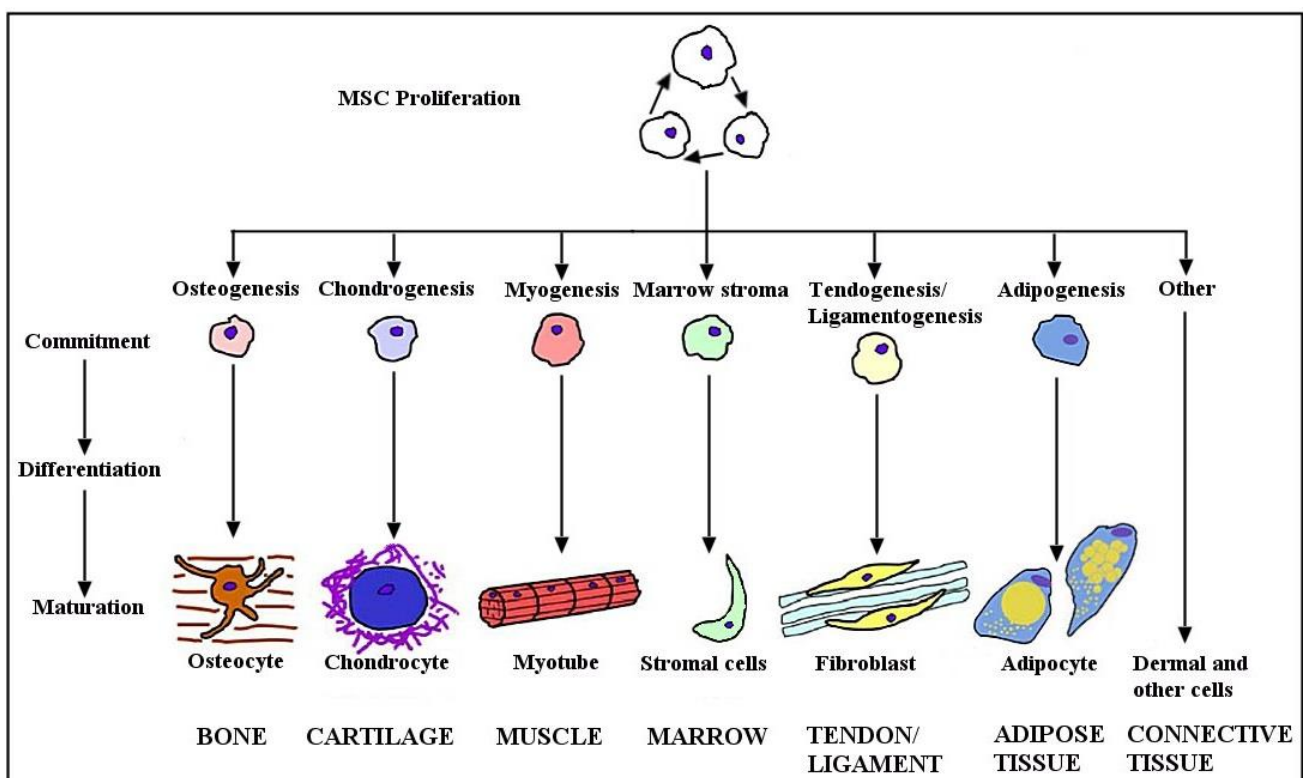


Figure 1. The mesengenic process. The mesenchymal stem cells differentiate into range of mesenchymal tissues and cells including bone, cartilage, muscle, stromal cells, tendon, ligaments and adipose tissue. Adapted from (Bonfield, Caplan 2010).

Mesenchymal stem cells are capable of multipotential differentiation to various mesenchymal lineages such as osteogenic, adipogenic and chondrogenic lineages (Pittenger et al. 1999, Caplan, Bruder 2001, Kern et al. 2006, Brignier, Gewirtz 2010, Sivasubramaniyan et al. 2012). Nonetheless, MSC have been shown to differentiate also to endo- and ectodermal lineages (Kern et al. 2006). Isolated MSCs can be differentiated in controlled manner (Pittenger et al. 1999) under appropriate culture conditions (Sivasubramaniyan et al. 2012) and with lineage-specific induction factors (Zuk et al. 2001). MSC populations isolated from various sources, although morphologically similar, might be functionally different (Brignier, Gewirtz 2010). For example, MSCs isolated from the umbilical cord do not have the same differentiation capabilities as bone marrow to give rise to osteoblasts, chondrocytes, and cardiomyocytes (Brignier, Gewirtz 2010) and in some studies presented lack of adipogenic differentiation (Kern et al. 2006).

2.1.2 Adipose stem cells

Adipose tissue is derived from the mesenchyme (Zuk et al. 2002, Strem et al. 2005) and contains bone marrow -like stem cells (Kern et al. 2006). This adipose stem cell population derives from the stromal vascular fraction (SVF) of adipose tissue (Varma et al. 2007, Wosnitza et al. 2007, Galateanu et al. 2012), and is isolated from the adipose tissue by collagenase digestion (Wosnitza et al. 2007). The adipose stem cell appears to be a common expression, however, also other terms have been suggested to these cells: processed lipoaspirate (PLA) (Zuk et al. 2001), adipose-derived stem cells (ADSCs) and adipose tissue-derived stem cells (Miranville et al. 2004).

Many studies have shown the similarities in differentiation capabilities between bone marrow -derived MSCs and ASCs (Weinzierl, Hemprich & Frerich 2006, Varma et al. 2007). The use of adipose tissue as a MSC source over bone marrow has several advantages. The donation procedure of bone marrow stem cells is highly invasive and the donor site morbidity limits the amount of marrow obtained (Strem et al. 2005, Kern et al. 2006, Weinzierl, Hemprich & Frerich 2006). In addition, the stem cells are scarce in bone marrow and the differentiation potential of the bone marrow stem cells (BMSC) diminishes with the increasing age of the donor (Kern et al. 2006, Weinzierl, Hemprich & Frerich 2006). On the contrary, adipose tissue exhibits minimal morbidity upon harvest (Strem et al. 2005, Galateanu et al. 2012, Buschmann et al. 2013). ASCs can be obtained larger quantities (Kern et al. 2006) and they are easily isolatable from adipose tissue (Zuk et al. 2002). The cells can be harvested from liposuction aspirates or excised fat samples (Zuk et al. 2002, Kern et al. 2006, Vermette et al. 2007, Wosnitza et al. 2007). Stem cell frequency is significantly higher in adipose tissue (1-5%) compared with bone marrow (0.001-0.1%) (Strem, Hedrick 2005, Varma et al. 2007,

Buschmann et al. 2013). Furthermore, stem cells isolated from adipose tissue exhibit stable growth and proliferation *in vitro* (Zuk et al. 2002).

Although many similarities between BMSCs and ASCs have been reported, the stem cells are not identical having differences in differentiation kinetics and in the CD marker profile (Zuk et al. 2002). The yield of ASCs has a negative correlation with the donor's age: the yield is diminished during the age (Buschmann et al. 2013). Also, variation has been reported in ASCs isolated from different body regions (Buschmann et al. 2013, Gnanasegaran et al. 2014). The study of Gnanasegaran and co-workers (2014) reveals that also the isolation method of ASCs has an effect on the gene expression of the stem cells. They concluded that ASCs from liposuction have a tendency to differentiate towards endoderm lineage whereas ASCs obtained from fat tissue biopsy have a propensity towards mesodermal and ectodermal lineages.

There are several ongoing studies investigating the use of ASCs in clinical applications. According to the database of clinical trials maintained by the US National Institutes of Health, 18 studies using ASCs and 30 studies using cells from SVF are listed at the moment (<http://clinicaltrials.gov>). Six of these studies focus on bone formation. In addition, ASCs are exploited in four trials of autologous fat grafting for soft tissue replacement. hASCs have been applied successfully in several clinical cases of treating craniomaxillo-facial defects. In Finland, 24 cases of bone and cartilage defects have been treated with adipose tissue derived stem cell products fabricated in Regea Cell and Tissue Center (Seppanen, Miettinen 2014). These products consist of the adipose stem cells, biological stimulus (e.g. growth factors) and a scaffold functioning as a substrate for cell adhesion and mechanical support of the construct (Giannitelli et al. 2015). In bone tissue engineering, the attachment of the cell to the scaffold is often enhanced with surface modifications of the biomaterials (Motamedian et al. 2015). For example, the addition of physicochemical factors (e.g. growth factors or ECM proteins) and nanoparticles to the material surface can improve the in cell response of bone scaffolds used (Motamedian et al. 2015). The scaffold materials and design in bone tissue engineering have been comprehensively reviewed recently by Velasco and co-workers (Velasco, Narvaez-Tovar & Garzon-Alvarado 2015).

2.1.3 Isolation and characterization of the adipose stem cells

The isolation of fat cells was first described by Rodbell (Rodbell 1964) who used collagenase and gentle stirring to disperse the adipose tissue of rats. The adipose stem cells from the stromal vascular fraction (SVF) of adipose tissue were isolated the first time from liposuction aspirates in 2001 by Zuk and collaborators (Zuk et al. 2001), the procedure is also described by Gimble and Guilak (2003) and Bunnell et al. (2008). Adipose stem cells are a heterogeneous cell population from SVF consisting of

various progenitor cells instead of a unique cell population (Zuk et al. 2001, Varma et al. 2007, Wosnitza et al. 2007). A more homogeneous population of adipose stem cells can be obtained by culture-expanding the cells in MSC growth supporting conditions (Strem et al. 2005, Varma et al. 2007) and by removing HSCs and other nonadherent cells from the culture with changes of the culture medium (Pittenger et al. 1999).

MSC characteristics include the expression of typical surface proteins (Pittenger et al. 1999, Kern et al. 2006) and lack of hematopoietic and endothelial markers (Kern et al. 2006). The minimal criteria for defining multipotent mesenchymal cells were proposed in 2006 by the Mesenchymal and tissue stem cell committee of the ISCT (Dominici et al. 2006). According to these criteria, human MSC must be plastic-adherent when maintained in standard culture conditions. MSCs must express specific surface markers (CD105, CD73 and CD90) and lack the expression of hematopoietic antigen molecules (CD45, CD34, CD14 or CD11b, CD79 α or CD19 and HLA-DR). In addition to these, MSCs must have the capacity for multilineage differentiation into osteoblasts, adipocytes and chondroblasts under standard *in vitro* conditions. (Dominici et al. 2006)

Adipose stem cells are commonly characterized as bone marrow -derived mesenchymal stem cells since they exhibit similar CD marker antigens (Zuk et al. 2002). However, ASC marker expression changes during *in vitro* culture complicating the identification (Zhang et al. 2014). Some reports have indicated that adipose tissue -derived MSCs express hematopoietic lineage surface antigen CD34 (Sivasubramaniyan et al. 2012, Gnanasegaran et al. 2014). Gnanasegaran and co-workers (2014) reported that in their study the ASCs were positive for CD34 but they suspected it resulting from the contamination of hematopoietic cells. Other studies have also demonstrated that the expression of marker CD34 is high in the freshly isolated SVF cells and in early passage (P0) ASCs (Mitchell et al. 2006, Varma et al. 2007). When cultured and successfully passaged, the expression of CD34 declines (Mitchell et al. 2006, Varma et al. 2007, Galateanu et al. 2012). On the other hand, some studies denote that the presence of CD34 indicates preadipocyte population of ASCs having an increased tendency towards fat tissue (Li et al. 2011).

2.2 Differentiation potential of the ASCs

The differentiation potential of ASCs has been studied extensively during the last decade. Adipose tissue -derived stem cells are known to possess multi-lineage differentiation capacity (Zuk et al. 2002, Strem et al. 2005, Wosnitza et al. 2007). ASCs have been cultured and differentiated to various cell lineages including adipocytes, osteoblasts, smooth muscle cells (Zuk et al. 2002, Weinzierl, Hemprich & Frerich 2006, Niemelä et al. 2007) and chondrocytes (Zuk et al. 2002, Niemelä et al. 2007). It has been proposed that the ASCs are also able to differentiate into non-mesenchymal lineages. The

neuronal differentiation of ASCs appears to be controversial as some articles suggest that ACSs are capable of differentiating into neuron-like cells (Strem et al. 2005, Niemelä et al. 2007) while more recent studies claim that there is no evidence yet that genuine neuronal differentiation is achieved (Franco Lambert et al. 2009, Arribas et al. 2014). In addition, several studies have shown the capability of animal ASCs to differentiate into cardiomyocytes spontaneously or when treated with 5-azacytidin (Rangappa et al. 2003, Planat-Benard et al. 2004). Also the human ASC cardiomyocyte differentiation has been described by for example Van Dijk and co-workers (Van Dijk et al. 2008). In addition, the *in vitro* endothelial differentiation of ASCs has been reported (Miranville et al. 2004).

The present study focuses on the osteogenic and adipogenic differentiation of ASCs. The basic mechanisms and the essential signaling events needed in the osteogenic and adipogenic differentiation are presented in Chapters 2.2.1 and 2.2.2, respectively.

2.2.1 Signaling events in the osteogenic differentiation

MSCs differentiate into osteoblasts through the steps of proliferation, maturation, matrix synthesis and mineralization (James 2013). Osteogenic differentiation is characterized by morphological changes of the cells, and by the osteoblast-specific expression of alkaline phosphatase (ALP), osteocalcin (OCN), osteopontin and hydroxyapatite-mineralized ECM (Niemelä et al. 2007, Salasnyk et al. 2007). At the early stage of MSC differentiation, the osteogenic genes are up-regulated with a simultaneous down-regulation of adipogenic, chondrogenic and muscular genes. Several signaling pathways are involved in MSC development from multipotent stem cells into mature osteoblasts. Runx2 (Runt-related transcription factor) is the major regulator of osteogenesis (Ge et al. 2009, Biggs, Dalby 2010, James 2013). It is responsible for the osteoblast-specific gene expression of ALP, OCN and osteopontin (Biggs, Dalby 2010). Runx2 is required for the commitment of mesenchymal stem cells to bone lineages and is therefore expressed very early in skeletal development (Ge et al. 2009). The bone-specific transcription factor, Cbfa1, regulates the expression of the osteocalcin gene and is also essential for bone formation (Xiao et al. 2000).

As reviewed by Lin and Hankenson (2011), the key signaling pathways in osteoblastogenesis include Wnt, Notch and bone morphogenetic protein (BMP). The canonical (β catenin mediated) Wnt signaling is involved in MSC osteogenic differentiation. In Wnt signaling ligand-receptor interactions ultimately lead to an increase in cytoplasmic β -catenin levels and its translocation into the nucleus, where it acts as a transcription factor (Hartmann 2006). Wnt signaling activates Runx2, but inhibits the transcription of peroxisome proliferator-activated receptor- γ (PPAR γ). (Lin, Hankenson 2011) PPAR γ is an essential transcription factor in adipogenesis, thus the expression of multiple Wnt family proteins suppresses the adipogenesis (Rajashekhar et al. 2008).

BMPs and other growth factors have been shown to enhance and accelerate the osteogenic differentiation of ASC (Bessa et al. 2009, Levi, Longaker 2011, Zhang et al. 2014). However, the studies regarding BMPs are conflicting. Some studies display the significance of BMPs to osteogenic gene regulation (Celil, Campbell 2005) while some indicate that there is no benefit from BMPs to osteogenic differentiation (Tirkkonen et al. 2013). Binding of BMPs to their receptors BMPR-I and BMPR-II activates intracellular Smad proteins that work as transcription factors activating expression of the osteogenic genes, such as Runx2. Notch is a transmembrane receptor that is involved in osteogenesis of MSCs through the regulation of either BMP or Wnt-induced osteogenesis. (Lin, Hankenson 2011)

In addition to the aforementioned pathways, also various other signaling cascades are involved in osteoblastogenesis including hedgehog (Hh), that has been linked to the skeletal development (Lin, Hankenson 2011), and MAPK pathways p38, JNK and ERK, out of which ERK signaling has been proven critical (Jaiswal et al. 2000, Greenblatt, Shim & Glimcher 2013). Integrin-mediated cell-ECM interactions play a central role in regulating hMSC osteogenesis. Integrins activate intracellular signaling cascades leading to the phosphorylation of Runx2/Cbfa1 (Salaszyk et al. 2007). Subsequent development of the osteoblast lineage requires at least two additional factors: osterix and ATF4, which regulates osteoblast activity, particularly in postnatal animals (Ge et al. 2009).

Cell morphology has been discovered to have a crucial role in stem cell commitment. Cell spreading increases osteoblast differentiation in preosteoblast cells (McBeath et al. 2004). In addition, the effect of cell density on the MSC commitment towards osteogenic or adipogenic lineages has been studied by McBeath and co-workers (2004). They discovered that the osteogenic differentiation favors lower cell density than adipogenesis. The control of osteogenic differentiation is complex and multifaceted and many factors of the osteogenic regulation are still unknown.

Osteogenic differentiation of ASCs can be induced *in vitro* using dexamethasone (DEX), ascorbic acid and β -glycerophosphate, as previously used with BMSCs (Jaiswal et al. 2000, Tirkkonen et al. 2013). These osteogenic supplements act also as mitogens by enhancing the cell division (Jaiswal et al. 2000). Recently, the concentrations of the supplements have been optimized for hASC osteogenic differentiation in our group (Kyllonen et al. 2013).

2.2.2 Signaling events in the adipogenic differentiation

Adipogenic differentiation can be divided into two phases: the determination phase and terminal differentiation phase. The determination phase includes the MSC commitment to adipogenic lineage whereas the terminal differentiation phase includes the conversion of pre-adipocytes into adipocytes (James 2013). Fibroblast-like pre-adipocytes lose their fibroblastic characteristics during

differentiation (Niemelä et al. 2007, James 2013). In the growth of white adipose tissue both adipocyte size and number increases (Niemelä et al. 2007) and dramatic changes takes place in the cell morphology, cytoskeletal components and ECM (Niemelä et al. 2007, Galateanu et al. 2012). The cell shape has turned out to regulate hMSC differentiation, round cell shape indicating adipogenic differentiation (McBeath et al. 2004). Furthermore, MSCs in high density form fat globules as a sign of adipogenic differentiation whereas at low cell density, no adipogenic differentiation is observed (McBeath et al. 2004). The adipose stem cell harvesting method has also shown to have impact on the differentiation potential, as the study of Vermette and co-workers indicates (Vermette et al. 2007).

The development of adipocyte phenotype is a sequentially and temporally organized process that is regulated by transcriptional factors (Galateanu et al. 2012). PPAR γ is considered as a master regulator of adipogenesis (Niemelä et al. 2007, Galateanu et al. 2012, James 2013). In the early stage of adipogenic lineage commitment, the level of pre-adipocyte factor-1 (pref-1) that maintains the pre-adipose phenotype decreases (Niemelä et al. 2007). PPAR γ acts co-operatively together with enhancer binding protein (C/EBP) activating each other's expression and regulating the downstream gene expression influencing fat cell development (Niemelä et al. 2007, Galateanu et al. 2012). These genes include adipocyte fatty acid-binding protein (aP2), lipoprotein lipase (LPL), fatty acid synthase (FAS), perilipin, fatty acid transport protein-1 (FATP-1), adiponectin and leptin (Galateanu et al. 2012). FAS, aP2 and perilipin are part of triacylglycerol (TAG) metabolism (Galateanu et al. 2012). During the terminal phase of differentiation mature adipocytes acquire new functions, such as lipid synthesis and storage (Niemelä et al. 2007, James 2013).

ASCs can be induced to adipogenic differentiation by using inducing agents in culture medium. Common inducing agents are DEX, 3-isobutyl-1-methylxantine (IBMX) and insulin (Pittenger et al. 1999, Niemelä et al. 2007, Galateanu et al. 2012). In the current study, xeno-free adipogenic medium containing 5% human serum was supplemented with the aforementioned agents and additionally biotin and pantothenate, as in the earlier studies done in our group (Lindroos et al. 2009). The above-mentioned agents induce adipogenesis via mechanisms that lead to increased activation of PPAR γ . According to Galateanu et al. (2012), IBMX upregulates C/EBP which in turn activates Krüppel-like transcription factor 5 (KLF5), that may trigger PPAR γ . Dexamethasone acts probably by inhibiting pre-adipocyte factor-1 and increasing C/EBP and PPAR γ expression, and insulin on the other hand, activates adipocyte specific genes (FAS, leptin and adiponectin). In some studies an additional agent troglitazone, a PPAR γ ligand, have been used to induce adipogenesis. (Galateanu et al. 2012)

2.3 Cell attachment

2.3.1 Integrins

Integrins are a large family of cell surface receptors. They are heterodimeric transmembrane glycoproteins (Cary, Guan 1999) that mediate signal transduction through the cell membrane in both directions (Liu, Calderwood & Ginsberg 2000, Hehlhans, Haase & Cordes 2007, Tilghman, Parsons 2008). Integrins link the ECM to the actin cytoskeleton through several actin-binding proteins (Tilghman, Parsons 2008), such as talin, α -actinin and filamin (Liu, Calderwood & Ginsberg 2000). Integrins are the main receptors for ECM proteins like collagen, fibronectin and laminin (Hehlhans, Haase & Cordes 2007). They mediate multiple cellular functions such as cell proliferation, apoptosis, migration, spreading (Cary, Guan 1999), signal transduction, gene expression (Liu, Calderwood & Ginsberg 2000), cell shape, adhesion and differentiation (Hehlhans, Haase & Cordes 2007).

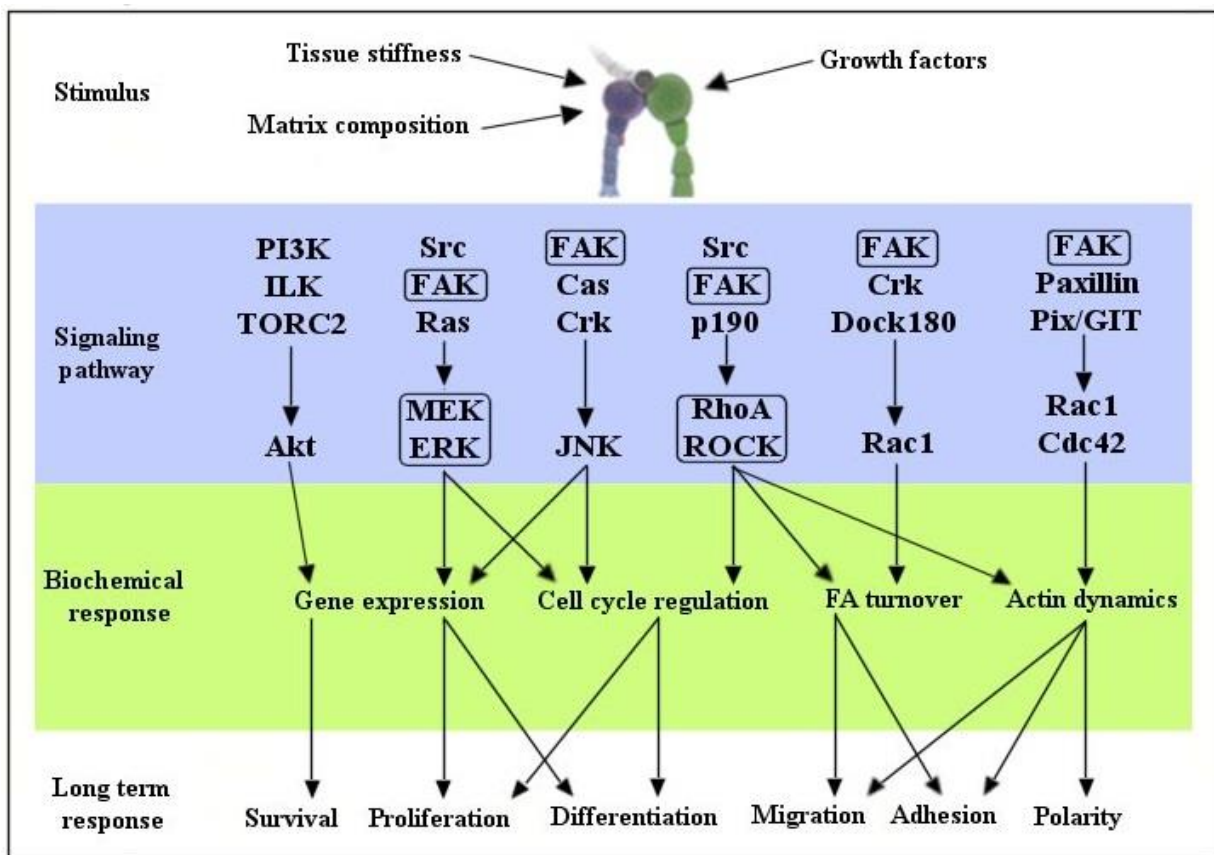


Figure 2. A schematical representation of signaling pathways located downstream of integrin activation. Extracellular stimuli such as ECM composition, its mechanical properties and growth factors regulate the integrin-mediated signaling. Signaling proteins central to the present study are bordered with black line. Modified from (Legate, Wickstrom & Fassler 2009).

Integrins consist of 18 α and 8 β subunits which form 24 known $\alpha\beta$ -heterodimers depending on cell type and cellular function in question (Hehlhans, Haase & Cordes 2007). The association of actin-binding proteins with β -cytoplasmic tails plays a central role in integrin functions (Liu, Calderwood

& Ginsberg 2000). Ligand binding to the extracellular integrin domain induces conformational changes and integrin clustering for the activation of intracellular signaling cascades (Schaller 2001). Integrins themselves lack kinase activity and therefore the signal transmission is conducted via adaptor molecules binding to integrin β tails including focal adhesion kinase (FAK), integrin linked kinase (ILK), talin, paxillin, parvins, p130Cas, Src-family kinases and GTPases of the Rho family (Liu, Calderwood & Ginsberg 2000, Hehlhans, Haase & Cordes 2007). Integrins regulate cell differentiation through various signaling routes. Regarding to the present study, the central integrin-associated signaling proteins include FAK, MEK-ERK and ROCK kinases that are schematically presented in Figure 2. The mechanisms of these signaling events are presented in detail in this literature review.

2.3.2 Focal adhesions

Focal adhesion (Figure 3) is a common type of adhesive contact that cells make with the ECM (Gumbiner 1996). These contacts serve as a link between the contractile actin cytoskeleton and the ECM (Tilghman, Parsons 2008). Focal adhesions are more prominent in adherent and stationary cells. Highly motile cells often lack easily distinguishable focal adhesions, probably since the focal adhesions are more transient, smaller and might be unevenly distributed (Gumbiner 1996). Focal adhesion forms when their receptors, integrins, are activated by interaction with ECM followed by the recruitment of numerous FA-associated proteins (Kuo 2013). FAs are associated with a wide range of cytoplasmic proteins, adaptor proteins such as vinculin and signaling proteins (kinases, phosphatases, phospholipases, GTPases) (Gumbiner 1996, Shih et al. 2011, Kuo 2013). Proteins being able to connect with actin cytoskeleton are termed as scaffolding proteins and include integrin, talin, paxillin, α -actinin and filamin (Gumbiner 1996, Shih et al. 2011, Kuo 2013). Signaling networks from focal adhesions are formed in a process called FA maturation in which FAs reorganize their protein composition to respond to specific biochemical or physical cues (Kuo 2013). Myosin II mediates FA maturation induced by cytoskeletal tension. Early after integrin activation, paxillin and α -actinin are recruited to focal adhesion where α -actinin together with talin provides a link between integrins and the actin cytoskeleton (Pasapera et al. 2010). FA-mediated signaling regulates cell growth and cytoskeletal dynamics, including changes in actomyosin contractility (Tilghman, Parsons 2008). Additionally, focal adhesions have a central role in the differentiation of MSCs. Osteogenesis of MSCs is more prevalent with spread actin cytoskeleton and greater number of focal adhesions. On the contrary, adipogenesis and chondrogenesis are encouraged by preventing focal adhesion attachment (Mathieu, Lobo 2012).

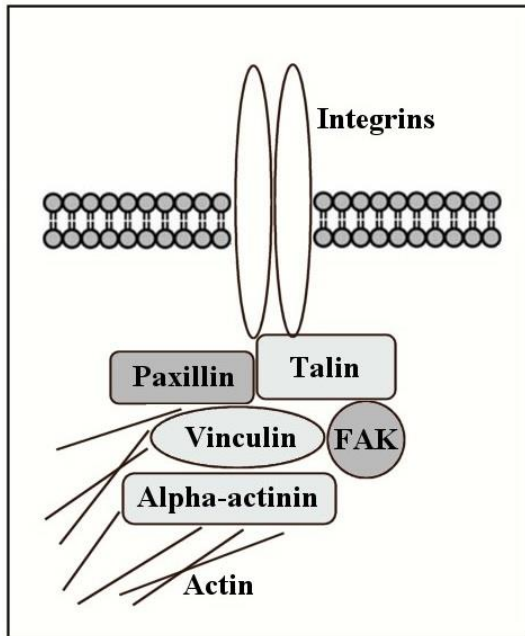


Figure 3. A simplified structure of focal adhesions. Focal adhesions are structures that function as anchoring complexes as well as integrin-mediated modulators of cellular functions via cytoplasmic proteins. Figure modified from (Van Tam et al. 2012).

2.3.3 Cell attachment mediated signaling in the cell differentiation

Focal adhesion kinase

Focal adhesion kinase is a non-receptor tyrosine kinase (Golubovskaya et al. 2008, Tilghman, Parsons 2008), a 125-kDa protein (Golubovskaya et al. 2008) that co-localizes with integrins to focal adhesions (Schaller et al. 1994, Golubovskaya et al. 2008). FAK is a central mediator of integrin-activated signaling (Liu, Calderwood & Ginsberg 2000). Protein tyrosine kinases (PTKs) regulate numerous signal transduction pathways, including those controlling cell growth and differentiation (Schaller et al. 1994). Focal adhesion kinase is involved in cell proliferation, survival, motility, invasion, angiogenesis (Golubovskaya, Cance 2007), adhesion and anchorage-dependent growth (Tilghman, Parsons 2008). In addition, FAK has been shown to be an important mediator in mechanotransduction pathways by both responding to substrate rigidity on the outside of the cell and regulating cellular tension via the actin cytoskeleton (Tilghman, Parsons 2008). FAK is expressed in a variety of species (including human) indicating that it is evolutionarily conserved (Cary, Guan 1999).

FAK is composed of N-terminal FERM domain, central catalytic kinase domain and C-terminal focal adhesion targeting (FAT) domain (Dunty et al. 2004, Lim et al. 2008). FERM domain mediates protein-protein interactions between FAK and cytoplasmic tails of the $\beta 1$ integrin subunit and growth factor receptors (Dunty et al. 2004). Focal adhesion -mediated signaling is initiated in response of receptor binding to integrins. Integrin clustering results in the increase in kinase activation of FAK and tyrosine autophosphorylation in a variety of cell types with the major site of phosphorylation identified as Y397 both *in vivo* and *in vitro* (Schaller et al. 1994, Cary, Guan 1999, Golubovskaya et

al. 2008). Unlike many other cytosolic PTKs, FAK does not contain a SH2 (src-homology 2) or SH3 (src-homology 3) domain (Cary, Guan 1999). Y397 is a critical component in downstream signaling providing highly specific (Schaller et al. 1994), high-affinity binding site for the SH2 domain of Src family kinases (Dunty et al. 2004, Golubovskaya et al. 2008). FAK contains also a proline-rich region between the catalytic domain and the FAT sequence providing docking sites for SH3 domain-containing proteins including p130^{Cas}, GRAF and ASAP1 (Dunty et al. 2004, Tilghman, Parsons 2008). The interaction between Y397-activated FAK and Src kinases leads to a cascade of tyrosine phosphorylation of multiple sites in FAK, as well as other signaling molecules including phosphatidylinositol 3-kinase (PI3), Akt, growth receptor -bound proteins 2 and 7 (Grb2 and 7), Shc, and other proteins resulting in the cytoskeletal changes and activation of other downstream signaling pathways (Cary, Guan 1999, Golubovskaya et al. 2008).

Table 1. Summary of previous studies on inhibiting FAK signaling. The FAK inhibition effects on osteogenesis and adipogenesis.

Cell type	Signaling pathway	Inhibition method	Results	Reference
hBMSCs	FAK-ERK1/2	FAK-specific siRNA (50µM or 100µM) and MEK1 inhibitor PD98059 (50µM)	FAK inhibition using FAK-specific siRNA knocked down the ERK1 and ERK2 phosphorylation and suppressed the levels of osterix, ALP activity and matrix mineralization. MEK inhibition using PD98059 reduced activity of Runx2/Cbfa-1. MEK inhibitor and FAK knockdown together resulted in further decrease in Runx2/Cbfa-1 phosphorylation.	Salasznyk et al., 2007
hBMSCs	FAK-ERK1/2	FAK inhibitor PF-573228 (100nM)	Type I collagene and osteocalcin gene expressions were significantly decreased and the mineralization was decreased. Inhibition of FAK also down-regulated ERK1/2 activation.	Shih et al., 2011
hBMCSs	FAK	FAK inhibitor PF-573228 (10µM)	FAK inhibition with PF-573228 promoted the adipogenesis. Gene expression of PPAR γ and the formation of lipid droplets were increased compared to the untreated samples in adipogenic differentiation medium.	Xu et al.,2014
hDFCs	FAK-ERK1/2	FAK inhibitor PF-573228	The inhibition of FAK repressed the activation of ERK signaling and the expression of osteogenic markers ALP and osteopontin.	Viale-Bouroncle et al., 2014b

Abbreviation: hDFCs, human dental follicle cells.

FAK has an important role in transmitting a cell survival signal. Inhibition of FAK can induce apoptosis and the overexpression of FAK can prevent anoikis (Schaller 2001), anoikis being apoptosis induced by lack of correct cell-ECM attachment (Gilmore 2005). Due to the cell survival supporting role of FAK, it is easily understandable that FAK is overexpressed in many types of tumors (Golubovskaya, Cance 2007, Golubovskaya et al. 2008, Tilghman, Parsons 2008). Tumor types mentioned in the literature include breast, colon, prostate, thyroid, ovarian and mesenchymal tumors (Schaller 2001, Golubovskaya, Cance 2007). The invasivity of the tumor has also been linked to FAK,

with a correlation between increased FAK expression and the aggressive metastatic tumors (Golubovskaya, Cance 2007, Roberts et al. 2008).

The effect of FAK-mediated signaling on the differentiation potential of MSCs has been evaluated with FAK inhibition studies. FAK inhibition by a FAK-specific inhibitor, PF-573228 or FAK silencing using FAK-specific siRNA resulted in decreased FAK activation and consequently reduced levels of osteogenic differentiation markers. In addition, the inhibition of FAK also down-regulated ERK1/2 phosphorylation (Salasznyk et al. 2007, Shih et al. 2011, Viale-Bouroncle, Gosau & Morscheck 2014b). FAK has been shown to work as a negative regulator of adipogenesis. FAK inhibition causes increased expression of adipogenic markers such as PPAR γ and promotes the formation of lipid droplets (Xu, Ju & Song 2014). Table 1 summarizes the inhibitor studies mentioned above.

Mitogen-activated protein kinases

In mammalian cells, mitogen activated protein kinase (MAPK) family consists of three group members ERK (extracellular signal-regulated kinase), JNK (c-Jun N-terminal kinase) and p38 (p38-reactivating kinase). ERK, JNK and p38 MAP kinases are structurally related and have similar kinase cascade pathways. Despite the similarities, the pathways are distinctly regulated: they are activated by different extracellular stimuli and have distinct substrates. (Jaiswal et al. 2000, Biggs, Dalby 2010, Zhao et al. 2012) JNK and p38 are activated by cytokines, environmental stress, ultraviolet and ionizing radiation while ERKs are activated primarily by growth factors (Jaiswal et al. 2000).

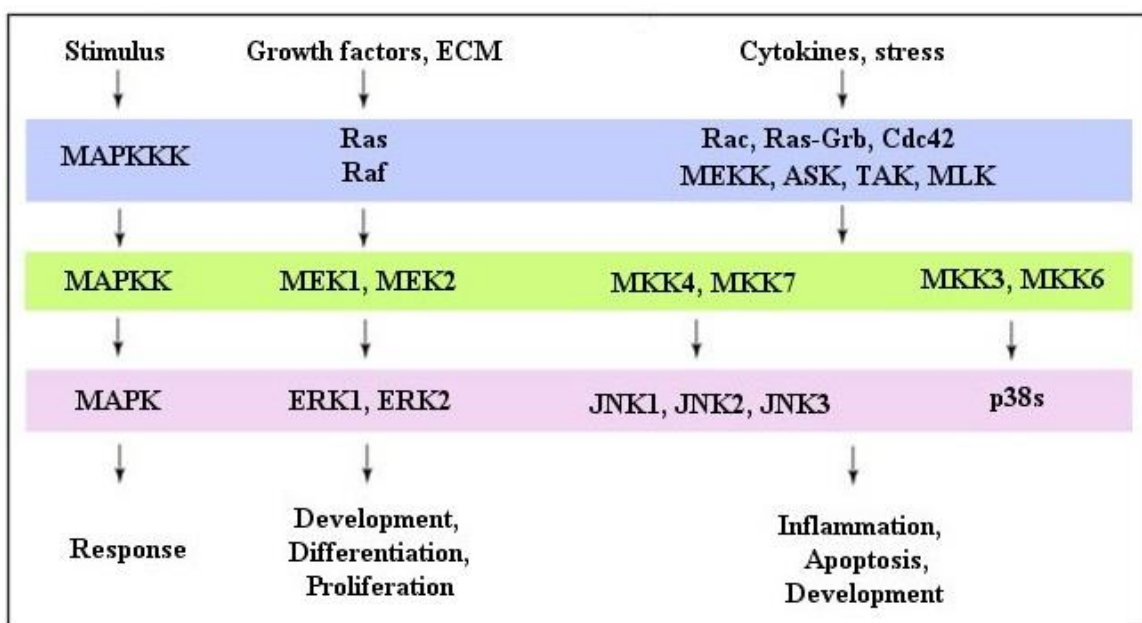


Figure 4. Small GTPases mediate extracellular signals via MAPK signaling pathways. A subsequent activation of MAPKK by MAPKKK triggers MAPK induced cellular responses and gene transcription. Modified from (Fantini et al. 2006).

MAPKs are essential proteins in the regulation of gene expression, mitosis, metabolism, survival, motility, apoptosis, proliferation and differentiation (Zhao et al. 2012). MAPK pathways are involved in MSC osteogenic commitment, especially ERK signaling been proven critical in the osteogenesis (Jaiswal et al. 2000, Xiao et al. 2000, Shih et al. 2011). MAPKs play a critical role in transmitting intracellular signaling of osteoinductive bone morphogenetic proteins (BMP2, BMP4 and BMP9) but their effect varies in different MAPK pathways (Zhao et al. 2012). ERK, JNK and p38 cascades are also known to be activated by mechanical stimuli (Kilian et al. 2010). MAPK signaling pathways are presented in Figure 4. ERK signaling is presented in more detail below since the effect of inhibiting the pathway on differentiation potential of hASCs was investigated in the present study.

MEK-ERK signaling

Activation of growth factor stimulated receptor tyrosine kinases or binding of integrin receptors to ECM proteins result in the activation of the small GTPase Ras (Jaiswal et al. 2000, Schindeler, Little 2006). Ras has many downstream targets including Raf family kinases (A-Raf, B-Raf and C-Raf) (Schindeler, Little 2006, McKay, Morrison 2007). Ras-Raf interaction is a first step for Raf activation followed by a highly complex process, involving the membrane localization, cycles of phosphorylation/dephosphorylation and protein interactions (McKay, Morrison 2007). The Raf kinases have restricted substrate specificity (Roskoski 2010). They are known to catalyse the activation of MEK1 and MEK2 kinases (MEK being an abbreviation of Mitogen-activated protein kinase/MAP kinase) (Roberts, Der 2007, Roskoski 2010). MEK1/2 kinases are dual-specificity kinases that activate their substrates ERK 1 and ERK 2 by phosphorylating both serine/threonine and tyrosine residues (Jaiswal et al. 2000, Roberts, Der 2007). ERK1 and ERK2, 44 and 42 kDa proteins respectively (Biggs, Dalby 2010), were the first MAPK family members to be discovered. MEK-ERK signaling pathway is activated primarily by the activation of receptor tyrosine kinases or integrin-mediated signaling including focal adhesion proteins (Schlaepfer, Jones & Hunter 1998, Schindeler, Little 2006, McKay, Morrison 2007) as presented in Figure 5.

The ERK signaling pathway is responsible for a wide range of biological processes including proliferation and differentiation events (Jaiswal et al. 2000), cellular metabolism, cell migration and survival (Takacs-Vellai 2014). Mutations that affect ERK signaling induce tumorigenesis in addition to some human syndromes (Takacs-Vellai 2014). ERKs are involved in MSC differentiation by working as a central molecular switch between adipogenic and osteogenic lineage commitment (Jaiswal et al. 2000). That said, there has been some debate about the role of Ras-MAPK in osteogenesis, with robust evidence demonstrating that bone formation may also be hindered as

committed osteoprogenitor cells have a choice of either proliferation or further differentiation, with Ras-MAPK being a key regulator of that balance (Schindeler, Little 2006). The major regulator of osteoblast-specific gene expression, Runx2 is phosphorylated and activated by ERK *in vitro* (Xiao et al. 2000, Shih et al. 2011). Runx2 controls osteoblast-specific genes (ALP, osteopontin, osteocalcin) and bone differentiation and formation in osteoprogenitor cells (Biggs, Dalby 2010). ERK controls also the key regulator of adipogenesis, PPAR γ , through phosphorylation (Jaiswal et al. 2000, Levi, Longaker 2011). Overexpression of MEK1 has shown to increase osteocalcin gene expression and Runx2 whereas the negative mutants of MEK decrease the osteogenic gene expression (Ge et al. 2009).

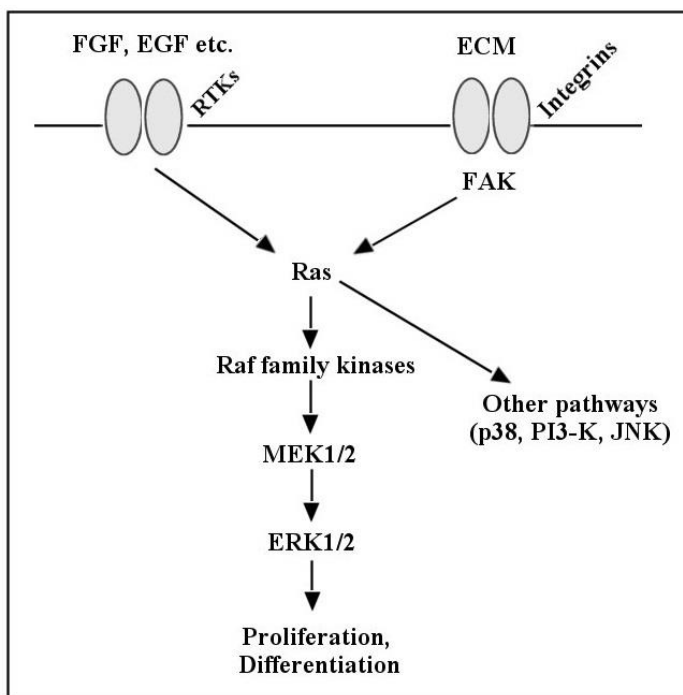


Figure 5. Receptor tyrosine kinase (RTK) or integrin-activated MEK-ERK pathway. Ras GTPase activates its downstream target Raf, that catalyzes the activation of MEK1/2. MEK1/2 kinases activate ERK1/2 by dual phosphorylation. ERK signalling leads to multiple functions such as proliferation and differentiation. Adapted from Schindeler and Little 2006.

The importance of MEK-ERK signaling to stem cell differentiation has been comprehensively studied with inhibitors targeted to the pathway (summarized in Table 2). ERK inhibition of hASCs and hBMSCs by inhibitor PD98059 blocks the osteogenic differentiation in a dose-dependent manner as seen in decreased ALP activity and mineralization (Jaiswal et al. 2000, Liu et al. 2009, Gu et al. 2011). On the contrary, adipogenic differentiation of hASCs and hBMSCs is increased concentration dependently with PD98059 inhibitor as seen by lipid droplet accumulation and increased the expression of adipogenesis-relative genes (Jaiswal et al. 2000, Liu et al. 2009). PD98059 repressed the activity of ALP also in dental follicle cells (Viale-Bouroncle, Gosau & Morsczeck 2014a). ERK 1/2 inhibitor FR180204 and the JNK 1/2/3 inhibitor SP600125 caused a decrease in osteogenesis with a concurrent increase in adipogenesis demonstrating the importance of these cascades in osteoblast differentiation (Kilian et al. 2010). Also MEK-ERK inhibitor U0126 blocked the osteogenic

differentiation in hBMSCs (Shih et al. 2011). On the contrary to these results, the inhibition of BMP9 activated ERK1/2 with PD98059 in mouse mesenchymal progenitor cells increased osteogenesis (Zhao et al. 2012).

Table 2. Summary of previous studies on inhibiting MEK-ERK signaling. The effect of MEK-ERK inhibition on osteogenesis and adipogenesis.

Cell type	Signaling pathway	Inhibition method	Results	Reference
hASCs	ERK1/2	MEK inhibitor PD98059	Osteogenic differentiation was blocked in a dose-dependent manner: there was a decrease in ALP activity, extracellular calcium deposition, osteocalcin and osteoblast specific gene expression. The MEK inhibition led to adipogenic differentiation as seen by lipid droplet accumulation and activation of adipogenesis-relative genes.	Liu et al., 2009
hASCs	ERK1/2	MEK inhibitor PD98059 (25µM and 50µM)	MEK inhibition caused concentration-dependent inhibition on ALP activity. Extracellular deposition of calcium was weakened with inhibitor addition and secretion of osteocalcin was suppressed.	Gu et al., 2011
hBMSCs	ERK	MEK inhibitor PD98059 (10µM, 25µM or 50µM)	Inhibition of ERK blocked the osteogenic differentiation in dose-dependent manner, shown as reduction of ALP activity and mineralization. Adipogenic differentiation was increased as seen from the expression of adipose-specific mRNAs PPARγ2, aP2 and lipoprotein lipase.	Jaiswal et al., 2000
hBMSCs	ERK1/2	ERK 1/2 inhibitor FR180204 (6µM)	ERK inhibition caused decrease in osteogenesis with a concurrent increase in adipogenesis	Kilian et al., 2010
hBMSCs	ERK1/2	MEK/ERK inhibitor U0126 (10 µM)	The inhibition of MEK-ERK pathway led to decreased type I collagen gene expression and the extent of mineralization.	Shih et al., 2011
MC3T3-E1	MAPK pathway	MEK inhibitor PD98059 (50µM, 100µM or 150µM)	In mouse preosteoblast cells, PD98059 inhibited ECM-dependent up-regulation of the osteocalcin gene promoter.	Xiao et al., 2000
MPCs	MAPK pathways, p38 and ERK	p38 inhibitor SB203580 and ERK 1/2 inhibitor PD98059 or RNAi	In mouse mesenchymal progenitor cells, the inhibition of p38 dramatically reduced BMP9-induced osteogenic differentiation and Smads signaling. Inhibition of ERK1/2 enhanced BMP9-induced osteogenic differentiation and Smads signaling, and increased BMP9-induced bone formation.	Zhao et al., 2012

Abbreviations: MC3T3-E1, mouse preosteoblast cells; MPCs, mouse mesenchymal progenitor cells.

The role of FAK in ECM-induced signaling in the activation of MEK-ERK signaling pathway has been proposed. Salasnyk and collaborators studied in 2007 the effect of FAK activated ERK1/2 signaling on the osteogenic differentiation in BMSCs. Their study revealed the importance of both FAK and ERK1/2 signaling mechanisms to the osteogenic lineage commitment of MSCs. FAK inhibition using FAK-specific siRNA knocked down the ERK1 and ERK2 phosphorylation

demonstrating that the ERK phosphorylation occurred through FAK signaling pathway (Salasznyk et al. 2007). Laminins are ECM proteins (the main constituent of the basal lamina) that induce osteogenesis in MSCs by binding integrins and activating FAK-ERK signaling pathways (Viale-Bouroncle, Gosau & Morsczeck 2014a).

2.4 Cell morphology as a regulator of cell differentiation

Cell shape is determined by cellular tension. The cellular tension is derived from forces generated by the contraction of the cytoskeleton within the cell and adhesions to the ECM or another cells that anchors the cellular contraction (Tilghman, Parsons 2008). The cytoskeleton of cells consists of actin, myosin, microtubules and intermediate filaments (Yim, Sheetz 2012). Actin filaments are cross-linked by myosin II which is the primary motor protein assembly that is responsible for generating cytoskeletal tension (Tilghman, Parsons 2008, Kilian et al. 2010, Chen, Jacobs 2013, Kuo 2013). Microtubules are normally arranged in spindle-like formation in mesenchymal stem cells and are re-organized during cell division and migration. The regulation of microtubule dynamics relies on a precise balance between microtubule growth, stabilization, and depolymerisation (Schofield, Steel & Bernard 2012).

Cytoskeletal components, particularly actin and its downstream effectors, are strong mediators of hMSC differentiation toward the osteoblastic lineage (Treiser et al. 2010). Several studies have emphasized the role of actomyosin contractility in promoting an osteogenic fate in MSCs (McBeath et al. 2004, Kilian et al. 2010). Kilian and co-workers used an inhibitor of myosin II (blebbistatin) to directly inhibit the contractility of the cells resulting in a decrease in osteogenesis and an increase in the adipogenesis (Kilian et al. 2010). Actomyosin contractility stimulates MAPK cascades and Wnt signaling to regulate osteoblast differentiation (Kilian et al. 2010). The canonical Wnt pathway is an important mediator in regulating cell proliferation and differentiation functioning through β -catenin (Hartmann 2006). In addition, cytoskeletal contractility regulates the FAK-mediated activation of Rho-ROCK signaling pathways (Tilghman, Parsons 2008), as described below in Chapter 2.4.1.

The role of microtubules in the differentiation of MSC is considered minor in comparison with actin cytoskeleton although it has been studied that the disruption of microtubule structure may increase the speed of differentiation (Mathieu, Lobo 2012). Integrins regulate a number of other signaling proteins that target microtubule dynamics, such as the Rho family of GTPases, which influence microtubule growth and stability (Colello et al. 2012). Cell migration can be increased by Rho activated ROCK signaling through ROCK substrate tubulin polymerization promoting protein 1 (TPPP1). TPPP1 phosphorylated by ROCK results in a decreased cellular level of acetylated tubulin and thereby increased cell motility (Schofield, Steel & Bernard 2012). Integrins regulate microtubule

nucleation also by promoting the formation of androgen receptor-Src signaling complexes to activate the MEK/ERK signaling pathway (Colello et al. 2012).

Cells undergo a number of morphological changes during the lineage commitment. Additionally, studies have demonstrated that cell shape in turn regulates the differentiation (Treiser et al. 2010). Studies of McBeath and co-workers (2004) and Kilian and co-workers (2010) demonstrate the effect of geometrical cues on guiding the lineage commitment. McBeath and co-workers used micro-patterns to regulate the culture area of MSCs. They found out that cell density has an effect on cell shape: MSCs cultured at relatively low densities were more spread and the differentiation was guided towards osteogenesis. Similar results were obtained in the study of Kilian and co-workers: MSCs grown in flower-like pattern with rounded edges favored adipogenesis while star-like pattern with sharp edges had a preference for an osteogenic fate. In addition, cells in star shapes showed larger focal adhesions and more stress fibers than cells in flower shapes. Cells in star shapes increased the levels of the noncanonical Wnt signaling molecules and their downstream effectors such as ERK and JNK leading to an elevated expression of master osteoblast regulators.

2.4.1 ROCK signaling pathway

Rho family GTPases are central regulators of cytoskeletal dynamics and contractility in many cells (Riento, Ridley 2003, McBeath et al. 2004, Tilghman, Parsons 2008). Rho, Rac and Cdc42 are the three best characterized members of the Rho family (Yim, Sheetz 2012). Rho family of GTPases mediate many of the integrin-dependent modifications of the actin cytoskeleton (Guo, Giancotti 2004, Hehlhans, Haase & Cordes 2007, Colello et al. 2012). The activation of RhoA can be FAK-mediated as well (Tilghman, Parsons 2008). RhoA is activated by multiple guanine nucleotide exchange factors (GEFs), several of which have been shown to be downstream of FAK signaling (Tilghman, Parsons 2008). RhoA regulate actin cytoskeleton through its downstream effector, ROCK, which stands for Rho-associated coiled-coil-containing kinase (Hehlhans, Haase & Cordes 2007), or simply Rho kinase (Riento, Ridley 2003). ROCKs are also involved in the regulation of the cell cycle, cell motility and invasion (Schofield, Steel & Bernard 2012).

ROCKs (isoforms ROCKI and ROCKII) are 160kDa protein serine/threonine kinases consisting of N-terminal kinase domain, coiled-coil forming region and C-terminal functional motifs such as Rho-binding domain, pleckstrin homology (PH) domain and ROCK kinase activity inhibiting autoinhibitory region. Rho binding enhances ROCK kinase activity and disrupts the negative regulatory interaction. (Riento, Ridley 2003) ROCKs work as a signal transmitters by phosphorylating various substrates that are involved in actin-filament assembly and contractility, such as myosin light chain (MLC) phosphatase, LIM motif-containing protein kinase (Riento, Ridley 2003,

Schofield, Steel & Bernard 2012) and ERM (ezrin-radixin-moesin) proteins (Riento, Ridley 2003). ROCK stimulates actomyosin contractility by sustaining MLC phosphorylation and by stimulating actin polymerisation to contractile stress fibres (Riento, Ridley 2003, Tilghman, Parsons 2008). LIM kinase phosphorylation inhibits cofilin-mediated actin depolymerisation resulting in an increase in the amount of actin filaments whereas ERM proteins function as linkers between actin filaments and cell surface proteins (Riento, Ridley 2003).

Table 3. Summary of previous studies on inhibiting ROCK signaling. The inhibitor effects on osteogenesis and adipogenesis.

Cell type	Signaling pathway	Inhibition method	Results	Reference
hASCs	ROCK	ROCK inhibitor Y-27632 (10 μ M)	Wnt5a induced changes in osteogenic markers via activation of ROCK. Y-27632 alone did not affect RUNX2 or osteocalcin gene expression, but down-regulated the effect of Wnt5a on RUNX2 and osteocalcin gene expression.	Santos et al., 2010
hBMSCs	ROCK	ROCK inhibitor Y-27632 (2 μ M)	ROCK inhibition caused decrease in osteogenesis with a corresponding increase in cells with adipocyte phenotypes.	Kilian et al., 2010
hBMSCs	ROCK-FAK-ERK1/2	ROCK inhibitor Y-27632 (5 μ M)	Type I collagen gene expression and the extent of mineralization were decreased in hBMSCs treated with ROCK inhibitor. Inhibition of ROCK down-regulated both FAK and ERK1/2 activation.	Shih et al., 2011
hMSC	Rho-ROCK	ROCK inhibitor Y-27632 (10 μ M) and myosin II inhibitor blebbistatin (50 μ M)	ROCK inhibition with Y-27632 led to decreased ALP activity and increased lipid production. Both inhibitors blocked osteogenesis demonstrating the significance of cytoskeletal tension in hMSC commitment to osteoblast fate.	McBeath et al., 2004
MEFs and MC3T3-L1	Rho-ROCK	ROCK inhibitor Y-27632 (10 μ M)	ROCK guided the lineage commitment to adipogenesis or myogenesis: inhibition of Rho GTPase activity was necessary for the adipogenic differentiation program. Active Rho-ROCK, on the other hand, was essential to myogenesis.	Sordella et al., 2003
C3H10T1/2	ROCK	Y-27632 (10 μ M), cytochalasin D (1 μ M) and blebbistatin (50 μ M)	Inhibition of ROCK with Y-27632, inhibition of myosin II with blebbistatin and disruption of actin polymerization with cytochalasin D resulted in lack or disruption of actin cytoskeleton leading to decreased Runx2 expression levels, demonstrating decreased osteogenesis.	Arnsdorf et al., 2009

Abbreviations: MEFs, mouse embryo-derived fibroblasts; MC3T3-L1, mouse preadipocyte cells; C3H10T1/2, murine MSCs.

The Rho-ROCK signaling pathway is essential in biophysically induced stem cell differentiation (Arnsdorf et al. 2009, Yim, Sheetz 2012). The pathway works as a molecular switch that controls stem cell lineage commitment. Changing RhoA activity by affecting cell shape can switch hMSC commitment to osteoblasts or adipocytes (McBeath et al. 2004). Several studies have

demonstrated this effect (summarized in Table 3): ROCK inhibition causes a decrease in osteogenesis with a corresponding increase in the number of cells with adipocyte phenotypes demonstrating the importance of ROCK signaling in osteogenic lineage commitment (McBeath et al. 2004, Kilian et al. 2010, Shih et al. 2011). ROCK is also a downstream effector of noncanonical Wnt signaling and triggers osteogenesis through a myosin-generated tension feedback loop (Kilian et al. 2010). In hASCs, Wnt5a induced osteogenic differentiation was decreased as seen in the down-regulation of Runx2 and osteocalcin gene expression when ROCK was inhibited with Y-27632 (Santos et al. 2010). In addition, lineage commitment to adipogenesis and myogenesis is similarly regulated. Rho-ROCK activity is essential to myogenesis, and in turn, inhibition of Rho GTPase activity is necessary for the adipogenic differentiation program (Sordella et al. 2003). The ROCK inhibitor reduces tumour cell spreading and may be thus used as a therapeutic agent (Riento, Ridley 2003). The Y-27632 inhibitor has been found to support the viability of multipotent stem cells (Watanabe et al. 2007, Pakzad et al. 2010, Zhang et al. 2011), but a recent study by Lamas and co-workers renounces this effect on hASCs. The effect of ROCK inhibition on hASCs was the opposite: Y-27632 decreased cell viability in dose-dependent manner (Lamas et al. 2015).

2.4.2 Mechanotransduction

Mechanotransduction is the process by which physical stimuli are converted into biochemical responses (Biggs, Dalby 2010, Yim, Sheetz 2012, Chen, Jacobs 2013). Stem cells are able to sense their mechanical environments through various mechanosensors including the cytoskeleton, focal adhesions, and primary cilia (Mathieu, Loba 2012, Chen, Jacobs 2013). Matrix stiffness is one such biophysical cue that cells respond to via initiation of mechanotransduction cascades (Shih et al. 2011). Focal adhesions work as integrin-mediated mechanosensors responding to mechanical stimuli generated by cell-ECM interactions (Yim, Sheetz 2012, Kuo 2013). FA recruitment of both the cytoskeletal adapter protein vinculin and FAK are myosin II and ECM stiffness dependent (Pasapera et al. 2010). Myosin II activity promotes the FAK-Src -mediated phosphorylation of paxillin and vinculin association with paxillin to drive FA maturation (Pasapera et al. 2010). Extracellular mechanical forces can promote the intracellular tension in a positive feedback loop through focal adhesion maturation and the RhoA mediated formation of stress fibers (Kuo 2013).

Mechanical forces play an important role in MSC lineage commitment (Shih et al. 2011, Mathieu, Loba 2012, Chen, Jacobs 2013). ECM stiffness that mimics developing bone results in higher levels of osteogenic phenotype (Shih et al. 2011). In addition, stable actin cytoskeleton is known to inhibit adipogenesis while adipogenesis is more likely with less-organized and less-stiff actin cytoskeleton (Mathieu, Loba 2012).

Several intracellular signal cascades are involved in mechanotransduction FAK and ROCK being the most pivotal (Riento, Ridley 2003, Pasapera et al. 2010, Shih et al. 2011). Rho-ROCK signaling is known to be a mechanotransducer of matrix stiffness during osteogenesis (Riento, Ridley 2003, Shih et al. 2011). Mechanically activated ROCK and FAK function also by subsequent activation of ERK1/2 (Shih et al. 2011) to increase osteogenic gene expression and mineralization in hMSCs (Chen, Jacobs 2013).

3. AIMS OF THE PRESENT STUDY

Adipose stem cells have proven to be an attractive MSC source for regenerative medicine and tissue engineering applications due to their various advantages, such as their multipotency and abundance. However, the intracellular signaling events regulating the differentiation of human adipose stem cells are not yet fully understood. The focus of the present study is in the mechanisms related to hASC adhesion and the cytoskeletal dynamics. The aim is to shed light on the cell attachment and morphology -related regulation of hASC differentiation. Three signaling pathways known to be involved in differentiation were chosen for the study based on the existing literature: cell attachment-mediated FAK and MEK-ERK signaling and morphology-related ROCK signaling pathways. Signaling cascades involving signaling proteins ROCK, FAK and ERK1/2 were studied in the context of adipogenic and osteogenic differentiation potential. To conduct the study, the signal transduction of the aforementioned pathways were inhibited with specific inhibitor molecules.

Specific aims of the study:

- 1) To evaluate the viability of hASCs with different concentrations of ROCK, FAK and MEK kinase inhibitors in the cell culture.
- 2) To study the effect of the specific inhibitors on hASC morphology and cell adhesion.
- 3) To evaluate the effect of these signaling cascades on the osteogenic and adipogenic differentiation potential of hASCs.

4. MATERIALS AND METHODS

4.1 The hASC culture

Four human adipose stem cell lines were used in this study: HFSC 1/13, HFSC 8/13, HFSC 9/13 and HFSC 1/14. The hASCs used had been previously isolated from adipose tissue samples of four female donors (aged 33-55) by the Adult stem cell group. The tissue samples had been collected from patients with their written informed consent in accordance with the Ethics Committee of the Pirkanmaa Hospital District, Tampere, Finland (ethical approval R03058).

Isolation of the adipose stem cells was performed by using a mechanical and enzymatic method described previously (Zuk et al. 2001, Gimble, Guilak 2003, Bunnell et al. 2008). Briefly, the adipose tissue samples were manually cut into small fragments and digested with collagenase type I (Gibco®/Thermo Fisher Scientific™, Waltham, Massachusetts, USA) in 37°C water bath under shaking conditions. After digestion, the hASCs were separated from the surrounding tissue by centrifugation and filtration. The isolated hASCs were resuspended in basic medium (BM) consisting of Dulbecco's Modified Eagle Medium/Ham's Nutrient Mixture F-12 (DMEM/F-12 1:1; Gibco®/Thermo Fisher Scientific™) supplemented with 5% Human serum (HS; PAA Laboratories GmbH, Pasching, Austria), 1% L-alanyl-L-glutamine (GlutaMAX™; Gibco®/Thermo Fisher Scientific™) and 1% antibiotics (Pen/Step 10000U Penicillin/ml, 10000U Streptomycin/ml; Lonza, Basel, Switzerland). The medium was sterile filtered before usage with VacuCap® 90 PF Filter unit with w/0.8/0.2µm Supor® membrane (PALL Corporation; Port Washington, New York, USA). The isolated cells were seeded into T-75cm² polystyrene culture flasks (Nunc™ Delta treated flask; Thermo Fisher Scientific™). This passage was designated as passage 0.

The hASCs were maintained and expanded in T-75cm² culture flasks in the cell incubator (Heracell™ 150; Heraeus®, Hanau, Germany) at 37°C. The cells were passaged after reaching 70-80% confluency. The cells were detached by using an animal origin free recombinant enzyme for detaching mammalian cells (TrypLE™ Select (1X); Gibco®/Thermo Fisher Scientific™). The expanded cells were cryo-preserved in gas phase nitrogen by resuspending the centrifuged cell pellet into freezing solution containing HS supplemented with 10% dimethyl sulfoxide (DMSO Hybri-Max™; Sigma-Aldrich, St. Louis, Missouri, USA). Prior to the experiments, the hASCs were thawed and expanded in BM. The workflow of the present study is presented in Figure 6.

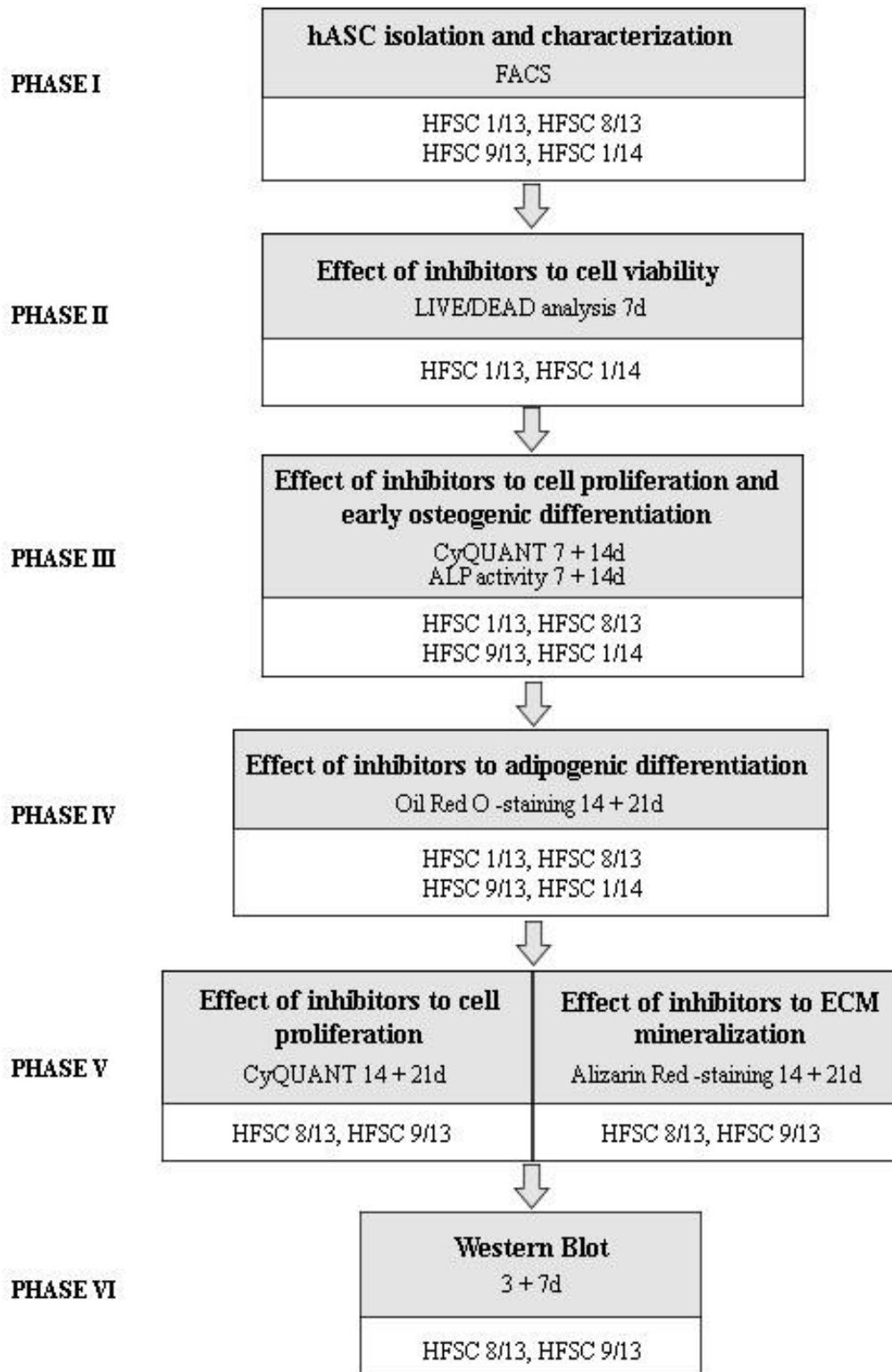


Figure 6. The workflow of the study. The figure demonstrates the analyses done in the study and the cell lines (HFSC) used in each analysis. The experiments done in the study were divided into phases I-VI.

4.2 Flow cytometric surface marker expression analysis

The hASC lines used in this study were characterized by their immunophenotype. The surface marker expression of HFSC 1/13, HFSC 8/13, HFSC 9/13 and HFSC 1/14 cell lines at passage 1 was analyzed with flow cytometry (fluorescence-activated cell sorting, FACS) (FACSAria™; BD Biosciences, Erembodgem, Belgium).

Monoclonal antibodies against CD3-PE, CD14-PE-Cy7, CD19-PE-Cy7, CD45R0-APC, CD54-FITC, CD73-PE, CD90-APC (BD Biosciences Franklin Lakes, New Jersey, USA), CD11a-APC, CD80-PE, CD86-PE, CD105-PE (R&D Systems, Minneapolis, Minnesota, USA), CD34-APC and HLA-DR-PE (ImmunoTools, Friesoythe, Germany) were used. The FACS analysis was performed on 10 000 cells per sample and the positive expression was defined as the fluorescence level greater than 99% of the comparable unstained cell sample.

4.3 Culture conditions of the hASCs in the experiments

The experiments were conducted at passages 3-5. The cells were plated to surface attachment enhancing Corning® CellBIND® (Corning Incorporation, Corning, New York, USA) polystyrene plates in basic medium. To study the role of ROCK, FAK and ERK signaling proteins in hASC differentiation, protein inhibitors to these targets were used. The protein inhibitors used were respectively ROCK1 inhibitor Y-27632 2HCl (Selleck Chemicals, Houston, Texas, USA), FAK inhibitor PF-562271 (Selleck Chemicals) and MEK inhibitor PD98059 (Calbiochem®/EMD Millipore, Billerica, Massachusetts, USA). The inhibitor concentrations in the experiments are listed in Table 4. The concentrations of the inhibitors had been previously optimized by the Adult stem cell group.

Table 4. Inhibitor concentrations used in the experiments. Three inhibitor concentrations of each inhibitor were used in LIVE/DEAD®, CyQUANT®, ALP activity, Oil Red O and Alizarin Red analyses. One inhibitor concentration was chosen to the Western Blot analysis.

	LIVE/DEAD CyQUANT	ALP activity Oil Red O Alizarin Red	Western Blot
ROCK Inhibitor Y-27632 2HCl	10µM, 15µM, 25µM		15µM
FAK Inhibitor PF-562271	0,5µM, 2µM, 5µM		2µM
MEK Inhibitor PD98059	30µM, 40µM, 60µM		30µM

Effects of the inhibitors were evaluated in three different culture environments: basic medium (BM), osteogenic medium (OM) and adipogenic medium (AM). Components of the differentiation media are presented in Table 5. Osteogenic medium (Table 5) consisted of basic medium supplemented with 200 μ M L-ascorbic acid 2-phosphate, 10mM β -Glycerophosphate, and 5nM Dexamethasone (the above-named reagents by Sigma-Aldrich). Adipogenic medium (Table 5) consisted of basic medium supplemented with 1 μ M Dexamethasone (DEX; Sigma-Aldrich), 100nM Insulin (Insulin, Human recombinant Zinc; Thermo Fisher Scientific™), 17 μ M Pantothenate (Sigma-Aldrich) and 33 μ M Biotin (Sigma-Aldrich). 0,25mM IBMX (3-isobutyl-1-methylxanthine; Sigma-Aldrich) was applied to the samples when inducing adipogenic differentiation. The differentiation media were sterile filtered before usage with VacuCap® 90 PF Filter unit w/0.8/0.2 μ m Supor® membrane (PALL Corporation). The media and the inhibitors were changed every three or four days during the culture and the experiments.

Table 5. 5% HS PAA Osteogenic medium (OM) and Adipogenic medium (AM).

Components	Quantity (OM)	Quantity (AM)
DMEM/F-12 1:1 1X		
Human serum	5 %	5 %
GlutaMAX	1 %	1 %
Pen/Strep	1 %	1 %
L-ascorbic acid 2-phosphate	200 μ M	-
β -Glycerophosphate	10mM	-
Dexamethasone	5nM	1 μ M
Insulin	-	100nM
Pantothenate	-	17 μ M
Biotin	-	33 μ M
IBMX	-	0,25mM

4.4 Cell attachment and viability

The effect of inhibitors on the attachment and viability of two of the hASC lines (HFSC 1/13 and HFSC 1/14) was evaluated using LIVE/DEAD® assay (Thermo Fisher Scientific™) at 7 day time point. The assay is based on two fluorescent dyes: green-fluorescent Calcein-AM (CaAM) indicating living cells and red-fluorescent Ethidium homodimer-1 (EthD-1) demonstrating necrotic cells. CaAM is enzymatically converted into calcein in the cytoplasm of living cells whereas EthD-1 enters the cells having damaged membranes and exhibits red fluorescence when binding nucleic acids (Sanfilippo et al. 2011).

For the experiment, 500 cells/well were plated in BM to 24-well Corning® CellBIND® plates. On the following day differentiation media supplemented with inhibitors were added to the plates. Different culture environments of the analysis are presented in Table 6. There were duplicates of each condition. The media and inhibitors were changed once during the 7 day culture period.

The protocol used in the analysis was a simplified version of the original manufacturer's instruction. Briefly, at 7 day time point the media were removed from the wells and the cells washed with 1X PBS (Dulbecco's Phosphate Buffered saline; Lonza). Working solution containing 0,25µM EthD-1 and 0,5µM CaAM in 1X PBS was added to the wells and incubated for 30 minutes at room temperature (RT). After incubation, the working solution was replaced with fresh 1X PBS solution. The fluorescence was visualized using a fluorescence microscope described in Chapter 4.10.

Table 6. Different culture environments of the experiments. Basic medium, osteogenic medium and adipogenic medium controls, and the media supplemented with three concentrations of each inhibitor.

BM	BM + ROCK 10µM	BM + ROCK 15µM	BM + ROCK 25µM	BM + FAK 0,5µM	BM + FAK 2µM	BM + FAK 5µM	BM + MEK-ERK 30µM	BM + MEK-ERK 40µM	BM + MEK-ERK 60µM
OM	OM + ROCK 10µM	OM + ROCK 15µM	OM + ROCK 25µM	OM + FAK 0,5µM	OM + FAK 2µM	OM + FAK 5µM	OM + MEK-ERK 30µM	OM + MEK-ERK 40µM	OM + MEK-ERK 60µM
AM	AM + ROCK 10µM	AM + ROCK 15µM	AM + ROCK 25µM	AM + FAK 0,5µM	AM + FAK 2µM	AM + FAK 5µM	AM + MEK-ERK 30µM	AM + MEK-ERK 40µM	AM + MEK-ERK 60µM

4.5 CyQUANT® cell proliferation assay

Proliferation of the hASC lines used in this study was assessed using a CyQUANT® cell proliferation assay kit (Molecular probes®; Thermo Fisher Scientific™) which is a method for measuring the total DNA amount per sample. CyQUANT GR Dye expresses fluorescence when bound to cellular nucleic acids (Jones et al. 2001). As in LIVE/DEAD® analysis, the cells were plated in 24-well Corning® CellBIND® plates at a density of 500 cells/well and incubated 24h in BM. The culture conditions used are presented in Table 6. There were 3 wells of each condition. The media and the inhibitors were changed every 3 or 4 days.

At 7, 14 and 21 day time points the cells were lysed with 0,1% Triton-X-100 buffer (Sigma-Aldrich). After freeze-thaw cycle the samples and Triton-X-100 blank were pipetted into flat bottom 96-well plates (Nunc™; Thermo Fisher Scientific™). Working solution consisting of Cell lysis buffer (20X concentrate) and GR-Dye (CyQUANT®GR Dye 400X concentrate in DMSO) in deionized water was added to the wells and fluorescence was measured with a microplate reader (Wallac Victor

1420 Multilabel Counter; Perkin Elmer, Waltham, Massachusetts, USA) at 480/520 nm. The fluorescence emission of Triton-X-100 was subtracted from the emission of the samples.

4.6 Oil Red O fat vacuole staining

The fat vacuole formation of four hASC lines was studied using Oil Red O method. hASCs were plated in 24-well Corning® CellBIND® plates as described in Chapter 4.4. There were duplicates of each culture condition, the culture conditions used are presented in table 6. The Oil Red O staining was done after 14 and 21 days of the culture.

For Oil Red O staining, after several washes with 1X PBS, the cells were fixed with 4% Paraformaldehyde (PFA; Sigma-Aldrich) for 1h at RT. Fixated cells were rinsed with deionized water and incubated for 4 minutes in 60% isopropanol (2-propanol; EMD Millipore) before adding the pre-filtered Oil Red O staining solution (Sigma-Aldrich). The staining solution was incubated for 10 minutes in room temperature. After several washing steps with deionized water, light microscope images of the wells were taken (described in chapter 4.10).

4.7 Alkaline phosphatase activity

The *in vitro* osteogenic differentiation potential of four hASC lines was evaluated quantitatively by measuring the alkaline phosphatase (ALP) activity at 7 and 14 day time points. ALP is an early marker of osteogenic differentiation. The method is based on a colorimetric reaction of ALP catalyzed cleavage of phosphate group from p-nitrophenyl phosphate under alkaline conditions. The reaction product p-nitrophenol has an intense yellow color which intensity is proportional to the catalytic concentration of ALP in the sample. (Tietz et al. 1983)

The analysis was done from the same samples as the analysis of cell proliferation. ALP activity was measured as follows. The samples in 0,1% Triton-X-100 were transferred to 96-well PCR plate (96-well Multiply® PCR plate; Sarstedt Nümbrecht, Germany), 0,1% Triton-X-100 was used as a blank. Working solution (preheated to 37°C) consisting of 1:1 10,8mM Phosphatase substrate (p-Nitrophenyl phosphate, disodium 40mg capsule; Sigma-Aldrich) in deionized water and 1,5M Alkaline buffer solution (Sigma-Aldrich) was added into the wells and the plates were incubated for 15 min at 37°C in the PCR-machine (Eppendorf, Hamburg, Germany). After incubation, the substrate reaction was halted by adding 1M Sodium hydroxide (NaOH; Sigma-Aldrich) into the wells. For measurement, the samples were transferred to flat bottom 96-well plates (Nunc™; Thermo Fisher Scientific™). The absorbance was measured with microplate reader (Wallac Victor 1420 Multilabel Counter; Perkin Elmer) at 405 nm. The mean absorbance value from Triton-X-100 was subtracted from the absorbance of the samples.

4.8 Mineralization

To further investigate the osteogenic differentiation potential of hASCs, the mineralization of the ECM of hASC lines (HFSC 8/13 and HFSC 9/13) was evaluated using Alizarin Red S staining protocol. For the experiment, cells were plated in 24-well Corning® CellBIND® plates at a density of 500 cells/well. The culture conditions used in the experiment are presented in Table 6. Corresponding samples were cultured for the cell proliferation analysis (CyQUANT®) for normalization of the Alizarin Red results. The highest concentration (25µM) of ROCK inhibitor was excluded from the experiment.

The analysis was executed quantitatively and qualitatively at 14 and 21 day time points. At each time point, the media were removed, cells rinsed gently with DPBS (Lonza) and fixed with 70% ethanol (Altia, Helsinki, Finland) for 1h at -20°C. After rinsing the cells with deionized water, the fixed cells were stained with 2% Alizarin Red S solution (Sigma-Aldrich) for 10 minutes. After washing steps with water and 70% ethanol, the dried cells were photographed (details given in chapter 4.10). The dye was extracted from the wells with 100mM Cetylpyridinium chloride monohydrate (Sigma-Aldrich) and the absorbance of the extracted dye was measured with a microplate reader (Wallac Victor 1420 Multilabel Counter; Perkin Elmer) at 544nm. The staining protocol was also executed to three empty wells that were used as blanks. The average absorbance value of blanks was subtracted from the absorbance values of the samples.

4.9 Western Blot analysis

For Western Blot analysis 30000 cells/well were plated in 6-well Corning® CellBIND® plates in BM and incubated 24h at 37°C. Starvation media containing 1% human serum (1% BM, 1% OM or 1% AM) were changed to the wells and the cells were incubated for another 24h. On the following day, fresh starvation media supplemented with 15µM ROCK, 2µM FAK or 30µM MEK inhibitors in addition to plain 1% BM, 1% OM and 1% AM that were used as controls were added to the wells. After 3 and 7 days of culture, the cells were washed with 1X PBS and lysed with 2X LAEMMLI sample buffer. The lysates were heated 5 min at 95°C, centrifuged shortly and stored at -20°C.

Before loading the samples into the wells of 10% SDS-PAGE gel the cell lysates were heated 5 min at 95°C and centrifuged shortly. 15µl of the samples were loaded for the analysis of the signaling proteins. For β-actin analysis only 3,5µl of samples were loaded. PageRuler™ Plus prestained protein ladder (Thermo Fisher Scientific™) was used as a molecular weight marker. Gels were electrophoresed (Mini-Protean®Tetra system; BIO-RAD; Hercules, California, USA) 120V until the loading buffer stain front was at the bottom of the gel. After electrophoresis, the proteins were transferred from gel to MetOH (EMD Millipore) activated PVDF (Amersham™Hybond™

0,45µm PVDF Blotting membrane; GE Healthcare, Little Chalfont, United Kingdom) membrane using 15V 300mA 1h (Trans-Blot®SD Semi dry transfer cell; BIO-RAD, Hercules, California, USA; Electrophoresis Power Supply EPS-601; GE Healthcare).

After transfer, the unspecific binding sites of the PVDF membrane were blocked with a blocking solution of 5% milk (Non-fat milk powder; Valio, Lapinlahti, Finland) in 0.05% Tween-TBS (Tween 20; Sigma-Aldrich).

Table 7. Primary antibodies used in Western Blot analysis.

Antibody	Host species	Dilution
anti-ERK2 (IgG) *	rabbit	1:1000
anti-pERK1/2 **	rabbit	1:2000
anti-FAK **	rabbit	1:1000
anti-pFAK **	rabbit	1:1000
anti-β-actin *	mouse	1:2000
anti-pMYL9 *	rabbit	1:500

* Santa Cruz Biotechnology, Dallas, Texas, USA

** Cell Signaling Technology, Danvers, Massachusetts, USA

Primary antibodies listed in Table 7 were used in immunodetection of the signaling proteins. The antibodies were diluted into blocking solution described above. The antibodies for phosphorylated proteins (pERK1/2, pFAK and pMYL9) were incubated overnight at +4°C, the other antibodies 2h at room temperature. The excess antibodies were rinsed from the membrane with 5 min washes in 1X TBS; 0,5% Tween-TBS; 0,1% Tween-TBS and 0,05% Tween-TBS. Horseradish peroxidase (HRP) -conjugated secondary antibodies (Goat anti-rabbit IgG HRP-linked antibody; Cell Signaling Technology, Danvers, Massachusetts, USA and Goat anti-mouse IgG HRP-conjugated antibody; Santa Cruz Biotechnology, Dallas, Texas, USA) were diluted 1:2000 in 5% milk blocking solution and incubated 1h RT. The excess antibodies were washed as after primary antibody incubation.

The proteins were visualized using luminol-based enhanced chemiluminescence detection (ECL). The detection reagents (ECL™ Prime Western Blotting Detection Reagent; GE Healthcare) were mixed 1:1 and incubated on top of the membranes for 5 min in dark room. The chemiluminescence caused by the HRP-catalyzed oxidation reaction of luminol at the presence of chemical enhancers was detected by exposure to light sensitive autoradiography film (Amersham™Hyperfilm™ECL; GE Healthcare). The exposure times varied from few seconds to 10 minutes. The intensities of the bands were quantified with ImageJ software. The phosphorylated

pERK1/2 and pFAK values obtained from quantification were normalized using the values of unphosphorylated forms of the proteins.

4.10 Microscopy, photography and image editing

Fluorescence microscopy in the LIVE/DEAD[®] analysis was performed using Olympus IX51 fluorescence microscope, fluorescence unit and camera DP30BW, Olympus, Finland. The microscope was operated with PC using the DP manager and DP controller software from Olympus. Alexa-488 filter was used to visualize Calcein-AM and Alexa-568 filter EthD-1. 4X and 10X air objectives were used for fluorescence imaging.

The time point images of the samples and the images of the Oil Red O stained wells were taken with a Nikon eclipse TS100 light microscope with 4X and 10X air objectives. The photographs of the Alizarin Red stained wells were taken with Panasonic Lumix DMC-TZ6 digital camera macro setting.

The fluorescence microscope images, light microscope images and the photographs were edited with Adobe Photoshop CS4. The black and white images obtained in the LIVE/DEAD[®] analysis were colored and the images from the two filters were stacked. Qualitative Alizarin Red results were presented as spherical images of the wells assembled into collages. The Western Blot films were scanned and the brightness and contrast of the images were adjusted to obtain better view of the protein bands. All the image panels of this thesis were created with Adobe Photoshop CS4.

4.11 Statistical analysis

The results of relative ALP activity and quantitative Alizarin Red analyses are presented in the graphs as a sample average. The error bars for these graphs are presented as standard deviation (SD) and were calculated in Microsoft Excel, with the formula given below.

$$SD = \sqrt{\frac{\sum (x - \bar{x})^2}{N - 1}}$$

Statistical analyses of CyQUANT[®], ALP activity and quantitative Alizarin Red results were made using GraphPad Prism 6. For analyzing the differences between control samples and the inhibitor-supplemented samples, non-parametric Mann-Whitney test was used. The test was done at the significance level $p < 0, 05$. The results are presented in the graphs as a sample average and standard error of the mean (SEM).

5. RESULTS

5.1 Flow cytometric surface marker expression analysis

Flow cytometric surface marker analysis was done to confirm the mesenchymal origin of the hASC lines used in the present study. The surface marker expression is presented in Table 8 below. The four hASC lines expressed the surface markers of CD73, CD90 and CD105 but lacked the expression of CD3, CD11a, CD14, CD19, CD45, CD80, CD86 and HLA-DR. The expression of hematopoietic marker CD34 was moderate, and the expression of CD54 varied between the cell lines. The expression of hematopoietic marker CD34 has been previously reported of hASC populations in early passages, but the expression has been shown to decrease when the cells are passaged (Mitchell et al. 2006, Varma et al. 2007, Galateanu et al. 2012).

Table 8. The surface marker expression of undifferentiated hASCs analyzed by flow cytometry (FACS analysis done in passage 1).

Surface marker	Antigen	HFSC 1/13	HFSC 8/13	HFSC 9/13	HFSC 1/14
Positive					
CD73	Ecto-5'-nucleotidase	99,3	98,3	81,8	98,4
CD90	Thymus cell antigen-1 (Thy-1)	99,7	99,6	90,8	99,6
CD105	Endoglin	99,8	98,6	97,7	99,4
Negative					
CD3	T-cell receptor	0,2	0,4	0,2	0,4
CD11a	Leucocyte function-associated antigen-1 (LFA-1)	0,4	0,4	0,3	0,8
CD14	Lipopolysaccharide binding protein	0,6	1,3	1,3	0,7
CD19	B-lymphocyte antigen	0,4	1,1	0,9	0,6
CD45	Leucocyte common antigen (LCA)	0,8	1,5	3	1,1
CD80	B-lymphocyte activation antigen (B7-1)	0,4	0,6	0,9	0,6
CD86	B-lymphocyte activation antigen (B7-2)	0,5	0,8	1,2	0,5
HLA-DR	Major histocompatibility complex, class II	0,3	0,9	1,2	0,7
Moderate expression					
CD34	Sialomucin-like adhesion molecule (hematopoietic progenitor cells)	27,9	11,7	5,7	9,7
CD54	Intercellular adhesion molecule 1 (ICAM-1)	28	23,3	3,7	2,8

5.2 Inhibitor effect on the cell viability and attachment

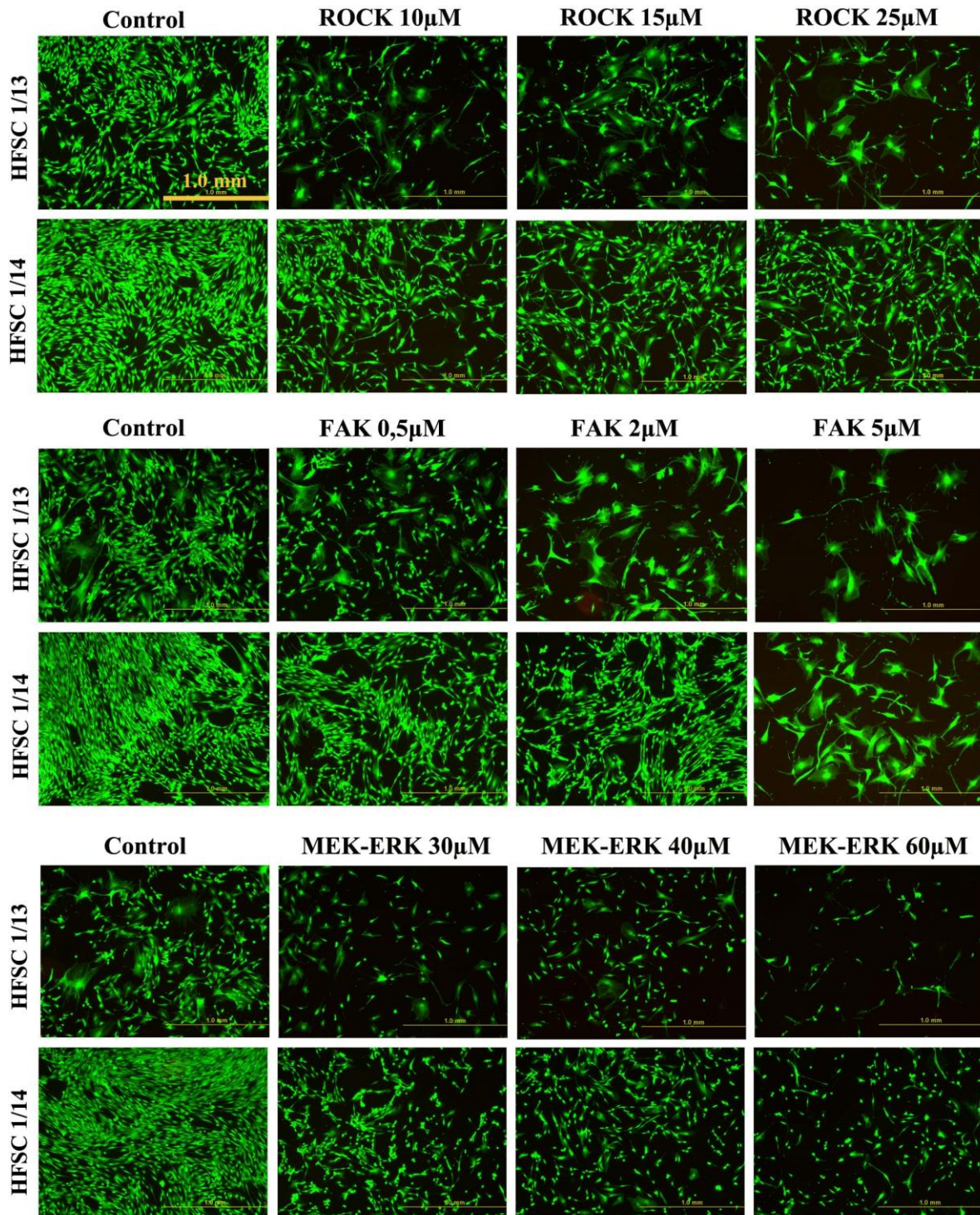


Figure 7. The effect of ROCK, FAK and MEK-ERK inhibitors on the viability of hASCs (HFSC 1/13 and 1/14 cell lines) in BM. 500 cells/well were plated and cultured 7 days in BM supplemented with ROCK, FAK and MEK-ERK inhibitors. The cell viability was assessed with LIVE/DEAD® staining. The green fluorescence indicates living cells while red fluorescence dead cells. The wells were imaged with fluorescence microscope, 4X magnification. Scale bar 1,0 mm (the same scale in every image).

FAK inhibitor used in the present study is PF-562271, a potent, ATP-competitive, reversible inhibitor of FAK and Pyk2 having a 10-fold increase in sensitivity to FAK over Pyk2 according to the manufacturer (Selleck Chemicals). ERK signaling was inhibited by inhibiting the activation of MAP kinase (MEK) with a selective, reversible inhibitor PD98059 to prevent the phosphorylation and activation of ERKs (Gu et al. 2011). ROCK signaling in the present study was inhibited by Y-27632 which is a widely used ROCK inhibitor (Riento, Ridley 2003).

The cell viability of two hASC lines was analyzed with LIVE/DEAD[®] assay at the 7th day of culture. Living cells were visualized with green fluorescent dye. Only a few singular attached dead cells exhibiting red fluorescent dye were observed in the analyzed wells. Plenty of living cells were observed in control samples of basic medium, osteogenic medium and adipogenic medium, cells growing in OM having the highest density in both HFSC 1/14 and HFSC 1/13 cell lines. Figure 7 represents cells cultured in BM, results in OM and AM are presented as a supplementary data (Appendices 1 and 2, respectively). Overall, the proliferation rate of 1/14 cell line was higher in comparison with 1/13 cell line.

The addition of ROCK, FAK or MEK-ERK inhibitor to the growth media caused reduction in the cell numbers in concentration dependent manner. Although fewer cells were observed in higher inhibitor concentrations, there were still some cells present in every culture condition. Decrease in the cell amount was seen especially with the two highest concentrations of FAK and MEK-ERK inhibitors. Morphology of the remaining attached cells in media supplemented with 2 μ M or 5 μ M FAK was different than the morphology of cells in 40 μ M or 60 μ M MEK-ERK inhibitor. Cells cultured in higher concentrations of FAK inhibitor were larger and exhibited more spread morphology than cells with MEK-ERK inhibitor. Also ROCK inhibitor caused a decrease in the number of attached cells. The reduction was seen especially with 1/13 cell line in BM (Figure 7) and AM (Appendix 2) as well as with 1/14 cell line in BM. OM condition supported cell growth the best with both cell lines studied (Appendix 1).

5.3 Cell morphology

The effect of ROCK, FAK and MEK-ERK inhibitors on the cell morphology was evaluated by light and fluorescence microscopy. hASC were cultured in BM, OM or AM condition supplemented with the inhibitors, inhibitor concentrations given in Table 4. Figure 8 represents the morphology changes occurred during the 14 day culture. Untreated human adipose stem cells exhibit fibroblast-like elongated morphology when growing attached to plastic culture dish. The highest cell density in this study was seen in OM control condition: the cells were growing tightly and partially on top of each other. BM and AM control conditions had slightly lower cell densities than the OM control.

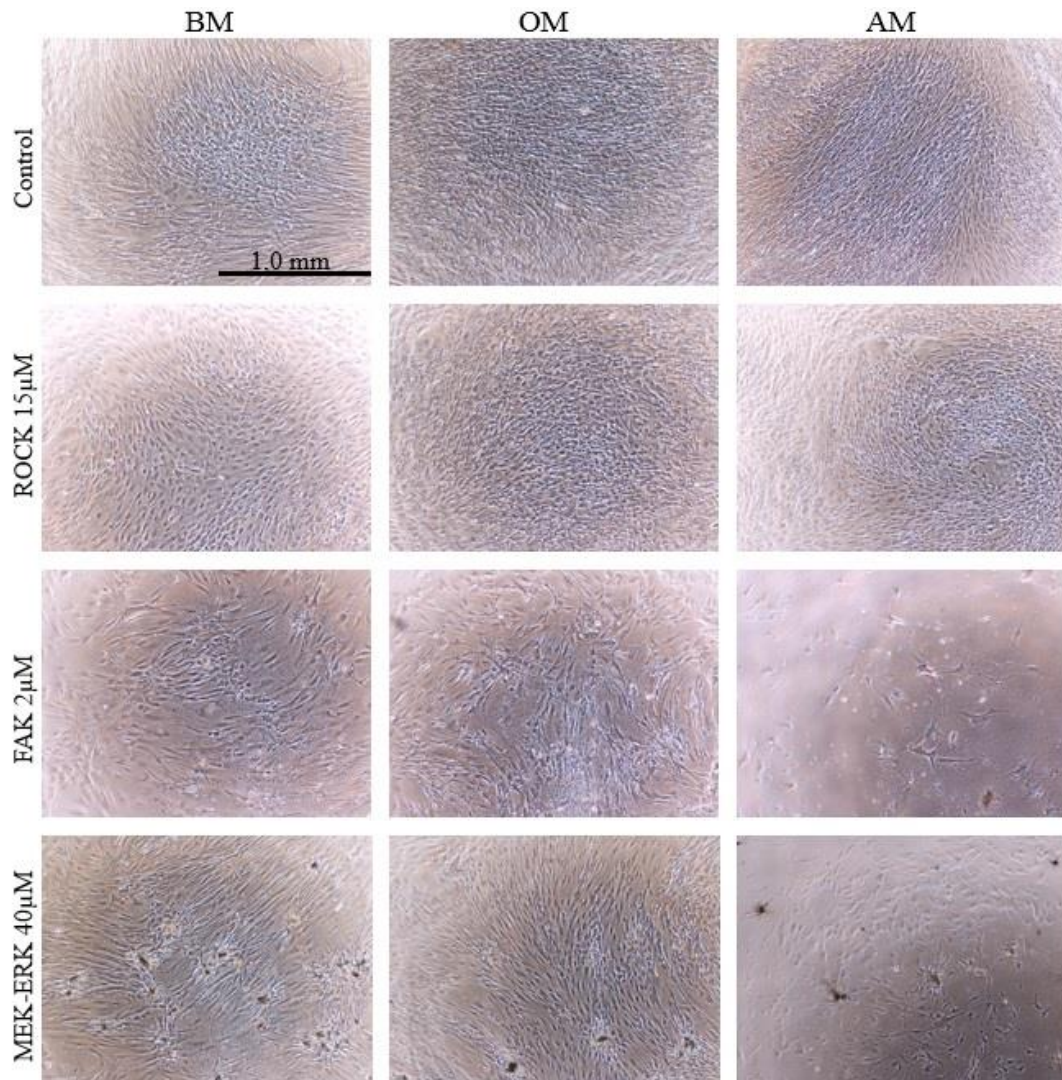


Figure 8. Inhibitor effect on the morphology of hASCs (HFSC 8/13 cell line) after 14 days of culture in BM, OM or AM condition. 15µM ROCK, 2µM FAK and 40µM MEK-ERK inhibitors are presented in the figure. 4X light microscope images, scale bar 1,0mm (the same scale in every image).

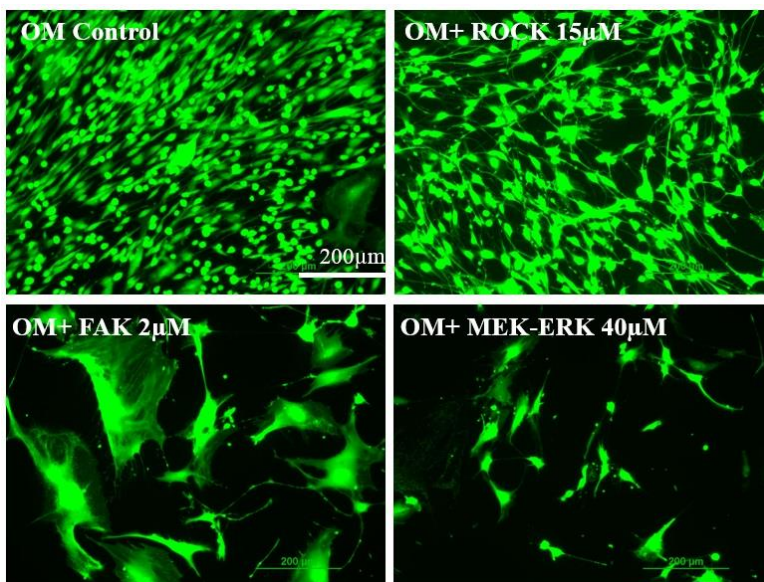


Figure 9. The fluorescence images of HFSC 1/13 cells cultured under osteogenic medium at 7 d time point. 500 cells/well were plated and cultured in OM supplemented with 15µM ROCK, 2µM FAK and 40µM MEK-ERK inhibitors. The green color represents the cytoplasmic calcein. Images taken with 10X magnification. Scale bar 200µm, the same scale in every image.

The inhibitors used in the current study affected both to the cell density and cell morphology. The fluorescence images of HFSC 1/13 cells in Figure 9 highlights the differences in cell morphology. hASCs growing in culture media supplemented with ROCK inhibitor appeared to exhibit more rounded morphology than the untreated hASCs. The cells were less spindle-like when treated with ROCK inhibitor, but had elongated extensions reaching out from the rounded nucleus, as seen in Figure 9. FAK inhibitor seemed to induce the cell spreading of those cells that remained attached to the culture dishes. The cells treated with FAK inhibitor were really large compared to the control cells or the cells treated with ROCK or MEK-ERK inhibitor. In the presence of MEK-ERK inhibitor, on the other hand, cells appeared less spread and dot-like.

During cell culture, an interesting effect of MEK inhibitor PD98059 was discovered. The inhibitor caused formation of crystal-like structures into the culture, as seen in Figure 10. The extent of crystal formation appeared to increase with growing inhibitor concentration and the duration of the culture.

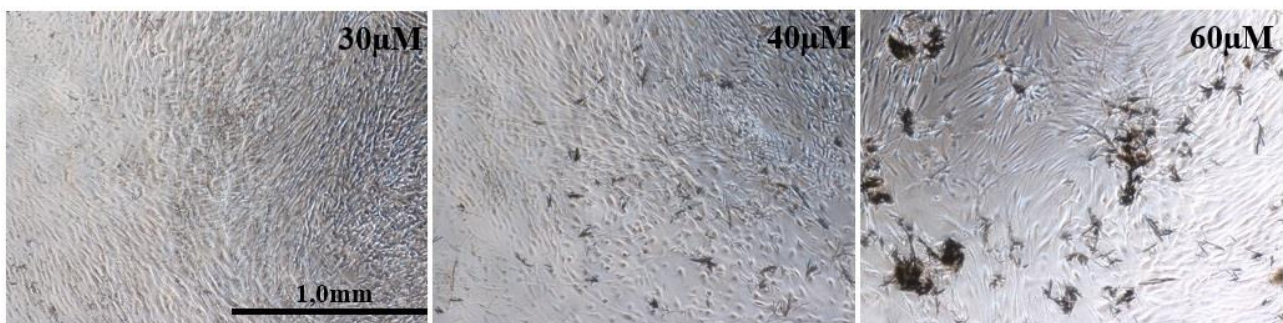


Figure 10. Crystals formed to the HFSC 9/13 culture in BM condition at day 21 as an effect of MEK inhibitor PD98059. 4X light microscope images, scale bar 1,0mm (same scale in every image).

5.4 Effect of FAK, ROCK and MEK kinase inhibition on the cell proliferation

In vitro proliferation of hASCs was evaluated with CyQUANT[®] Cell proliferation assay kit by measuring the total DNA amount of the wells, using GR Dye that expresses fluorescence when bound to cellular nucleic acids. The analysis was done at 7 and 14 day time points. The fluorescein results from all four cell lines (HFSC 1/13, HFSC 8/13, HFSC9/13 and HFSC 1/14) (data not shown) appeared convergent and due to that, the results were combined. Cell proliferation in osteogenic medium was clearly enhanced in all the experiments compared to basic medium. The cell amount in BM control was about one third of the cell amount in OM at the 14 day time point. Also adipogenic medium appeared to support the cell proliferation more than basic medium. Statistical analysis was done of the 14th day CyQUANT[®] results (Figure 11).

ROCK inhibitor had a slight decreasing effect on the cell proliferation in basic, osteogenic and adipogenic culture media at 7 and 14 day time points (14 d results presented in Figure 11 A).

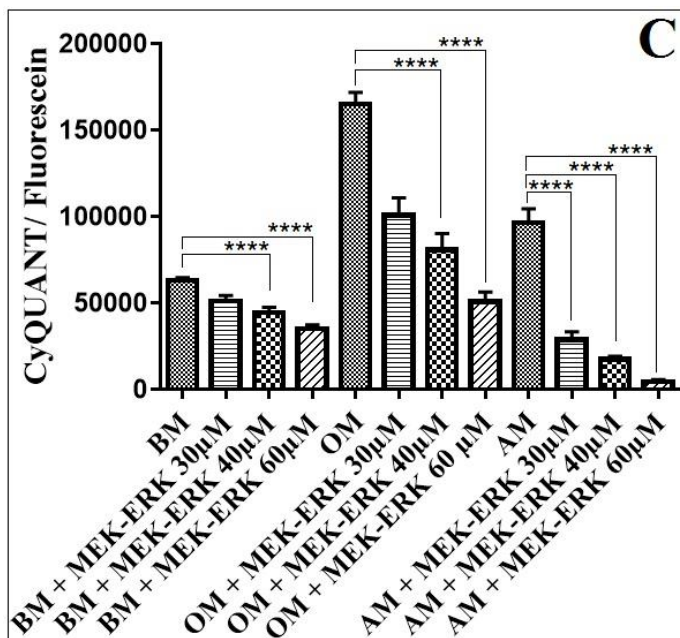
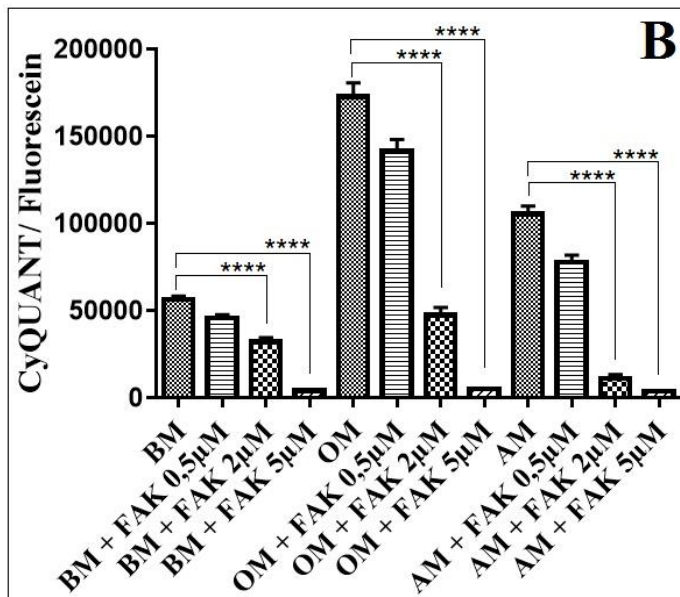
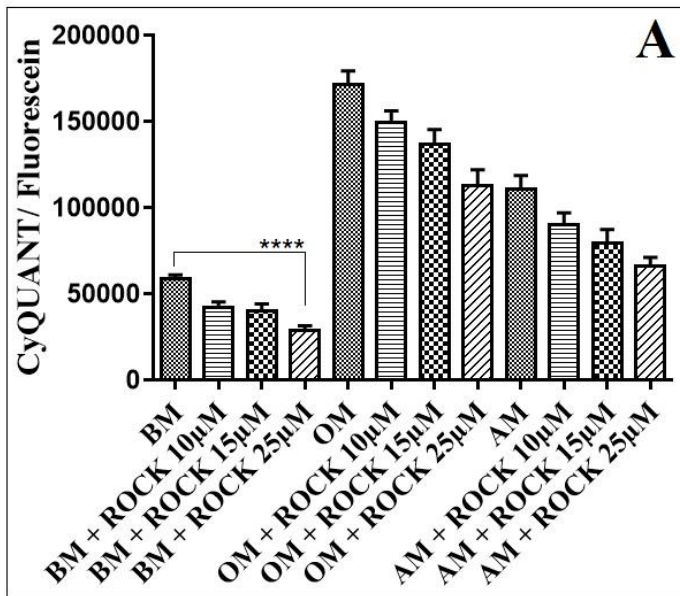


Figure 11. Quantitative analysis of cell number at day 14. Statistical Mann-Whitney analysis was done to analyze the combined CyQUANT® results of the HFSC 1/13, 8/13, 9/13 and 1/14 cell lines. Graph A) represents results of ROCK inhibition, B) FAK inhibition and C) MEK-ERK inhibition. The results are presented as mean and SEM, N=12. The most significant inhibitor effects are presented in the graphs, **** P<0,0001.

The suppressing effect was dependent on the inhibitor concentration: increased inhibitor concentration caused a decrease in the fluorescein values. Most significant repression in cell proliferation was seen with the highest concentration (25 μ M) of ROCK inhibitor in BM condition. P values of the statistical analysis are given as a supplementary data (Appendix 3).

FAK inhibitor caused a dramatic diminishing effect to the fluorescein values. The inhibitor repressed cell proliferation in dose-dependent manner in all culture media at both 7 and 14 day time points. The statistical results of the 14 day time point are presented in Figure 11 B and P values in Appendix 3. The weakest concentration of FAK (0,5 μ M) had the smallest reducing effect on fluorescein values. On the contrary, the cells were almost completely detached from the wells containing the highest concentration of FAK (5 μ M) in basic and osteogenic medium condition. In adipogenic medium, both 2 μ M and 5 μ M concentrations of FAK inhibitor were sufficient to decrease the proliferation and detach the cells from the wells.

Similarly as FAK inhibitor, also MEK-ERK inhibitor reduced the cell proliferation at 7 and 14 day time points. The statistical results of the 14 day time point are presented in Figure 11 C and P values in Appendix 3. The inhibitor effect was dose-dependent in the way that highest concentration (60 μ M) had the largest effect. The most dramatic effect was seen in OM and AM conditions, though osteogenic medium supported cell proliferation more than adipogenic medium.

5.5 The effect of FAK, ROCK and MEK-ERK inhibition on differentiation potential of the hASCs

In vitro adipogenic differentiation was examined by qualitative Oil Red O staining. Fat vacuoles formed in the culture were stained with red dye at 14 and 21 day time points and imaged with a light microscope. Osteogenic differentiation of hASCs was evaluated studying the expression of two osteogenic markers. Alkaline phosphatase activity was measured as an early osteogenic marker and late osteogenic differentiation was assessed using Alizarin Red staining for matrix mineralization.

5.5.1 Adipogenic differentiation

Induction of adipogenic differentiation was observed by the accumulation of lipid-rich vacuoles within cells. Fat vacuole formation was studied in BM, OM and AM conditions. The extent of adipogenic differentiation varied greatly between different culture conditions. Culture medium supplemented with adipogenesis-inducing agents supported the differentiation towards fat cells the most resulting in the accumulation of large and abundant fat vacuoles, as seen in Figure 12 on the right. Osteogenic medium appeared to induce both adipogenesis and osteogenesis (Figure 12 in the middle). Adipogenic differentiation of hASC lines used in the current study was noticeable at 14 day time point (data not shown), but the differentiation was more evident at 21 day time point. The size

and amount of accumulated lipid-rich vacuoles within the cells increased during culture. The fat vacuoles were not uniformly distributed to the culture plates, rather large clusters of lipid droplets had been formed.

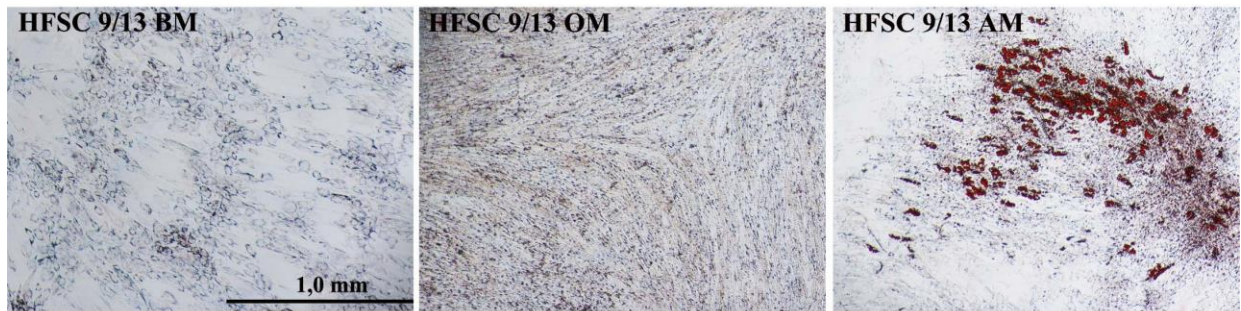


Figure 12. Oil Red O staining of HFSC 9/13 cell line, control samples at 21 d time point. 500 cells/well were plated and cultured three weeks in BM, OM and AM conditions. Adipogenic differentiation was analyzed with Oil Red O staining. Fat vacuoles can be seen as bright red dots in the images. 4X magnification, scale bar 1,0mm, scale bar 1,0 mm, same scale in all images.

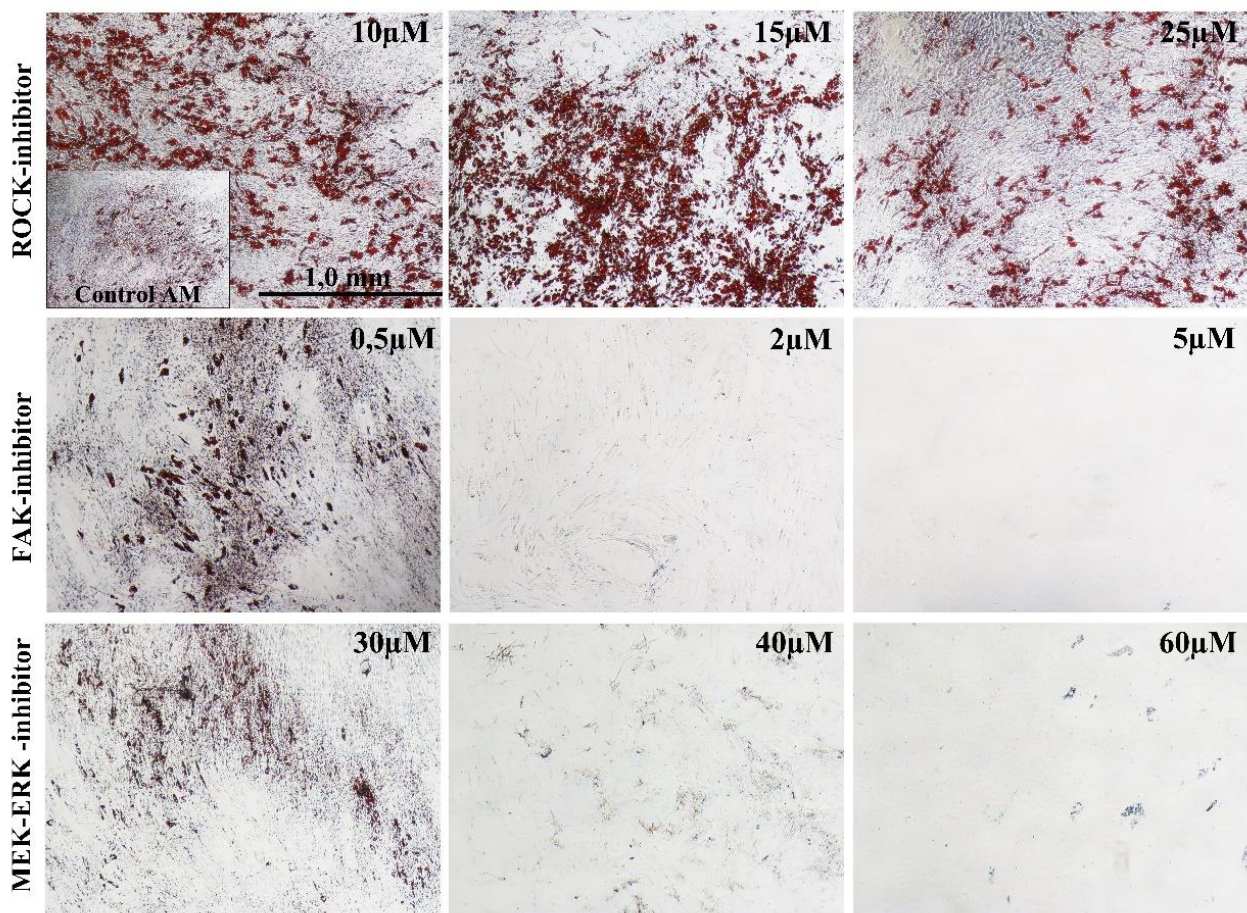


Figure 13. Inhibitor effect on lipid-rich vacuole accumulation in adipogenic medium. 500 cells/well were plated and cultured three weeks in adipogenic medium supplemented with ROCK, FAK and MEK-ERK inhibitors. Fat vacuole formation was assessed with Oil Red O staining. Images of HFSC 1/13 cell line in 21 d time point are presented in the image panel. 4X magnification, scale bar 1,0mm, same scale in every image.

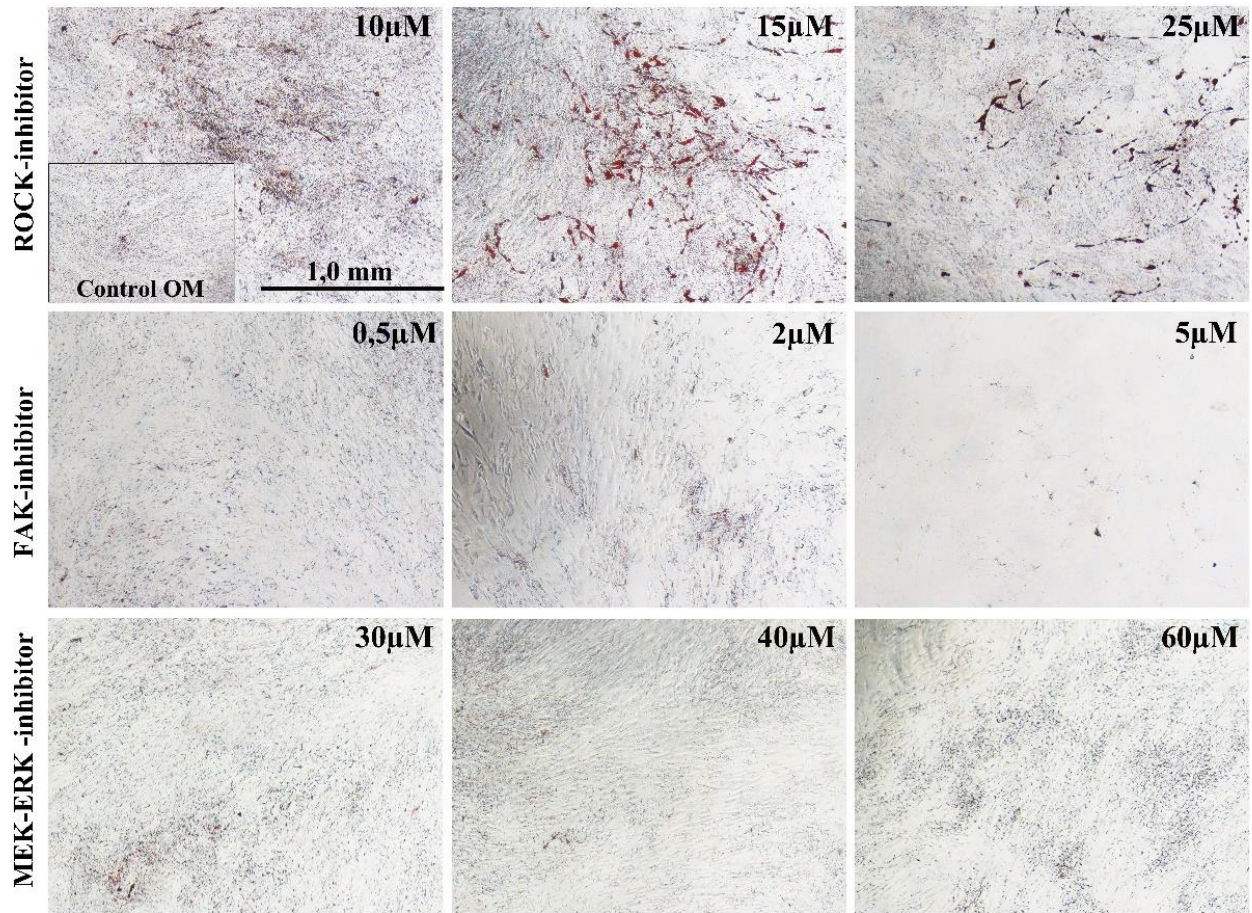


Figure 14. Inhibitor effect on lipid-rich vacuole accumulation in osteogenic medium. 500cells/well were plated and cultured three weeks in osteogenic medium supplemented with ROCK, FAK and MEK-ERK inhibitors. Fat vacuole formation was assessed with Oil Red O staining. Images of HFSC 1/13 cell line in 21 day time point are presented in the image panel. 4X magnification, scale bar 1,0mm, same scale in every image.

Basic medium had the smallest effect on inducing adipogenesis. Small fat vacuoles, which could be seen as small red or black dots at the borders of the cells (Figure 12 on the left), were formed within cells in BM condition during the 14 and 21 day culture periods (14th day results, data not shown). The extent of adipogenesis of hASCs cultured in basic medium was minor in comparison with AM or OM conditions and thus only the detailed results of AM and OM conditions are presented below.

ROCK inhibitor induced adipogenic differentiation substantially in adipogenic culture medium (Figure 13). Large red-stained lipid-rich vacuoles were apparent in AM supplemented with 10µM, 15µM and 25µM ROCK inhibitor. With 1/13, 9/13 and 1/14 cell lines, the addition of ROCK inhibitor increased the amount of large lipid vacuoles compared to control AM sample. On the contrary, with 8/13 cell line AM supplemented with 25µM ROCK contained slightly fewer lipid droplets than the other inhibitor concentration in AM (data not shown). Adipogenic induction of

hASCs was also seen in samples of AM supplemented with 0,5 μ M FAK inhibitor (images of cell line 1/13 presented in Figure 13). With three of the hASC lines used, 0,5 μ M FAK inhibitor even augmented the adipogenesis compared to the control, as seen by the accumulation of large fat vacuoles (data not shown). Increasing concentrations of FAK inhibitor suppressed adipogenic differentiation together with the inhibitor's decreasing effect on cell amount. Samples containing 2 μ M or 5 μ M FAK inhibitor exhibited no detectable adipogenic differentiation in three of the cell lines studied. HFSC 1/14 cell line was an exception exhibiting some degree of adipogenic differentiation in AM supplemented with 2 μ M FAK inhibitor (data not shown). This could be due to that 1/14 cell line possessed a high proliferation rate and the high cell density supported cell attachment also in culture environment containing higher concentration of FAK inhibitor. According to current study, MEK-ERK inhibitor suppressed lipid accumulation in dose-dependent manner. Large red-stained lipid vacuoles were seen at 21 day time point in AM supplemented with 30 μ M MEK-ERK inhibitor with HFSC 1/13 (Figure 13), 40 μ M MEK-ERK with HFSC8/13, and both concentrations 30- and 40 μ M of MEK-ERK with HFSC1/14 cell line (data not shown). AM supplemented with 60 μ M MEK-ERK inhibitor contained least cells and the lowest number of fat vacuoles compared to the weaker inhibitor concentrations.

The results in osteogenic medium condition followed similar trend as described above with AM condition. Large fat vacuoles were present in OM supplemented with ROCK inhibitor (Figure 14), but in less degree than in AM condition. In OM, the amount of large fat vacuoles seemed to increase slightly with increased ROCK inhibitor concentration with cell lines 1/13 (the uppermost images in Figure 14) and 9/13 while with 8/13 and 1/14 cell lines, there was no visually detectable increase in adipogenesis (data not shown). Small lipid-rich vacuoles were present in OM supplemented with 0,5 μ M FAK inhibitor. However, 2 μ M and 5 μ M FAK inhibitor concentrations suppressed the adipogenesis. Similarly as FAK inhibitor, also MEK-ERK inhibitor reduced the adipogenic differentiation in dose-dependent manner. OM supported the cell proliferation and attachment the best, thus the 60 μ M MEK-ERK inhibitor caused smaller decrease in hASC proliferation and differentiation in OM compared to AM (1/13 cell line presented in Figures 13 and 14). Some HFSC 1/14 samples in OM were overgrown and detached from the wells during the 21 day culture period (data not shown).

5.5.2 Early osteogenic differentiation

Early osteogenic differentiation of hASCs was analyzed quantitatively by determining the activity of alkaline phosphatase. ALP activity was examined after 7 and 14 days of culture. The ALP results were normalized by dividing the ALP activity with the total DNA amount (results from CyQUANT[®]

cell proliferation assay). This way, the results could be examined on a single cell level, without the distorting effect of different cell amounts growing in different wells of the plates.

At 7 day time point, the ALP activity was still very low in most of the samples, as seen in Figures 15, 16 and 17. HFSC 9/13 cell line appeared to express slightly more ALP activity at day 7 compared to the other cell lines (data not shown). At 14 day time point significant ALP activation in OM was observed. ALP activation was also present in some of the samples in BM. Inhibition of ROCK signaling caused a dose-dependent decrease in ALP activity in three of the cell lines studied (Figure 15). Similarly as ROCK inhibition, FAK inhibition caused a decrease in the ALP activity of the same cell lines (Figure 16). The effect of MEK-ERK inhibition was more coherent between the cell lines studied (Figure 17). ALP activity was seen predominantly only in OM control samples. All three inhibitor concentrations of MEK-ERK resulted in the suppression of ALP activity in BM, OM and AM conditions.

To examine the statistical differences between different culture conditions, normalized 14th day results of the four cell lines were combined. In this case, the separate results of the four cell lines were not presented relative to the 7th day BM control sample since it would have led to a biased result. The P values of non-parametric Mann-Whitney tests are listed in Appendix 4. The most significant statistical differences are shown in Figure 18.

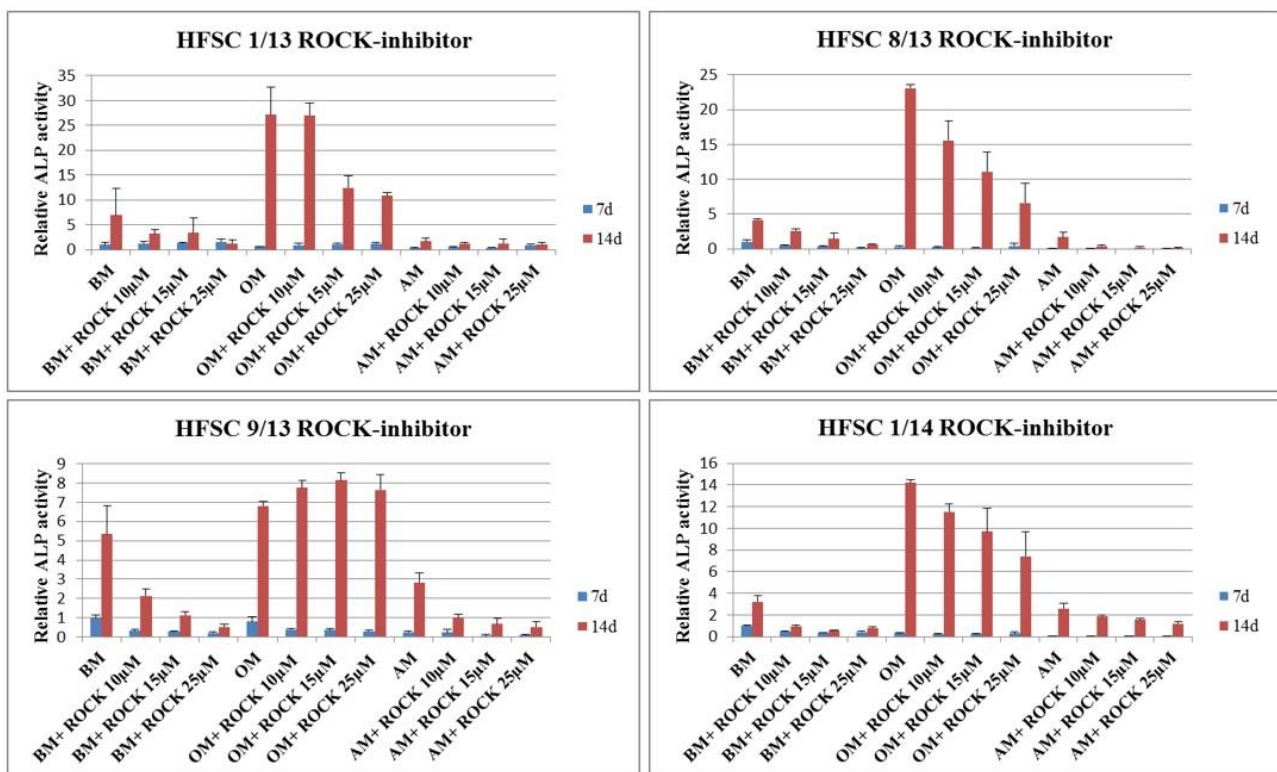


Figure 15. The effect of ROCK inhibition on relative ALP activity in BM, OM and AM conditions after 7 and 14 days of culture. Relative ALP activity was obtained by presenting the results relative to the 7 day BM control sample (=1).

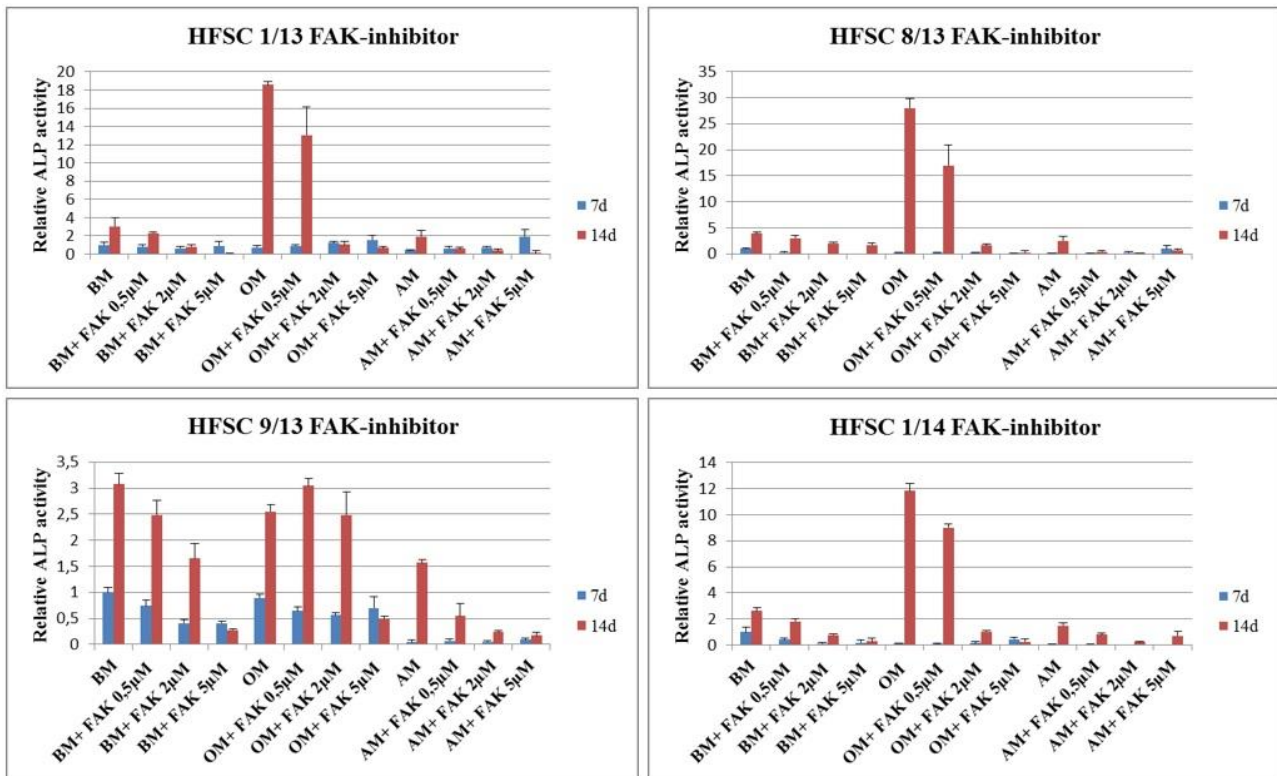


Figure 16. The effect of FAK inhibition on relative ALP activity in BM, OM and AM conditions after 7 and 14 days of culture. Relative ALP activity was obtained by presenting the results relative to the 7 d BM control sample (=1).

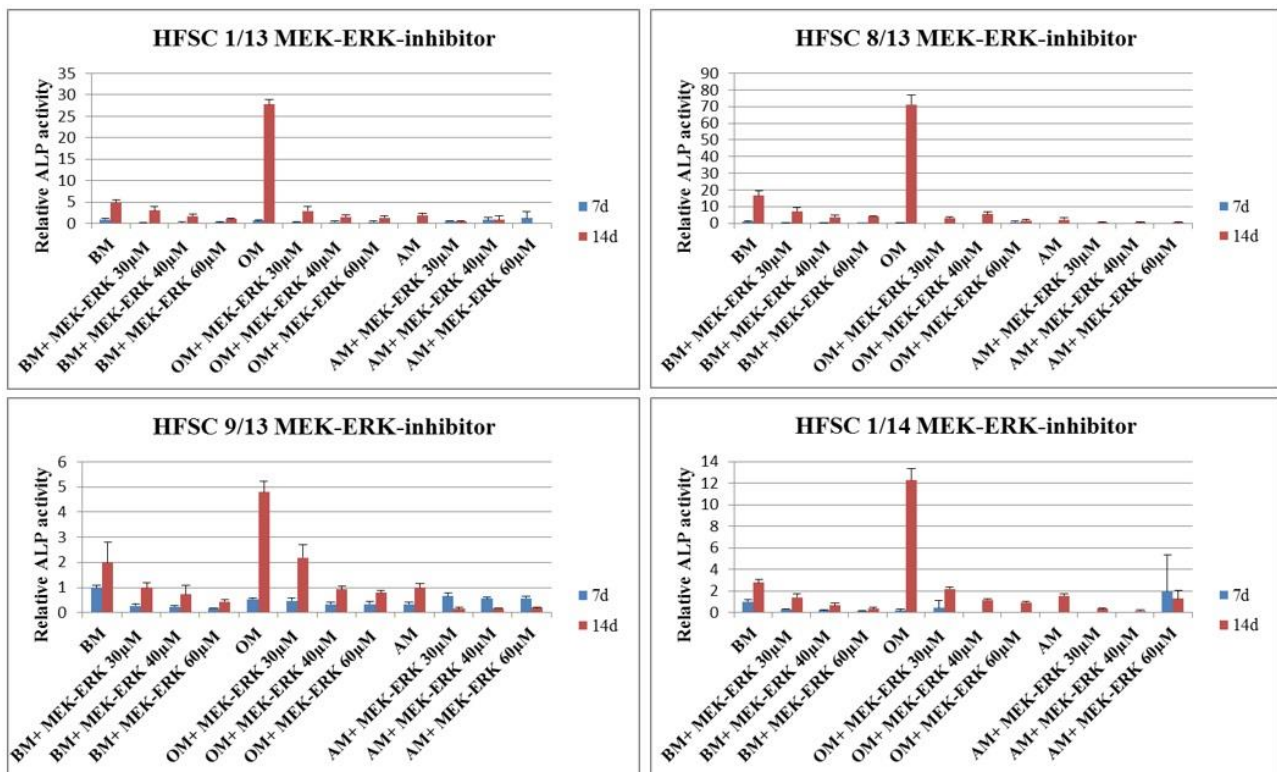


Figure 17. The effect of MEK-ERK inhibition on relative ALP activity in BM, OM and AM conditions after 7 and 14 days of culture. Relative ALP activity was obtained by presenting the results relative to the 7 d BM control sample (=1).

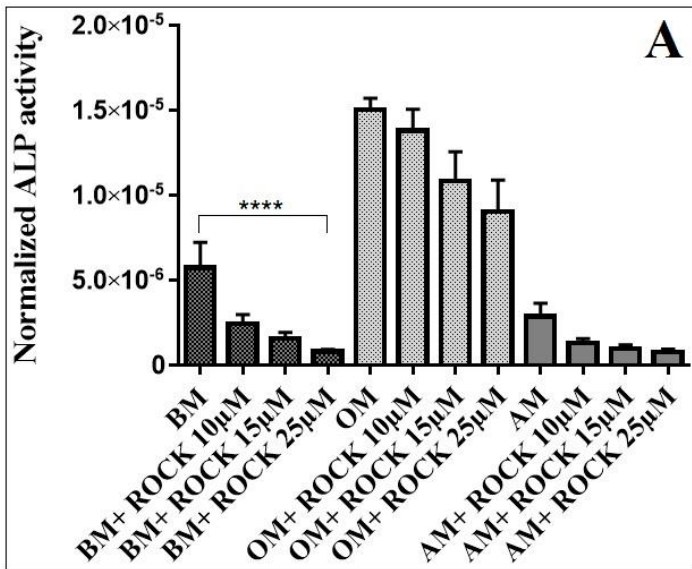
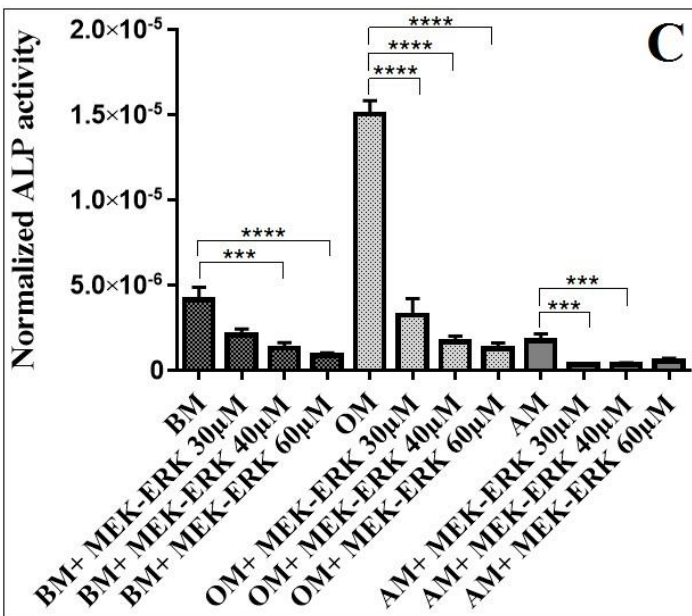
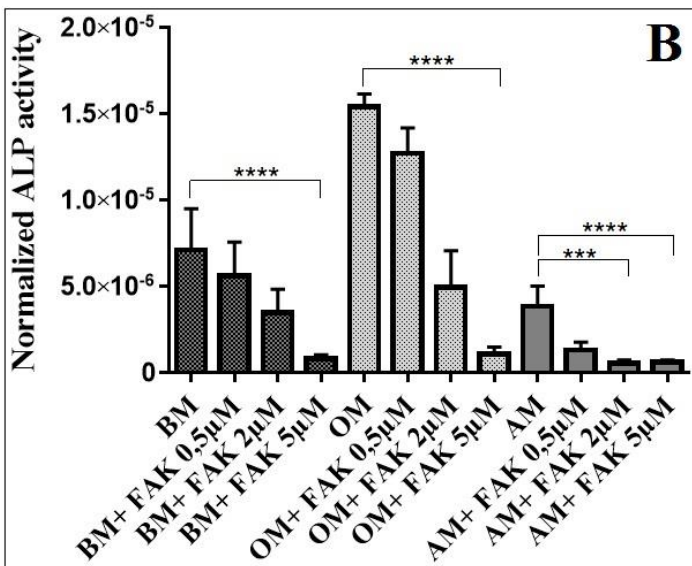


Figure 18. Normalized ALP activity after 14 days of culture. The normalized values of four cell lines were combined (N=12) and the inhibitor effect in each culture condition was analyzed with Mann-Whitney test. **A)** ROCK inhibitor, **B)** FAK inhibitor and **C)** MEK-ERK inhibitor. The statistical results are presented as mean and SEM. The most significant differences are presented in the graphs, *** P<0,0007 and **** P<0,0001.



According to these results, the inhibition of ROCK signaling has the smallest effect on ALP activity (Figure 18 A), whereas the inhibition of FAK and MEK-ERK signaling has a notable decreasing effect on ALP activity. With FAK inhibitor, the two highest inhibitor concentrations caused significant reduction in ALP activity (Figure 18 B) while with MEK-ERK inhibitor the effect was seen already with the weakest concentration (Figure 18 C).

5.5.3 Mineralization

An important marker of late phase osteogenic differentiation is mineralization: the accumulation of calcium in the extracellular space and its organization into hydroxyapatite crystals. The matrix mineralization was evaluated by qualitative and quantitative Alizarin Red staining at 14 and 21 day time points. With both HFSC 8/13 and 9/13 cell lines, the extent of mineralization was still very low after 14 days of culture (data not shown). However, at the 21 day time point, clear signs of matrix mineralization were seen. In qualitative analysis, images of stained mineral deposits were taken with digital camera. Bright red color represented mineralization, whereas pale pink and purple colors were signs of unspecific staining. Results from the two cell lines studied were alike. Images of HFSC 8/13 21 day time point are presented in Figure 19. The 21 day qualitative results of 9/13 cell line are presented in Appendix 5.

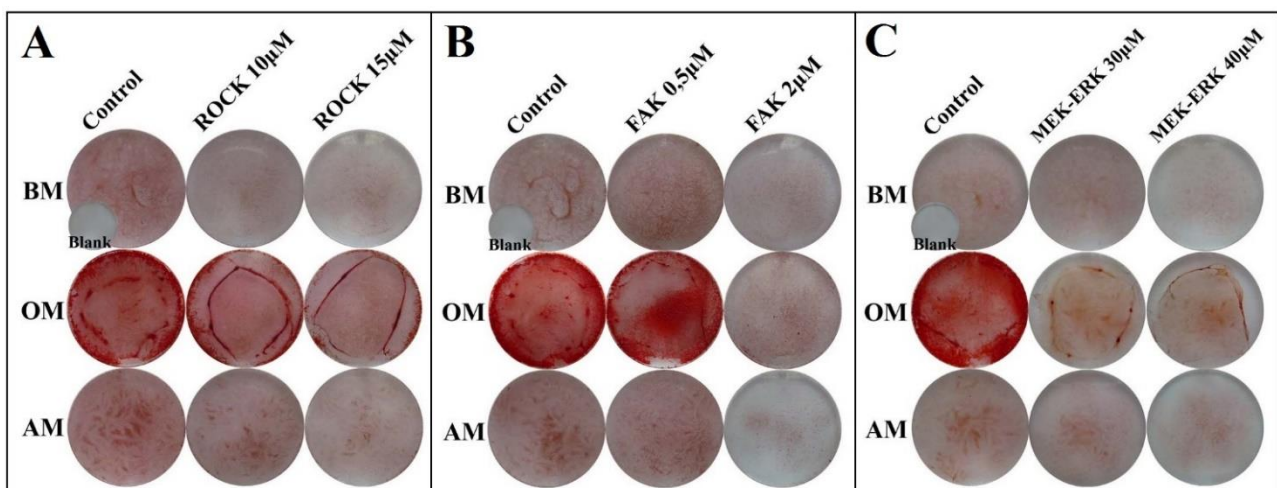


Figure 19. Qualitative Alizarin Red staining of cell line HFSC 8/13 (day 21). hASCs were cultured three weeks in BM, OM and AM conditions supplemented with ROCK, FAK and MEK-ERK inhibitors. Qualitative mineral deposition was analyzed with Alizarin Red staining. The inhibitor effect on matrix mineralization is presented in the figure: **A)** ROCK inhibitor, **B)** FAK-inhibitor and **C)** MEK-ERK inhibitor. Mineralization is visualized by the bright red color of the well. The spherical images represent the surface area of the 24-well plates.

Cells grown in BM and AM failed to deposit any detectable calcium throughout the culture period. After 21 days of culture, the inhibitor-treated cells exhibited a significant reduction in matrix

mineralization. Untreated cells in OM, however, induced significant increase in calcium deposition. Matrix mineralization was also seen in OM supplemented with 0,5 μ M FAK inhibitor and some extent of mineralization was seen in OM supplemented with 10 μ M ROCK inhibitor.

The quantitative Alizarin Red analysis gave convergent results, as seen in Figure 20. The results are presented here as absorbance values of the extracted dye and not as normalized results since the normalization with the corresponding CyQUANT[®] results led to biased results. Increased calcium accumulation was observed in untreated OM samples. ROCK, FAK and MEK-ERK inhibitors suppressed calcium deposition in a dose-dependent manner with all concentrations tested. The effect was the most evident with PD98059, already the weakest inhibitor concentration inhibited matrix mineralization. Statistical analysis was done to compare the calcium deposition of OM control sample versus two inhibitor concentrations of ROCK, FAK and MEK-ERK. Box blot graph of the statistical results is shown in Figure 20 D.

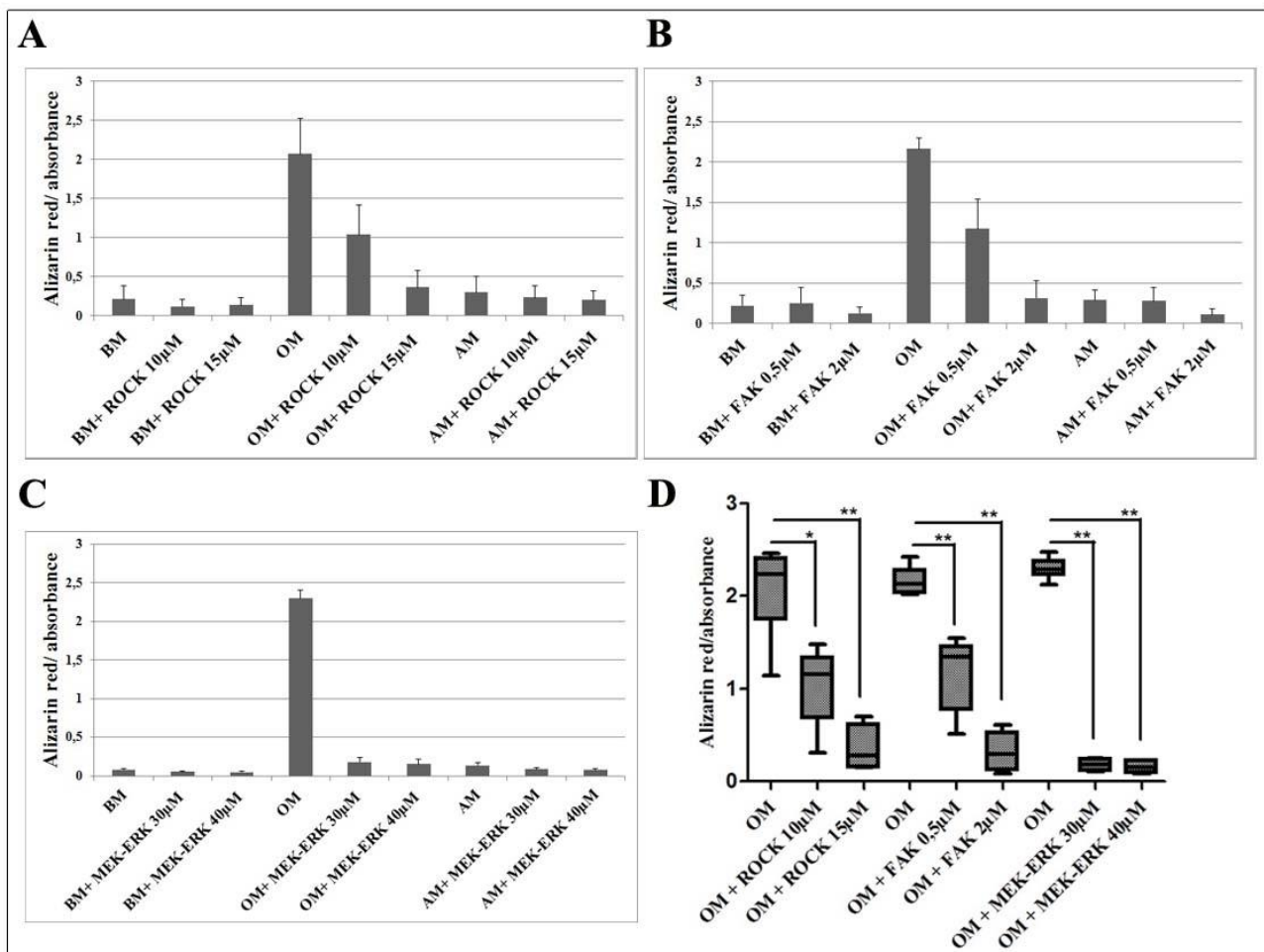


Figure 20. Quantitative matrix mineralization of hASCs is repressed by inhibiting ROCK, FAK and MEK-ERK signaling. hASCs were cultured three weeks in BM, OM and AM supplemented with ROCK, FAK and MEK-ERK inhibitors. ECM mineralization was studied by quantitative Alizarin Red analysis. The absorbance values representing mineral deposition are presented in graphs **A**, **B** and **C**. **A)** ROCK inhibitor, **B)** FAK inhibitor and **C)** MEK-ERK inhibitor. **D)** The inhibitor effect in OM condition. Statistical Mann-Whitney test, N=6, * P=0,0152 ** P=0,0022.

5.6 Western Blot analysis of the inhibitor functionality

Protein activation and the inhibitor function were confirmed by Western Blot analysis. Two cell lines (HFSC 8/13 and 9/13) were studied after 3 and 7 days of culture in 1% starvation BM, OM or AM supplemented with ROCK, FAK or MEK-ERK inhibitor. The sample lysates in LAEMMLI sample buffer were run in electrophoresis, the protein bands were transferred from the SDS-PAGE gel to PVDF-membrane and immunoblotted. Immunoblot analysis was performed with antibodies binding to β -actin, FAK, ERK2 and the phosphorylated forms of FAK, ERK1/2 and MYL9 signaling proteins. The immunoblotting with pMYL9 (myosin light chain 9) antibody was unsuccessful. The unspecific binding to the membrane was too strong to reveal the actual protein bands, thus the results of pMYL Western Blot are not presented here.

To become functional, FAK and ERK signaling proteins are activated by phosphorylation. With HFSC 8/13 cell line, the phosphorylation of ERK was down-regulated in the presence of PD98059, as seen in Figure 21 A, suggesting that the inhibition of MEK signaling protein suppresses the activation of ERK. The phosphorylation of pFAK was similarly down-regulated in the presence of FAK inhibitor and also to less extent with ROCK inhibitor.

Convergent results to these findings could be also obtained from the semiquantification of these signaling proteins. The graphs in Figure 21 B and C represent semiquantified results of FAK and ERK activation. The band intensities of phosphorylated protein forms were divided with the band intensities of unphosphorylated forms to gain insight of the ratio of these proteins. Functionality of FAK and MEK-ERK inhibitors are confirmed in graphs B and C of the Figure 21. FAK inhibitor causes reduction in column height of semiquantified FAK signaling protein in all three culture media. In the same way, MEK inhibitor suppresses the ratio of activated ERK in the cells. The suppressive impact appears to be the most evident in cells cultured in 1% OM.

The Western Blot results of the 9/13 cell line (supplementary data, Appendices 6 and 7) differed slightly from results of the 8/13 cell line. The bands of pFAK and FAK were even more faded than with 8/13 cell line making the interpretation of the results and the semiquantification of the band intensities more difficult. However, at least pERK suppression in the presence of MEK inhibitor was noticed. Taken together, these results confirm both the inhibitor function and the presence of functional forms of FAK and ERK signaling proteins.

A

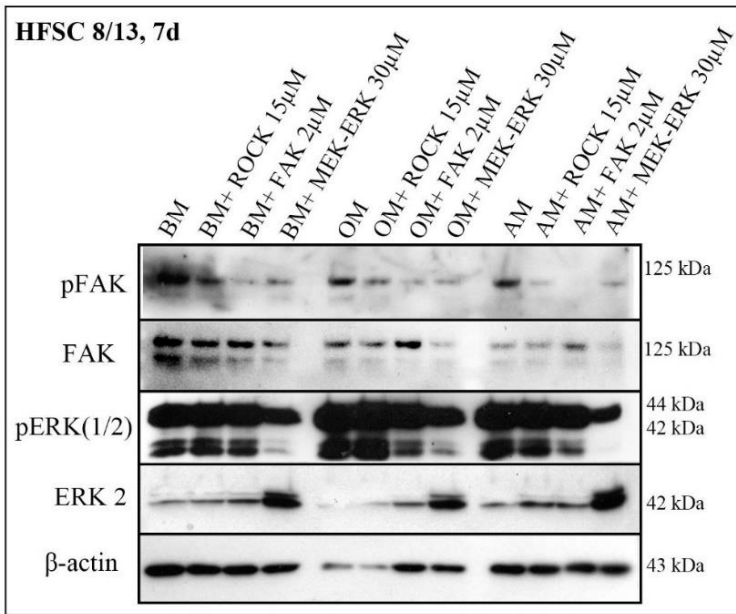
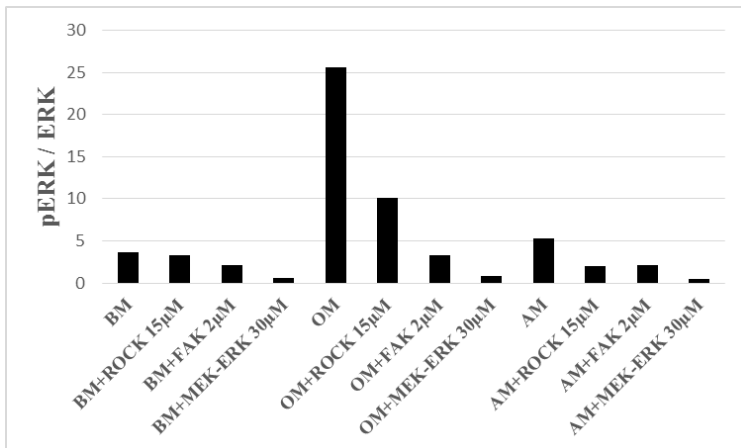


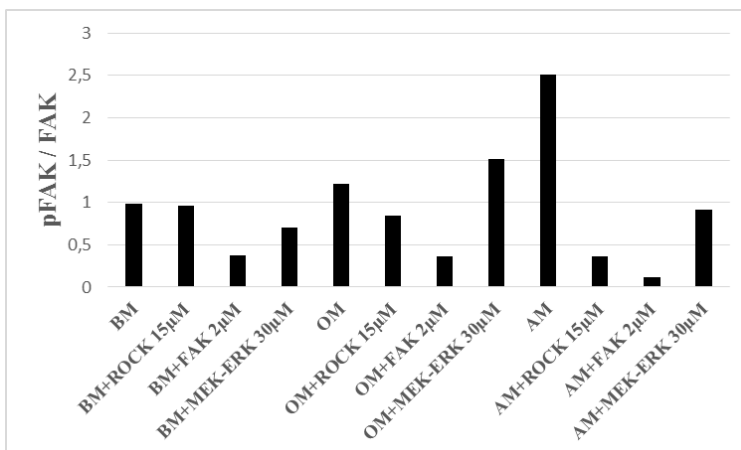
Figure 21. A) Western blot of 7th day HFSC 8/13 sample lysates. 30 000 cells/well were plated and cultured in 1% starvation BM, OM or AM; all culture media were supplemented with 15μM ROCK, 2μM FAK or 30μM MEK-ERK inhibitor. Cells were lysed in 2X LAEMMLI sample buffer (100μl/well) and 15μl sample lysates were run in electrophoresis. Signaling molecules pFAK, FAK, pERK(1/2), ERK2 and β-actin were analyzed. For β-actin analysis, only 3,5μl of each lysates was run.

B



B) Semiquantification of the activation of signaling molecules. The band intensities were measured with Image J software. pFAK intensities were divided with corresponding FAK intensities.

C



C) Similarly, pERK(1/2) intensities were divided with the intensities of ERK bands.

6. DISCUSSION

The aim of this study was to analyze the significance of integrin-mediated cell adhesion and cell morphology to hASC differentiation potential. The role of ROCK, FAK and MEK-ERK signaling pathways in hASC osteogenic and adipogenic differentiation were assessed. Chemical inhibitors against signal transduction were used to investigate these signaling cascades. In addition to differentiation studies, hASC morphology, viability and proliferation were studied in response of inhibition of these signaling cascades.

6.1 The cell attachment and proliferation are interfered with the inhibitors

In this study, the cells were grown on an attachment promoting CellBIND[®] culture plates from Corning. The polystyrene surface of CellBIND[®] culture vessels has been treated with plasma surface treatment, which increases the oxygen content of the polymer surface resulting in improved hydrophilicity and wettability (Pardo et al. 2005). The oxygen incorporation to the polystyrene surfaces has been shown to result in increased cell proliferation. Furthermore, the production of the adhesion-related proteins such as cadherin-5, FAK and RhoA has been shown to increase on surfaces with higher wettability, indicating a better attachment. (Van Kooten, Spijker & Busscher 2004)

The attachment promoting culture vessel allowed to study inhibitors that have a negative effect on cell adhesion. In addition, the CellBIND[®] plate provided a suitable growth environment for a prolonged culture. The cells were cultured a 21 day period for analyzing the late osteogenic differentiation and the adipogenic differentiation. Based on the prior experiments done in our research group, the cells would have detached more easily from a regular polystyrene culture plate.

The LIVE/DEAD[®] cell viability and CyQUANT[®] cell proliferation analyses revealed the importance of the ROCK, FAK and MEK-ERK signaling to cell proliferation. All three inhibitors used in this study had a negative effect on the amount of hASCs in culture. The inhibitor effect was dose-dependent: the highest inhibitor concentration resulted in greatest decrease in the cell number. FAK inhibitor PF-562271 and MEK inhibitor PD98059 caused a significant concentration-dependent suppression of cell proliferation in hASCs and contributed to detachment of the cells from the culture plates. The inhibitor effect was also observed from the fluorescence images taken after 7 days of culture. Similar results have been reported before in context of other cell types. FAK inhibition in breast cancer cells (BT474) increased cell detachment and inhibited cell adhesion in a dose-dependent manner (Golubovskaya et al. 2008). Taken together, the inhibition of pathways that are essential to cell adhesion diminishes the number of adherent hASCs.

Both FA kinase (Schaller 2001) and the MAPK pathways (Zhao et al. 2012) have an essential role in transmitting a cell survival signal. Overexpression of FAK and ERK pathways have been noted

in many types of tumors (Golubovskaya, Cance 2007, Tilghman, Parsons 2008, Takacs-Vellai 2014), and therefore inhibitors targeted against these signaling cascades have been investigated as a possible anti-tumor drugs (Roberts et al. 2008, Sun et al. 2010, Wiemer et al. 2013). The overexpression of these survival-enhancing pathways may prevent the programmed cell death, termed anoikis. Anoikis, a subset of apoptosis, originates from inadequate or inappropriate cell-matrix contacts (Frisch, Screaton 2001). Resistance of anoikis is associated with the malignancy of cancers (Frisch, Screaton 2001). The integrin-mediated signaling is an essential component regulating the attachment-regulated cell death. Integrins respond to the lack of appropriate cell-ECM contacts by activating various downstream pathways, the most important being FAK, Shc, ILK (integrin-linked kinase) and the ERK pathway. Additionally, the cell spreading and morphology influence the cell survival. The cytoskeletal integrity has proven to be critical in preventing the anoikis. (Frisch, Screaton 2001, Gilmore 2005)

In respect of the current study, it remains unclear whether the cells underwent anoikis or remained viable as they detached from the culture plates as a response of the inhibitors. According to the LIVE/DEAD[®] analysis done with the hASCs, the cells analyzed were predominantly viable. However, the staining was done only to the adherent cells still remaining attached to the culture plates. To confirm the anoikis of the detached cells, the cell viability staining should have been done also with the suspended cells, prior to medium changes (the detached cells were removed as the old media were removed). The suspended cells could have been stained and studied with flow cytometry using FACSAria[™], as in the surface marker expression analysis, for example.

6.2 The hASC morphology changes as a result of the inhibitor treatments

The hASCs exhibit fibroblast-like elongated morphology when growing attached to plastic culture vessels. Minor morphology differences between cell lines were observed. Some of the cell lines used in this study represented slightly more spindle-like morphology than others and some grew rather in clusters than equally distributed. The small differences seen in freshly plated stem cells became even when the cell density increased. The cell density was markedly lower with BM and AM than with OM condition. During the culture, the cells expanded and migrated to cover the surface of the entire vessel.

The inhibitor effect on cell morphology was evaluated with light and fluorescence microscopy. The treatment with ROCK inhibitor Y-27632 caused the adipose stem cells to appear less elongated and spread while being more rounded. In the presence of FAK inhibitor PF-562271 the adherent cells were spread, but much larger than the control cells and the cells treated with ROCK inhibitor. MEK inhibitor PD98059 seemed to hamper the spreading. Instead of typical spindle-like morphology, the

cells appeared more rounded and dot-like. In the presence of PD98059, the cells appeared also smaller than the control cells and the cells treated with the other inhibitors. Presumably, these morphology differences were caused by the changes in the actin cytoskeleton. ROCK inhibitor has a direct effect on the cytoskeletal integrity. Inappropriate formation of the actin fibers leads to rounded shape of the cells. Inhibition of FAK causes decreased numbers of focal adhesions leading to detachment of the cells. FAK inhibition may also affect through ROCK signaling since ROCK has been suggested to be a downstream target of FAK signaling. However, instead of being rounded, the adherent cells treated with FAK inhibitor PF-562271 were large, elongated and spread. In these cells the mechanisms of adhesion and cytoskeletal changes may be somewhat different than in the detached cells.

To confirm these findings, more specific analyses on cell shape should be done. One suitable method is immunocytochemistry. The cell morphology could be analyzed by immunostaining the focal adhesions and actin cytoskeleton, and the changes caused by the inhibitors could be observed with fluorescence microscopy. Another method named Cell-IQ[®], a live cell imaging technology, would allow observations of real time morphology changes after inhibitor addition.

6.3 ROCK works as a molecular switch between osteogenesis and adipogenesis in hASC differentiation

The Rho-ROCK signaling is an essential pathway mediating cytoskeletal dynamics and contractility in many cells (Riento, Ridley 2003, McBeath et al. 2004, Tilghman, Parsons 2008). The pathway is also crucial in biophysically induced stem cell differentiation (Arnsdorf et al. 2009, Yim, Sheetz 2012). In the current study, the significance of Rho-ROCK signaling in the hASC lineage commitment towards osteogenesis and adipogenesis was assessed. The effects of actin cytoskeletal alterations was evaluated using a pharmacological agent Y-27632 (10 μ M, 15 μ M and 25 μ M concentrations) to test the importance of ROCK and the cytoskeletal tension on hASC differentiation.

Previous studies have proven the significance of Rho-ROCK signaling in the osteogenic differentiation of stem cells (McBeath et al. 2004, Arnsdorf et al. 2009, Santos et al. 2010, Shih et al. 2011). In bone marrow MSCs, 5 μ M ROCK inhibitor Y-27632 resulted in down-regulation of ROCK activation followed by decrease in type I collagen, osteocalcin gene expression and the extent of mineralization (Shih et al. 2011). Similarly to BMCSs, we found out that the commitment of hASCs to the osteoblastic lineage required the proper functionality of ROCK signaling cascade. Inhibition of ROCK signaling caused a dose-dependent decrease in ALP activity, a marker of early osteogenic differentiation, in three of the cell lines studied. The progression of osteogenic differentiation was also suppressed with ROCK inhibitor, as seen from the qualitative and quantitative Alizarin Red

results. The matrix mineralization was markedly greater in the samples without the addition of Y-27632. The importance of ROCK signaling to osteogenesis is comprehensible, since the osteogenesis has been shown to be more prevalent with spread cytoskeleton (McBeath et al. 2004), and the main function of RhoA-ROCK is to stimulate actomyosin contractility and the actin polymerization leading to accumulation of contractile stress fibres in the cell (Tilghman, Parsons 2008). Presumably, disruption of the actomyosin contractility and formation of the actin cytoskeleton inhibits the spread morphology and through that, the osteogenic differentiation.

The Rho-ROCK pathway has been indicated to be an important molecular switch that controls stem cell lineage commitment. The commitment of hBMSCs and MSCs into osteoblasts or adipocytes have been demonstrated to be regulated by ROCK signaling (McBeath et al. 2004, Kilian et al. 2010). Additionally, ROCK also regulates the switch between adipogenesis and myogenesis (Sordella et al. 2003). The qualitative Oil Red O results of this study revealed that the inhibition of ROCK induced substantial adipogenic differentiation in AM but also to a less extent in OM condition. In the presence of 10 μ M, 15 μ M and 25 μ M ROCK inhibitor in adipogenic medium, large red-stained lipid-rich vacuoles were apparent. The addition of all three ROCK inhibitor concentrations caused predominantly increased adipogenesis in comparison with the untreated cells in AM. Large fat vacuoles were also present in the osteogenic medium supplemented with ROCK inhibitor, however, with minor extent than in AM. In BM, on the contrary, there was no detectable induction of adipogenesis either in control samples or with any concentrations of ROCK inhibitor. Gene expression studies (RT-PCR) conducted in our group confirmed these results in genetic level (unpublished data). PCR studies indicated that the hASCs expressed increased levels of the master regulator of adipogenesis, PPAR γ , when treated with 15 μ M ROCK inhibitor. The expression of PPAR γ was higher in AM supplemented with ROCK inhibitor than in the AM control samples.

The results obtained from the present study are convergent with the reviewed literature. Studies of McBeath et al. (2004), Arnsdorf et al. (2009) and Kilian et al. (2010) also witnessed the importance of cell morphology to stem cell differentiation. Lack of ROCK activity leads to disruption of the cytoskeleton and cytoplasmic tension leading to rounded morphology. The rounded shape of the cells, on the other hand, is a strong signal in initiating adipogenic differentiation. These findings together with previous studies demonstrate that the cell morphology, regulated through ROCK signaling, is an essential regulator of hASC differentiation.

ROCK is one of the pathways mediating extracellular physical stimuli through mechanotransduction. The cytoskeletal effects as a response of mechanical forces, such as matrix stiffness, can guide the differentiation process in MSCs. In the future studies, it will be increasingly important to study the effects of mechanical stimuli on hASC differentiation. The impact of forces

surrounding the cells becomes more important in the *in vivo* situation. The information gained from studies of the impact of the mechanical stimulations would guide the design and the biomaterial surfaces of the tissue engineering constructs.

6.4 FAK mediated attachment is required for the hASC osteogenic differentiation

Focal adhesions are the essential links connecting cells to the surrounding ECM through integrins (Tilghman, Parsons 2008), whereas FAK is the trafficker of the extracellular messages (Liu, Calderwood & Ginsberg 2000). As well as ROCK also FAK has been shown to be an important mediator of mechanotransduction pathways by both responding to substrate rigidity on the outside of the cell and regulating cellular tension via the actin cytoskeleton (Tilghman, Parsons 2008). In the present study, FAK activation was inhibited with a FAK specific inhibitor, PF-562271 to find out the relevance of cell adhesion to the intracellular events of hASCs. The main research problem was whether the lack of adequate cell-ECM contacts prevents the differentiation of hASCs.

The inhibitor used in the present study PF-562271 (formula: $C_{21}H_{20}F_3N_7O_3S$, Selleck Chemicals) is a small-molecule inhibitor of FAK that has been extensively used in analyses associated with different kind of tumors (Roberts et al. 2008, Sun et al. 2010, Wiemer et al. 2013). The functionality of the FAK inhibitor was evaluated with Western Blot by determining the ratio of basal and phosphorylated FAK proteins from the 7 day band intensities of immunoblotted samples. The activation of FAK was distinctly lowered when the samples were treated with FAK inhibitor compared to the untreated samples in BM, OM and AM with HFSC 8/13 cell line (Figure 21). That said, with HFSC 9/13 cell line, the FAK inhibitor suppressed the activation of FAK only in OM and, conversely, the activation of FAK was slightly increased in BM and AM (Appendices 6 and 7). This may denote the lineage specific operability of the inhibitor molecule. However, based on the LIVE/DEAD[®] cell viability test and the CyQUANT[®] cell proliferation test, the inhibitor can be stated operational, since the inhibitor addition led to similar results in all of the cell lines studied. To confirm the functionality of the FAK inhibitor, the Western Blot experiment should be repeated and done also with other hASC lines.

To our knowledge, the inhibitor in question has not been used in comparable studies of cell adhesion in hASCs or hMCSs before. However, a similar compound, PF-573228 (formula: $C_{22}H_{20}F_3N_5O_3S$, Sigma-Aldrich) has been used in hBMSCs and in hDFCs to study the effect of FAK inhibition on osteogenic and adipogenic differentiation. Studies with the PF-573228 inhibitor has demonstrated the importance of cell attachment to the differentiation potential. Based on the literature reviewed, FAK inhibition with PF-573228 or FAK silencing using FAK-specific siRNA resulted in

decreased FAK activation and therefore reduced levels of osteogenic differentiation markers (Salasznyk et al. 2007, Shih et al. 2011, Viale-Bouroncle, Gosau & Morsczeck 2014b).

The results of this study support the previous findings. The expression of osteogenic markers studied was distinctly lowered as a result of FAK inhibition, although the scope of methods in this study included only the analyses of ALP activity and the matrix mineralization. In the present study, the ALP activity was more evident at 14 day time point. Significant ALP activation had occurred in the control OM condition, and also less extent in OM supplemented with 0,5 μ M FAK inhibitor. The inhibition of FAK signaling caused a dose-dependent decrease in ALP activity in three of the cell lines studied. Two highest inhibitor concentrations (2 μ M and 5 μ M) caused the most significant reduction in ALP activity. The late osteogenic differentiation was also hindered with FAK inhibition. Based on qualitative and quantitative Alizarin Red analysis, calcium deposition was induced only in untreated cells in OM and in OM supplemented with 0,5 μ M FAK inhibitor. In the presence of the two higher inhibitor concentrations, the cells failed to deposit any detectable calcium. In sum, the osteogenesis of hASC lines was efficiently blocked with increasing concentrations of FAK inhibitor. Also studies of gene expression have marked this suppressing effect. In the study of Shih and co-workers (2011) a significant reduction in gene expression of type 1 collagen and osteocalcin were demonstrated in the presence of 100nM PF-573228.

In addition of being a positive regulator of osteogenesis, a study published last year claims that FAK work as a negative regulator of adipogenesis in MCSs isolated from bone marrow (Xu, Ju & Song 2014). In the study of Xu and co-workers, FAK inhibition was shown to increase the expression of adipogenic markers such as PPAR γ and promote the formation of lipid droplets in hBMSCs (Xu, Ju & Song 2014). Contrary to these results, our results indicate that the adipogenesis is dose-dependently suppressed with PF-562271. However, the weakest concentration (0,5 μ M) enhanced the formation of large lipid rich vacuoles with three of the hASC lines studied. Additionally, some degree of adipogenic differentiation in AM supplemented with 2 μ M FAK inhibitor was observed with HFSC1/14 cell line. On the contrary, the adipogenic differentiation was suppressed in the other three cell lines studied when supplemented with 2 μ M or 5 μ M PF-562271.

This difference may be explained with the high proliferation rate of the 1/14 cell line. The cell densities in the wells containing 1/14 cell line were visibly much higher than the wells of 1/13, 8/13 or 9/13 cell lines. In MSCs the high cell density has been found to induce adipogenic differentiation and increase the formation of fat vacuoles (McBeath et al. 2004). In our study, the high cell density supported cell attachment and simultaneously worked against the detaching effect of the FAK inhibitor. Thus, with the 1/14 cell line, the cell density in AM supplemented with 2 μ M was still high enough to support the adipogenesis. As a conclusion, the decreasing effect of FAK inhibition on

adipogenesis was accompanied with the inhibitor's decreasing effect on cell amount. Whether the adipogenesis is decreased because of too low cell density as a result of the detaching effect of the inhibitor or through other mechanisms remains unknown.

6.5 Functional MEK-ERK signaling is required in the hASC differentiation

The MAPK signaling pathways, especially the ERK pathway, have been suggested to be critical for osteogenic differentiation in hBMSCs (Jaiswal et al. 2000, Shih et al. 2011). To determine the involvement of MEK-ERK signaling in hASC differentiation the cells were treated with specific inhibitor of this pathway, MEK inhibitor PD98059. Three inhibitor concentrations were chosen to this study: 30 μ M, 40 μ M and 60 μ M, based on prior optimization done in our research group.

The functionality of the MEK inhibitor was confirmed with Western Blot and immunodetection of ERK2 and pERK1/2 signaling proteins. The ratio of basal and phosphorylated ERK was determined from the 7 day band intensities. MEK inhibitor distinctly lowered the amount of activated ERK compared to the control samples in BM, OM and AM, indicating the operability of the inhibitor.

The significance of MEK-ERK signaling for osteogenic differentiation of hASCs was studied by evaluating the ALP activity and matrix mineralization as a response of addition of MEK inhibitor PD98059. Based on these results, the effect of MEK-ERK inhibition on osteogenesis was apparent: the osteogenesis was significantly suppressed. The ALP activity and the calcium deposition were radically suppressed in a dose-dependent manner with all inhibitor concentrations tested. The present study showed that the culture media (BM, OM or AM) supplemented with 60 μ M PD98059 failed to deposit any detectable calcium throughout the 21 day culture period. Taken together, the osteogenesis of hASCs was efficiently blocked by preventing the phosphorylation and activation of ERK signaling. The results of the present study were convergent with the existing inhibition studies with PD98059 in hASCs (Liu et al. 2009, Gu et al. 2011) and in hBMSCs (Jaiswal et al. 2000).

Jaiswal et al. (2000) showed that the inhibition of ERK activation with PD98059 resulted in concentration-dependent inhibition of ALP activity at 7 day time point. In addition to ALP activity, ECM mineralization was declined by the inhibitor as well: there was no evidence of calcium formation in MSCs grown in medium containing 50 μ M inhibitor (Jaiswal et al. 2000). Similar results were obtained in 2011 in the study of Gu and co-workers. The inhibition of hASCs with PD98059 blocked the osteogenic differentiation in a dose-dependent manner as seen in decreased ALP activity, weakened extracellular deposition of calcium and the suppressed secretion of osteocalcin (Gu et al. 2011). The importance of MEK-ERK signaling in osteogenesis has also been demonstrated with other chemical inhibitors of the signal transduction (Kilian et al. 2010, Shih et al. 2011) and with murine cells (Xiao et al. 2000, Zhao et al. 2012).

While simultaneously decreasing osteogenesis, the PD98059 inhibitor has been shown to induce adipogenesis in hASCs and hBMSCs in a dose-dependent manner. This is shown by lipid droplet accumulation and the increased expression of adipogenesis-relative genes (Jaiswal et al. 2000, Liu et al. 2009, Kilian et al. 2010). On the contrary to the literature reviewed, the present study denotes that the inhibition of MEK-ERK signaling does not induce adipogenesis in the human adipose stem cell lines studied. Based on the results of Oil Red O staining, the inhibition of MEK-ERK cascade with MEK inhibitor PD98059 slightly suppressed the lipid accumulation in dose-dependent manner compared to the control samples. Large red-stained lipid vacuoles were only seen at 21 day time point in adipogenic medium control and to less extent in the two lowest concentrations of PD98059 in AM. Similar results were obtained from the RT-PCR studies done in our group (unpublished data). The expression of PPAR γ was not increased compared to the control samples. Instead, OM supplemented with 30 μ M MEK inhibitor markedly reduced the expression of PPAR γ .

This study reveals the importance of MEK-ERK signaling to both osteogenic and adipogenic differentiation potential of hASCs. The cascade is involved in various important cellular events in addition to differentiation, including the control of cell survival, proliferation, metabolism and migration (Jaiswal et al. 2000, Takacs-Vellai 2014). Hence, the inhibition of this signaling may affect hASC differentiation potential directly or indirectly through the inhibition of other cellular effects. Further investigation is needed to understand the cellular mechanisms of this cascade in detail.

6.6 Cross-talk between ROCK, FAK and MEK-ERK cascades

Instead of being separate, the intracellular signaling pathways are highly interconnected, affecting each other in various ways. Hence, the communication between ROCK, FAK and MEK-ERK cascades must be considered in the differentiation process of hASCs.

The inhibition of ROCK has been shown to affect other intracellular signaling cascades. In study of Shih et al. (2011), ROCK inhibition down-regulated both FAK and ERK1/2 activation after 3 days of osteogenic induction in bone marrow stem cells (Shih et al. 2011). In the present study, the activation of FAK and ERK2 were studied at 3 and 7 day time points with Western Blot and immunodetection of FAK, pFAK, ERK2 and pERK1/2 signaling proteins. The ratio of basal and phosphorylated FAK and ERK were determined from the 7 day band intensities. This ratio works as a tool for evaluating the activation of signaling pathways. The inhibition of ROCK repressed the extent of FAK and ERK activation with HFSC 8/13 cell line (Figure 21). However, opposite results were obtained with the 9/13 cell line: the inhibition of ROCK increased the activation of both FAK and ERK (Appendices 6 and 7). The decreasing effect of ROCK inhibition to FAK activation can be explained by the inhibitor effect to the cytoskeleton of the cells. In the presence of ROCK inhibitor,

the cells are less spread and more rounded leading to decreased amount of focal adhesions (Mathieu, Lobo 2012), and hence less FAK activation. The differences in the results could be explained by the possible morphological differences between the cell lines in the presence of ROCK inhibitor. However, the morphology of the cells should be studied before further conclusions can be made.

FAK is involved in various signaling cascades as well. Inhibition studies of FAK have revealed that the inhibition of FAK also down-regulates the ERK1/2 activation (Salasznyk et al. 2007, Shih et al. 2011, Wiemer et al. 2013). The results of the present study support the previously obtained results. The activation of ERK was decreased compared to the control samples in the presence of 2 μ M FAK inhibitor in BM, OM and AM conditions. The results were coherent between the two cell lines studied. The down-regulation of ERK signaling as a result of FAK inhibition may indicate that ERK is a downstream target of FAK mediated cell signaling. The MAPK pathways ERK, JNK and p38 are known to be activated by mechanical stimuli (Kilian et al. 2010) and the cross-talk between FAK and ERK signaling can be one possible way for mediating the intracellular signaling events regulated by extracellular mechanical forces.

6.7 Donor variation

Donor variation affects the interpretation of the results, regardless of the analysis method. The variation in the adipose tissue samples diminishes the statistical significance of the results. The differences in the tissue samples and hASC lines derived from the samples may arise from donor age, body mass index (BMI), sample type (liposuction/tissue biopsy) (Buschmann et al. 2013, Gnanasegaran et al. 2014), the harvesting technique (Iyyanki et al. 2015) and harvesting site (Peptan, Hong & Mao 2006). In the present study, the isolation procedure should cause minimal variation to the samples, since a standardized isolation protocol is used in the Adult stem cell group.

In the present study, donor variation was seen particularly in the proliferation speed of the cell lines and in the analysis of ALP activity. The proliferation of the HFSC 1/14 cell line was markedly higher compared to the other hASC lines used in the study. This was seen in all the experiments. During the 21 day culture period in Oil Red O experiment, the cells were overgrown in some of the wells in BM and OM conditions. When the cells reached their confluency, they started to detach from the borders of the wells as a uniform cell layer. With the other three cell lines, the cell layers remained attached to the plastic culture vessels the whole culture period. The cell lines used were isolated from adipose tissue samples (subcutaneous fat from abdomen or breast) of four female donors aged 33-55. Interestingly, the 1/14 cell line was derived from the youngest donor, with a 10 year age difference to the following aged donor. Additionally, the freezing process and cryostorage of hASCs has been noted to have deleterious effects on the cell proliferation and differentiation (James et al. 2011). The

1/14 cell line was the most recently isolated from the cell lines studied, thus the cryostorage time was also shorter in comparison with the other cell lines. In sum, the donor age and the duration of the cryostorage may explain the high proliferation rate of the 1/14 cell line.

When considering the ALP activity analysis, HFSC 9/13 cell line appeared to exhibit the highest differentiation potential towards bone tissue. 9/13 cells expressed slightly more ALP activity at day 7 compared to the other cell lines. In other words, there was signs of osteogenic differentiation already after 7 days of culture. Since the ALP activity was already seen at day 7, the relative ALP activity values at 14 day time point were lower than in the other cell lines. This is due to the mathematical operation that gives the relative values: the ALP result is initially divided with CyQUANT® results, and then the results from the other samples are presented relative to 7 day BM control sample, given value 1. Because of this calculation method, the resulting values are biased and do not represent the actual values. Thus, instead of comparing the exact values between different inhibitor experiments, the ALP activity trends should be compared.

In ROCK and FAK experiments, there was a concentration-dependent repression in ALP activity with three of the cell lines studied. With 9/13 cell line, such dependency was not observed. This difference may stem from the high ALP activity seen in 9/13 cells. Absorbances of the samples were measured with Wallac Victor microplate reader at 405 nm. The absorbance results can be considered reliable when the absorbance values range from 0 to 2,5. In the ALP activity results obtained from the present study the highest absorbances were over 2,5 and thus not reliable. Dilution of the samples would ensure that the results are reliable and allow the inspection of the samples with highly activated ALP.

Finally, as only two or four hASC lines were studied depending on the analysis, no general deductions of hASC differentiation potential can be made. In order to form general conclusions, more adipose stem cell lines need to be analyzed. In addition, the experiments should be repeated to confirm the findings of this study.

7. CONCLUSIONS

The aim of my thesis work was to evaluate the significance of cell adhesion and cell morphology to hASC differentiation potential towards osteoblasts and adipocytes. My primary goal was to analyze the ROCK, FAK and MEK-ERK signaling in hASC differentiation. Specific inhibitor molecules (ROCK inhibitor Y-27632, FAK inhibitor PF-562271 and MEK inhibitor PD98059) were used to block the signal transduction in these cascades. Additionally, the inhibitor effect on cell morphology, viability, proliferation and differentiation was evaluated.

The main conclusions of this thesis are:

1. Based on the results, ROCK, FAK and MEK inhibitors reduce cell proliferation dose-dependently. FAK and MEK inhibitors have the most significant decreasing effect on the cell amount, most likely caused by the detachment of the cells from the culture plates. The adherent hASCs studied were predominantly viable.
2. Adipose stem cells isolated from four donors (four hASC lines) possess the ability of multilineage differentiation at least into two lineages, as confirmed by the evidence of osteogenic and adipogenic differentiation *in vitro*.
3. This work confirms that the cell attachment is a critical step for promoting the osteogenic differentiation of hASCs. Disruption of the cell adhesion with FAK or ROCK inhibition suppresses the osteogenic differentiation, as evidenced by decreased ALP activity and mineralization of the extracellular matrix.
4. This work further confirms that cell morphology works as a cue that guides hASC lineage commitment. Spread actin cytoskeleton of the cells induces osteogenesis while the disruption of cytoskeleton with ROCK inhibition leads to rounded cells favouring adipogenic commitment.
5. ROCK protein works as a molecular switch between adipogenesis and osteogenesis in the hASC lines studied. Normal functionality of ROCK pathway is required for the osteogenic differentiation of hASCs while lack of functional ROCK guides the differentiation towards adipogenesis.
6. Functional MEK-ERK pathway is a prerequisite for various intracellular processes in hASCs including cell proliferation and differentiation.
7. The results suggest, that the differentiation process of hASCs *in vitro* is guided by a cross-talk between ROCK, FAK and MEK-ERK signaling cascades.

8. REFERENCES

- Arnsdorf, E.J., Tummala, P., Kwon, R.Y. & Jacobs, C.R. 2009, "Mechanically induced osteogenic differentiation - The role of RhoA, ROCKII and cytoskeletal dynamics", *Journal of cell science*, vol. 122, no. 4, pp. 546-553.
- Arribas, M.I., Ropero, A.B., Reig, J.A., Fraga, M.F., Fernandez, A.F., Santana, A. & Roche, E. 2014, "Negative neuronal differentiation of human adipose-derived stem cell clones", *Regenerative medicine*, vol. 9, no. 3, pp. 279-293.
- Bessa, P.C., Cerqueira, M.T., Rada, T., Gomes, M.E., Neves, N.M., Nobre, A., Reis, R.L. & Casal, M. 2009, "Expression, purification and osteogenic bioactivity of recombinant human BMP-4, -9, -10, -11 and -14.", *Protein Expression & Purification*, vol. 63, no. 2, pp. 89-94.
- Biggs, M.J. & Dalby, M.J. 2010, "Focal adhesions in osteoneogenesis", *Proceedings of the Institution of Mechanical Engineers.Part H, Journal of engineering in medicine*, vol. 224, no. 12, pp. 1441-1453.
- Bonfield, T.L. & Caplan, A.I. 2010, "Adult mesenchymal stem cells: an innovative therapeutic for lung diseases", *Discovery medicine*, vol. 9, no. 47, pp. 337-345.
- Brignier, A.C. & Gewirtz, A.M. 2010, "Embryonic and adult stem cell therapy", *The Journal of allergy and clinical immunology*, vol. 125, no. 2 Suppl 2, pp. S336-344.
- Bunnell, B.A., Flaat, M., Gagliardi, C., Patel, B. & Ripoll, C. 2008, "Adipose-derived stem cells: isolation, expansion and differentiation", *Methods (San Diego, Calif.)*, vol. 45, no. 2, pp. 115-120.
- Buschmann, J., Gao, S., Harter, L., Hemmi, S., Welti, M., Werner, C.M., Calcagni, M., Cinelli, P. & Wanner, G.A. 2013, "Yield and proliferation rate of adipose-derived stromal cells as a function of age, body mass index and harvest site-increasing the yield by use of adherent and supernatant fractions?", *Cytotherapy*, vol. 15, no. 9, pp. 1098-1105.
- Caplan, A.I. 1994, "The mesengenic process", *Clinics in plastic surgery*, vol. 21, no. 3, pp. 429-435.
- Caplan, A.I. & Bruder, S.P. 2001, "Mesenchymal stem cells: building blocks for molecular medicine in the 21st century", *Trends in molecular medicine*, vol. 7, no. 6, pp. 259-264.
- Cary, L.A. & Guan, J.L. 1999, "Focal adhesion kinase in integrin-mediated signaling", *Frontiers in bioscience : a journal and virtual library*, vol. 4, pp. D102-113.
- Celil, A.B. & Campbell, P.G. 2005, "BMP-2 and insulin-like growth factor-I mediate Osterix (Osx) expression in human mesenchymal stem cells via the MAPK and protein kinase D signaling pathways", *The Journal of biological chemistry*, vol. 280, no. 36, pp. 31353-31359.
- Chen, J.C. & Jacobs, C.R. 2013, "Mechanically induced osteogenic lineage commitment of stem cells", *Stem cell research & therapy*, vol. 4, no. 5, pp. 107-117.
- Choumerianou, D.M., Dimitriou, H. & Kalmanti, M. 2008, "Stem cells: promises versus limitations", *Tissue engineering.Part B, Reviews*, vol. 14, no. 1, pp. 53-60.

- Colello, D., Mathew, S., Ward, R., Pumiglia, K. & LaFlamme, S.E. 2012, "Integrins regulate microtubule nucleating activity of centrosome through mitogen-activated protein kinase/extracellular signal-regulated kinase/extracellular signal-regulated kinase (MEK/ERK) signaling", *The Journal of biological chemistry*, vol. 287, no. 4, pp. 2520-2530.
- Dominici, M., Le Blanc, K., Mueller, I., Slaper-Cortenbach, I., Marini, F., Krause, D., Deans, R., Keating, A., Prockop, D. & Horwitz, E. 2006, "Minimal criteria for defining multipotent mesenchymal stromal cells. The International Society for Cellular Therapy position statement.", *Cytotherapy*, vol. 8, no. 4, pp. 315-317.
- Dunty, J.M., Gabarra-Niecko, V., King, M.L., Ceccarelli, D.F., Eck, M.J. & Schaller, M.D. 2004, "FERM domain interaction promotes FAK signaling", *Molecular and cellular biology*, vol. 24, no. 12, pp. 5353-5368.
- Fantini, M.C., Becker, C., Kiesslich, R. & Neurath, M.F. 2006, "Drug insight: novel small molecules and drugs for immunosuppression", *Nature clinical practice.Gastroenterology & hepatology*, vol. 3, no. 11, pp. 633-644.
- Franco Lambert, A.P., Fraga Zandonai, A., Bonatto, D., Cantarelli Machado, D. & Pegas Henriques, J.A. 2009, "Differentiation of human adipose-derived adult stem cells into neuronal tissue: does it work?", *Differentiation; research in biological diversity*, vol. 77, no. 3, pp. 221-228.
- Frisch, S.M. & Screaton, R.A. 2001, "Anoikis mechanisms", *Current opinion in cell biology*, vol. 13, no. 5, pp. 555-562.
- Galateanu, B., Dinescu, S., Cimpean, A., Dinischiotu, A. & Costache, M. 2012, "Modulation of adipogenic conditions for prospective use of hADSCs in adipose tissue engineering", *International journal of molecular sciences*, vol. 13, no. 12, pp. 15881-15900.
- Ge, C., Xiao, G., Jiang, D., Yang, Q., Hatch, N.E., Roca, H. & Franceschi, R.T. 2009, "Identification and functional characterization of ERK/MAPK phosphorylation sites in the Runx2 transcription factor", *The Journal of biological chemistry*, vol. 284, no. 47, pp. 32533-32543.
- Giannitelli, S.M., Basoli, F., Mozetic, P., Piva, P., Bartuli, F.N., Luciani, F., Arcuri, C., Trombetta, M., Rainer, A. & Licocchia, S. 2015, "Graded porous polyurethane foam: A potential scaffold for oro-maxillary bone regeneration", *Materials science & engineering.C, Materials for biological applications*, vol. 51, pp. 329-335.
- Gilmore, A.P. 2005, "Anoikis", *Cell death and differentiation*, vol. 12, Suppl 2, pp. 1473-1477.
- Gimble, J. & Guilak, F. 2003, "Adipose-derived adult stem cells: isolation, characterization, and differentiation potential", *Cytotherapy*, vol. 5, no. 5, pp. 362-369.
- Gnanasegaran, N., Govindasamy, V., Musa, S. & Kasim, N.H. 2014, "Different isolation methods alter the gene expression profiling of adipose derived stem cells", *International journal of medical sciences*, vol. 11, no. 4, pp. 391-403.
- Golubovskaya, V.M. & Cance, W.G. 2007, "Focal adhesion kinase and p53 signaling in cancer cells", *International review of cytology*, vol. 263, pp. 103-153.

- Golubovskaya, V.M., Nyberg, C., Zheng, M., Kweh, F., Magis, A., Ostrov, D. & Cance, W.G. 2008, "A small molecule inhibitor, 1,2,4,5-benzenetetraamine tetrahydrochloride, targeting the y397 site of focal adhesion kinase decreases tumor growth.", *Journal of medicinal chemistry*, vol. 51, no. 23, pp. 7405-7416.
- Greenblatt, M.B., Shim, J.H. & Glimcher, L.H. 2013, "Mitogen-activated protein kinase pathways in osteoblasts", *Annual Review of Cell and Developmental Biology*, vol. 29, pp. 63-79.
- Gu, H., Guo, F., Zhou, X., Gong, L., Zhang, Y., Zhai, W., Chen, L., Cen, L., Yin, S., Chang, J. & Cui, L. 2011, "The stimulation of osteogenic differentiation of human adipose-derived stem cells by ionic products from akermanite dissolution via activation of the ERK pathway", *Biomaterials*, vol. 32, no. 29, pp. 7023-7033.
- Gumbiner, B.M. 1996, "Cell adhesion: the molecular basis of tissue architecture and morphogenesis", *Cell*, vol. 84, no. 3, pp. 345-357.
- Guo, W. & Giancotti, F.G. 2004, "Integrin signalling during tumour progression", *Nature reviews.Molecular cell biology*, vol. 5, no. 10, pp. 816-826.
- Hehlgans, S., Haase, M. & Cordes, N. 2007, "Signalling via integrins: implications for cell survival and anticancer strategies", *Biochimica et biophysica acta*, vol. 1775, no. 1, pp. 163-180.
- Hipp, J. & Atala, A. 2008, "Sources of stem cells for regenerative medicine", *Stem cell reviews*, vol. 4, no. 1, pp. 3-11.
- Horwitz, E.M., Le Blanc, K., Dominici, M., Mueller, I., Slaper-Cortenbach, I., Marini, F.C., Deans, R.J., Krause, D.S., Keating, A. & International Society for Cellular Therapy 2005, "Clarification of the nomenclature for MSC: The International Society for Cellular Therapy position statement", *Cytotherapy*, vol. 7, no. 5, pp. 393-395.
- Iyyanki, T., Hubenak, J., Liu, J., Chang, E.I., Beahm, E.K. & Zhang, Q. 2015, "Harvesting technique affects adipose-derived stem cell yield", *Aesthetic surgery journal / the American Society for Aesthetic Plastic surgery*, vol. 35, no. 4, pp. 467-476.
- Jaiswal, R.K., Jaiswal, N., Bruder, S.P., Mbalaviele, G., Marshak, D.R. & Pittenger, M.F. 2000, "Adult human mesenchymal stem cell differentiation to the osteogenic or adipogenic lineage is regulated by mitogen-activated protein kinase.", *Journal of Biological Chemistry*, vol. 275, no. 13, pp. 9645-9652.
- James, A.W. 2013, "Review of Signaling Pathways Governing MSC Osteogenic and Adipogenic Differentiation.", *Scientifica (Cairo)*, vol. 2013, Article ID 684736, Epub.
- James, A.W., Levi, B., Nelson, E.R., Peng, M., Commons, G.W., Lee, M., Wu, B. & Longaker, M.T. 2011, "Deleterious effects of freezing on osteogenic differentiation of human adipose-derived stromal cells in vitro and in vivo", *Stem cells and development*, vol. 20, no. 3, pp. 427-439.
- Jones, L.J., Gray, M., Yue, S.T., Haugland, R.P. & Singer, V.L. 2001, "Sensitive determination of cell number using the CyQUANT cell proliferation assay.", *Journal of immunological methods*, vol. 254, no. 1-2, pp. 85-98.

- Kern, S., Eichler, H., Stoeve, J., Kluter, H. & Bieback, K. 2006, "Comparative analysis of mesenchymal stem cells from bone marrow, umbilical cord blood, or adipose tissue.", *Stem cells*, vol. 24, no. 5, pp. 1294-1301.
- Kilian, K.A., Bugarija, B., Lahn, B.T. & Mrksich, M. 2010, "Geometric cues for directing the differentiation of mesenchymal stem cells.", *Proceedings of the National Academy of Sciences of the United States of America*, vol. 107, no. 11, pp. 4872-4877.
- Kuo, J.C. 2013, "Mechanotransduction at focal adhesions: integrating cytoskeletal mechanics in migrating cells", *Journal of Cellular & Molecular Medicine*, vol. 17, no. 6, pp. 704-712.
- Kyllonen, L., Haimi, S., Mannerstrom, B., Huhtala, H., Rajala, K.M., Skottman, H., Sandor, G.K. & Miettinen, S. 2013, "Effects of different serum conditions on osteogenic differentiation of human adipose stem cells in vitro", *Stem cell research & therapy*, vol. 4, no. 1, pp. 17-32.
- Lamas, N.J., Serra, S.C., Salgado, A.J. & Sousa, N. 2015, "Failure of Y-27632 to improve the culture of adult human adipose-derived stem cells", *Stem cells and cloning : advances and applications*, vol. 8, pp. 15-26.
- Legate, K.R., Wickstrom, S.A. & Fassler, R. 2009, "Genetic and cell biological analysis of integrin outside-in signaling", *Genes & development*, vol. 23, no. 4, pp. 397-418.
- Levi, B. & Longaker, M.T. 2011, "Concise review: adipose-derived stromal cells for skeletal regenerative medicine", *Stem cells (Dayton, Ohio)*, vol. 29, no. 4, pp. 576-582.
- Li, H., Zimmerlin, L., Marra, K.G., Donnenberg, V.S., Donnenberg, A.D. & Rubin, J.P. 2011, "Adipogenic potential of adipose stem cell subpopulations", *Plastic and Reconstructive Surgery*, vol. 128, no. 3, pp. 663-672.
- Lim, S.T., Mikolon, D., Stupack, D.G. & Schlaepfer, D.D. 2008, "FERM control of FAK function: implications for cancer therapy", *Cell cycle (Georgetown, Tex.)*, vol. 7, no. 15, pp. 2306-2314.
- Lin, G.L. & Hankenson, K.D. 2011, "Integration of BMP, Wnt, and notch signaling pathways in osteoblast differentiation", *Journal of cellular biochemistry*, vol. 112, no. 12, pp. 3491-3501.
- Lindroos, B., Boucher, S., Chase, L., Kuokkanen, H., Huhtala, H., Haataja, R., Vemuri, M., Suuronen, R. & Miettinen, S. 2009, "Serum-free, xeno-free culture media maintain the proliferation rate and multipotentiality of adipose stem cells in vitro", *Cytotherapy*, vol. 11, no. 7, pp. 958-972.
- Lindroos, B., Suuronen, R. & Miettinen, S. 2011, "The potential of adipose stem cells in regenerative medicine", *Stem cell reviews*, vol. 7, no. 2, pp. 269-291.
- Liu, Q., Cen, L., Zhou, H., Yin, S., Liu, G., Liu, W., Cao, Y. & Cui, L. 2009, "The role of the extracellular signal-related kinase signaling pathway in osteogenic differentiation of human adipose-derived stem cells and in adipogenic transition initiated by dexamethasone", *Tissue engineering. Part A*, vol. 15, no. 11, pp. 3487-3497.
- Liu, S., Calderwood, D.A. & Ginsberg, M.H. 2000, "Integrin cytoplasmic domain-binding proteins", *Journal of cell science*, vol. 113, no. Pt 20, pp. 3563-3571.

- Mathieu, P.S. & Lobo, E.G. 2012, "Cytoskeletal and focal adhesion influences on mesenchymal stem cell shape, mechanical properties, and differentiation down osteogenic, adipogenic, and chondrogenic pathways.", *Tissue Engineering Part B-Reviews*, vol. 18, no. 6, pp. 436-444.
- McBeath, R., Pirone, D.M., Nelson, C.M., Bhadriraju, K. & Chen, C.S. 2004, "Cell shape, cytoskeletal tension, and RhoA regulate stem cell lineage commitment.", *Developmental Cell*, vol. 6, no. 4, pp. 483-495.
- McKay, M.M. & Morrison, D.K. 2007, "Integrating signals from RTKs to ERK/MAPK", *Oncogene*, vol. 26, no. 22, pp. 3113-3121.
- Miranville, A., Heeschen, C., Sengenès, C., Curat, C.A., Busse, R. & Bouloumie, A. 2004, "Improvement of postnatal neovascularization by human adipose tissue-derived stem cells", *Circulation*, vol. 110, no. 3, pp. 349-355.
- Mitchell, J.B., McIntosh, K., Zvonic, S., Garrett, S., Floyd, Z.E., Kloster, A., Di Halvorsen, Y., Storms, R.W., Goh, B., Kilroy, G., Wu, X. & Gimble, J.M. 2006, "Immunophenotype of human adipose-derived cells: temporal changes in stromal-associated and stem cell-associated markers", *Stem cells (Dayton, Ohio)*, vol. 24, no. 2, pp. 376-385.
- Motamedian, S.R., Hosseinpour, S., Ahsaie, M.G. & Khojasteh, A. 2015, "Smart scaffolds in bone tissue engineering: A systematic review of literature", *World journal of stem cells*, vol. 7, no. 3, pp. 657-668.
- Ng, A.M., Saim, A.B., Tan, K.K., Tan, G.H., Mokhtar, S.A., Rose, I.M., Othman, F. & Idrus, R.B. 2005, "Comparison of bioengineered human bone construct from four sources of osteogenic cells", *Journal of orthopaedic science : official journal of the Japanese Orthopaedic Association*, vol. 10, no. 2, pp. 192-199.
- Niemelä, S.M., Miettinen, S., Konttinen, Y., Waris, T., Kellomäki, M., Ashammakhi, N.A. & Ylikomi, T. 2007, "Fat tissue: views on reconstruction and exploitation.", *Journal of Craniofacial Surgery*, vol. 18, no. 2, pp. 325-335.
- Pakzad, M., Totonchi, M., Taei, A., Seifinejad, A., Hassani, S.N. & Baharvand, H. 2010, "Presence of a ROCK inhibitor in extracellular matrix supports more undifferentiated growth of feeder-free human embryonic and induced pluripotent stem cells upon passaging", *Stem cell reviews*, vol. 6, no. 1, pp. 96-107.
- Pappa, K.I. & Anagnostou, N.P. 2009, "Novel sources of fetal stem cells: where do they fit on the developmental continuum?", *Regenerative medicine*, vol. 4, no. 3, pp. 423-433.
- Pardo, A.M.P., Bryhan, M., Krasnow, H., Hardin, N., Riddle, M., LaChance, O., Gagnon, P., Upton, T. & Hoover, D.S. 2005, *Corning® CellBIND® Surface: An Improved Surface for Enhanced Cell Attachment. Technical Report.*, Corning Incorporated, USA.
- Pasapera, A.M., Schneider, I.C., Rericha, E., Schlaepfer, D.D. & Waterman, C.M. 2010, "Myosin II activity regulates vinculin recruitment to focal adhesions through FAK-mediated paxillin phosphorylation", *The Journal of cell biology*, vol. 188, no. 6, pp. 877-890.

- Passier, R. & Mummery, C. 2003, "Origin and use of embryonic and adult stem cells in differentiation and tissue repair", *Cardiovascular research*, vol. 58, no. 2, pp. 324-335.
- Peptan, I.A., Hong, L. & Mao, J.J. 2006, "Comparison of osteogenic potentials of visceral and subcutaneous adipose-derived cells of rabbits", *Plastic and Reconstructive Surgery*, vol. 117, no. 5, pp. 1462-1470.
- Pittenger, M.F., Mackay, A.M., Beck, S.C., Jaiswal, R.K., Douglas, R., Mosca, J.D., Moorman, M.A., Simonetti, D.W., Craig, S. & Marshak, D.R. 1999, "Multilineage potential of adult human mesenchymal stem cells", *Science (New York, N.Y.)*, vol. 284, no. 5411, pp. 143-147.
- Planat-Benard, V., Menard, C., Andre, M., Puceat, M., Perez, A., Garcia-Verdugo, J.M., Penicaud, L. & Casteilla, L. 2004, "Spontaneous cardiomyocyte differentiation from adipose tissue stroma cells", *Circulation research*, vol. 94, no. 2, pp. 223-229.
- Rajashekhar, G., Traktuev, D.O., Roell, W.C., Johnstone, B.H., Merfeld-Clauss, S., Van Natta, B., Rosen, E.D., March, K.L. & Clauss, M. 2008, "IFATS collection: Adipose stromal cell differentiation is reduced by endothelial cell contact and paracrine communication: role of canonical Wnt signaling", *Stem cells (Dayton, Ohio)*, vol. 26, no. 10, pp. 2674-2681.
- Rangappa, S., Fen, C., Lee, E.H., Bongso, A. & Sim, E.K. 2003, "Transformation of adult mesenchymal stem cells isolated from the fatty tissue into cardiomyocytes", *The Annals of Thoracic Surgery*, vol. 75, no. 3, pp. 775-779.
- Riento, K. & Ridley, A.J. 2003, "Rocks: multifunctional kinases in cell behaviour", *Nature Reviews Molecular Cell Biology*, vol. 4, no. 6, pp. 446-456.
- Roberts, P.J. & Der, C.J. 2007, "Targeting the Raf-MEK-ERK mitogen-activated protein kinase cascade for the treatment of cancer", *Oncogene*, vol. 26, no. 22, pp. 3291-3310.
- Roberts, W.G., Ung, E., Whalen, P., Cooper, B., Hulford, C., Autry, C., Richter, D., Emerson, E., Lin, J., Kath, J., Coleman, K., Yao, L., Martinez-Alsina, L., Lorenzen, M., Berliner, M., Luzzio, M., Patel, N., Schmitt, E., LaGreca, S., Jani, J., Wessel, M., Marr, E., Griffor, M. & Vajdos, F. 2008, "Antitumor activity and pharmacology of a selective focal adhesion kinase inhibitor, PF-562,271", *Cancer research*, vol. 68, no. 6, pp. 1935-1944.
- Rodbell, M. 1964, "Metabolism of Isolated Fat Cells. I. Effects of Hormones on Glucose Metabolism and Lipolysis", *The Journal of biological chemistry*, vol. 239, pp. 375-380.
- Roskoski, R., Jr 2010, "RAF protein-serine/threonine kinases: structure and regulation", *Biochemical and biophysical research communications*, vol. 399, no. 3, pp. 313-317.
- Salasznyk, R.M., Klees, R.F., Williams, W.A., Boskey, A. & Plopper, G.E. 2007, "Focal adhesion kinase signaling pathways regulate the osteogenic differentiation of human mesenchymal stem cells.", *Experimental cell research*, vol. 313, no. 1, pp. 22-37.
- Sanfilippo, S., Canis, M., Ouchchane, L., Botchorishvili, R., Artonne, C., Janny, L. & Brugnon, F. 2011, "Viability assessment of fresh and frozen/thawed isolated human follicles: reliability of two methods (Trypan blue and Calcein AM/ethidium homodimer-1).", *Journal of Assisted Reproduction & Genetics*, vol. 28, no. 12, pp. 1151-1156.

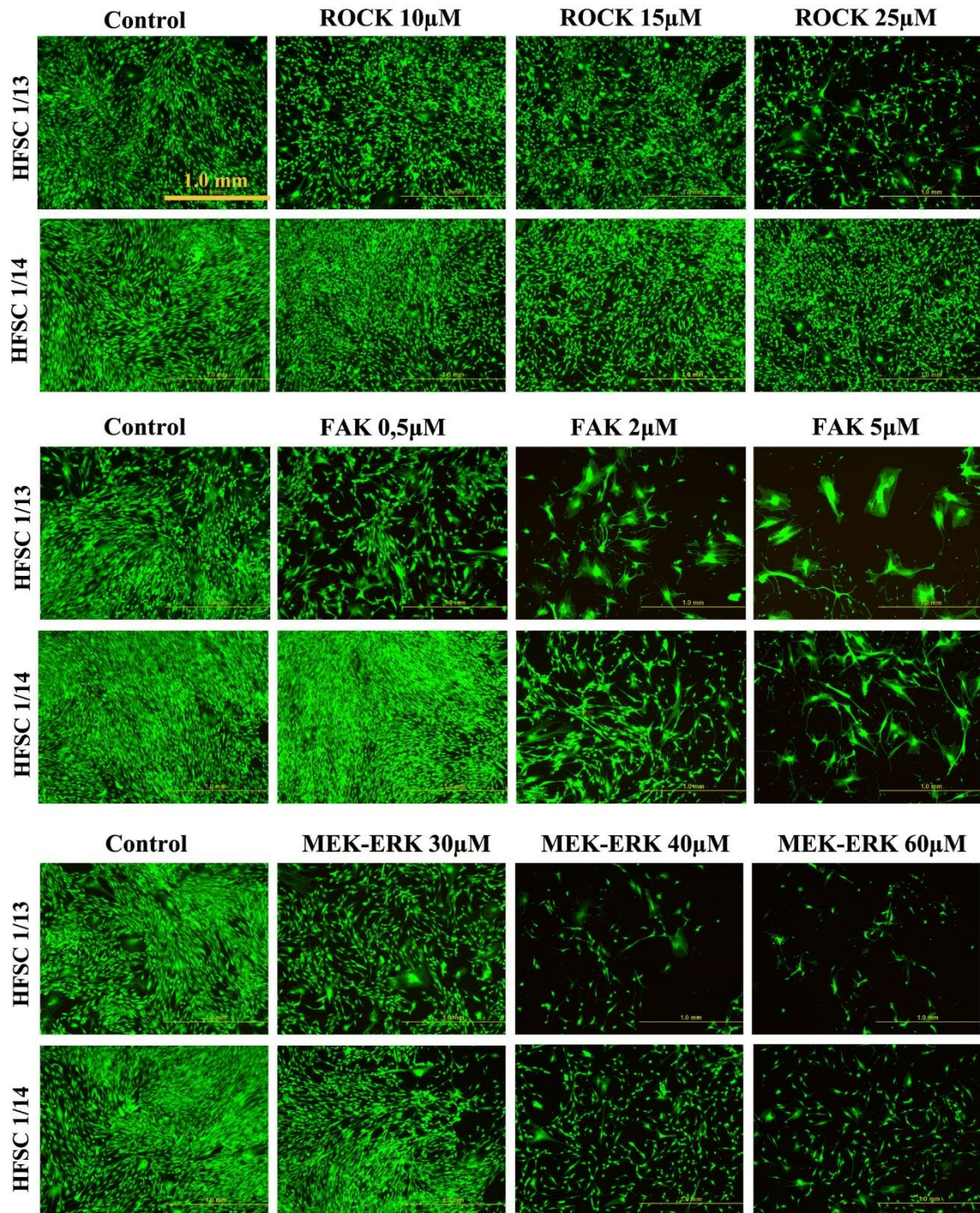
- Santos, A., Bakker, A.D., de Blicck-Hogervorst, J.M. & Klein-Nulend, J. 2010, "WNT5A induces osteogenic differentiation of human adipose stem cells via rho-associated kinase ROCK", *Cytotherapy*, vol. 12, no. 7, pp. 924-932.
- Schaller, M.D. 2001, "Biochemical signals and biological responses elicited by the focal adhesion kinase", *Biochimica et biophysica acta*, vol. 1540, no. 1, pp. 1-21.
- Schaller, M.D., Hildebrand, J.D., Shannon, J.D., Fox, J.W., Vines, R.R. & Parsons, J.T. 1994, "Autophosphorylation of the focal adhesion kinase, pp125FAK, directs SH2-dependent binding of pp60src", *Molecular and cellular biology*, vol. 14, no. 3, pp. 1680-1688.
- Schindeler, A. & Little, D.G. 2006, "Ras-MAPK signaling in osteogenic differentiation: friend or foe?", *Journal of bone and mineral research : the official journal of the American Society for Bone and Mineral Research*, vol. 21, no. 9, pp. 1331-1338.
- Schlaepfer, D.D., Jones, K.C. & Hunter, T. 1998, "Multiple Grb2-mediated integrin-stimulated signaling pathways to ERK2/mitogen-activated protein kinase: summation of both c-Src- and focal adhesion kinase-initiated tyrosine phosphorylation events", *Molecular and cellular biology*, vol. 18, no. 5, pp. 2571-2585.
- Schofield, A.V., Steel, R. & Bernard, O. 2012, "Rho-associated coiled-coil kinase (ROCK) protein controls microtubule dynamics in a novel signaling pathway that regulates cell migration", *The Journal of biological chemistry*, vol. 287, no. 52, pp. 43620-43629.
- Seppanen, R. & Miettinen, S. 2014, "Bone to the chin from adipose-derived stem cells", *Duodecim; laaketieteellinen aikakauskirja*, vol. 130, no. 19, pp. 2009-2016.
- Shih, Y.R., Tseng, K.F., Lai, H.Y., Lin, C.H. & Lee, O.K. 2011, "Matrix stiffness regulation of integrin-mediated mechanotransduction during osteogenic differentiation of human mesenchymal stem cells", *Journal of bone and mineral research : the official journal of the American Society for Bone and Mineral Research*, vol. 26, no. 4, pp. 730-738.
- Sivasubramaniyan, K., Lehnen, D., Ghazanfari, R., Sobiesiak, M., Harichandan, A., Mortha, E., Petkova, N., Grimm, S., Cerabona, F., de Zwart, P., Abele, H., Aicher, W.K., Faul, C., Kanz, L. & Buhning, H.J. 2012, "Phenotypic and functional heterogeneity of human bone marrow- and amnion-derived MSC subsets", *Annals of the New York Academy of Sciences*, vol. 1266, pp. 94-106.
- Sordella, R., Jiang, W., Chen, G.C., Curto, M. & Settleman, J. 2003, "Modulation of Rho GTPase signaling regulates a switch between adipogenesis and myogenesis", *Cell*, vol. 113, no. 2, pp. 147-158.
- Strem, B.M. & Hedrick, M.H. 2005, "The growing importance of fat in regenerative medicine", *Trends in biotechnology*, vol. 23, no. 2, pp. 64-66.
- Strem, B.M., Hicok, K.C., Zhu, M., Wulur, I., Alfonso, Z., Schreiber, R.E., Fraser, J.K. & Hedrick, M.H. 2005, "Multipotential differentiation of adipose tissue-derived stem cells", *The Keio journal of medicine*, vol. 54, no. 3, pp. 132-141.

- Sun, H., Pisle, S., Gardner, E.R. & Figg, W.D. 2010, "Bioluminescent imaging study: FAK inhibitor, PF-562,271, preclinical study in PC3M-luc-C6 local implant and metastasis xenograft models.", *Cancer Biol Ther*, vol. 10, no. 1, pp. 38-43.
- Takacs-Vellai, K. 2014, "The metastasis suppressor Nm23 as a modulator of Ras/ERK signaling", *Journal Of Molecular Signaling*, vol. 9, no.1, pp. 4-11.
- Takahashi, K. & Yamanaka, S. 2006, "Induction of pluripotent stem cells from mouse embryonic and adult fibroblast cultures by defined factors", *Cell*, vol. 126, no. 4, pp. 663-676.
- Thomson, J.A., Itskovitz-Eldor, J., Shapiro, S.S., Waknitz, M.A., Swiergiel, J.J., Marshall, V.S. & Jones, J.M. 1998, "Embryonic stem cell lines derived from human blastocysts", *Science (New York, N.Y.)*, vol. 282, no. 5391, pp. 1145-1147.
- Tietz, N.W., Burtis, C.A., Duncan, P., Ervin, K., Petitclerc, C.J., Rinker, A.D., Shuey, D. & Zygowicz, E.R. 1983, "A reference method for measurement of alkaline phosphatase activity in human serum.", *Clinical chemistry*, vol. 29, no. 5, pp. 751-761.
- Tilghman, R.W. & Parsons, J.T. 2008, "Focal adhesion kinase as a regulator of cell tension in the progression of cancer", *Seminars in cancer biology*, vol. 18, no. 1, pp. 45-52.
- Tirkkonen, L., Haimi, S., Huttunen, S., Wolff, J., Pirhonen, E., Sandor, G.K. & Miettinen, S. 2013, "Osteogenic medium is superior to growth factors in differentiation of human adipose stem cells towards bone-forming cells in 3D culture", *European cells & materials*, vol. 25, pp. 144-158.
- Treiser, M.D., Yang, E.H., Gordonov, S., Cohen, D.M., Androulakis, I.P., Kohn, J., Chen, C.S. & Moghe, P.V. 2010, "Cytoskeleton-based forecasting of stem cell lineage fates", *Proceedings of the National Academy of Sciences of the United States of America*, vol. 107, no. 2, pp. 610-615.
- Van Dijk, A., Niessen, H.W., Zandieh Doulabi, B., Visser, F.C. & van Milligen, F.J. 2008, "Differentiation of human adipose-derived stem cells towards cardiomyocytes is facilitated by laminin", *Cell and tissue research*, vol. 334, no. 3, pp. 457-467.
- Van Kooten, T.G., Spijker, H.T. & Busscher, H.J. 2004, "Plasma-treated polystyrene surfaces: model surfaces for studying cell-biomaterial interactions", *Biomaterials*, vol. 25, no. 10, pp. 1735-1747.
- Van Tam, J.K., Uto, K., Ebara, M., Pagliari, S., Forte, G. & Aoyagi, T. 2012, "Mesenchymal stem cell adhesion but not plasticity is affected by high substrate stiffness", *Science and Technology of Advanced Materials*, vol. 13, no. 6, pp. 64205-64212.
- Varma, M.J., Breuls, R.G., Schouten, T.E., Jurgens, W.J., Bontkes, H.J., Schuurhuis, G.J., van Ham, S.M. & van Milligen, F.J. 2007, "Phenotypical and functional characterization of freshly isolated adipose tissue-derived stem cells", *Stem cells and development*, vol. 16, no. 1, pp. 91-104.
- Velasco, M.A., Narvaez-Tovar, C.A. & Garzon-Alvarado, D.A. 2015, "Design, Materials, and Mechanobiology of Biodegradable Scaffolds for Bone Tissue Engineering", *BioMed research international*, vol. 2015, Article ID 729076, Epub.

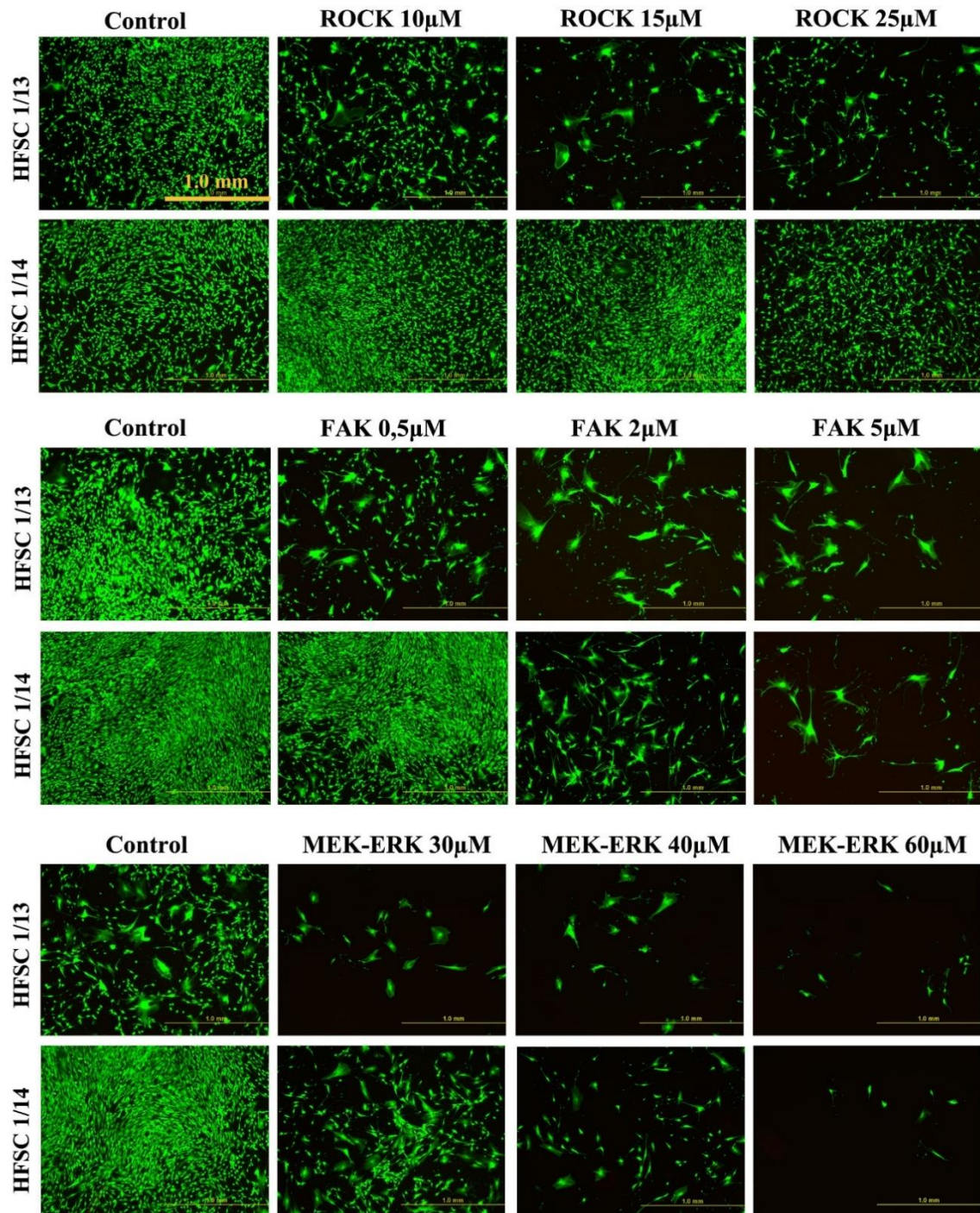
- Vermette, M., Trottier, V., Menard, V., Saint-Pierre, L., Roy, A. & Fradette, J. 2007, "Production of a new tissue-engineered adipose substitute from human adipose-derived stromal cells", *Biomaterials*, vol. 28, no. 18, pp. 2850-2860.
- Viale-Bouroncle, S., Gosau, M. & Morsczeck, C. 2014a, "Laminin regulates the osteogenic differentiation of dental follicle cells via integrin- α 2/ β 1 and the activation of the FAK/ERK signaling pathway.", *Cell Tissue Res*, vol. 357, no. 1, pp. 345-354.
- Viale-Bouroncle, S., Gosau, M. & Morsczeck, C. 2014b, "Collagen I induces the expression of alkaline phosphatase and osteopontin via independent activations of FAK and ERK signalling pathways", *Archives of Oral Biology*, vol. 59, no. 12, pp. 1249-1255.
- Watanabe, K., Ueno, M., Kamiya, D., Nishiyama, A., Matsumura, M., Wataya, T., Takahashi, J.B., Nishikawa, S., Nishikawa, S., Muguruma, K. & Sasai, Y. 2007, "A ROCK inhibitor permits survival of dissociated human embryonic stem cells", *Nature biotechnology*, vol. 25, no. 6, pp. 681-686.
- Weinzierl, K., Hemprich, A. & Frerich, B. 2006, "Bone engineering with adipose tissue derived stromal cells", *Journal of cranio-maxillo-facial surgery : official publication of the European Association for Cranio-Maxillo-Facial Surgery*, vol. 34, no. 8, pp. 466-471.
- Wiemer, A.J., Wernimont, S.A., Cung, T.D., Bennin, D.A., Beggs, H.E. & Huttenlocher, A. 2013, "The focal adhesion kinase inhibitor PF-562,271 impairs primary CD4+ T cell activation", *Biochemical pharmacology*, vol. 86, no. 6, pp. 770-781.
- Wobus, A.M. & Boheler, K.R. 2005, "Embryonic stem cells: prospects for developmental biology and cell therapy", *Physiological Reviews*, vol. 85, no. 2, pp. 635-678.
- Wosnitza, M., Hemmrich, K., Groger, A., Graber, S. & Pallua, N. 2007, "Plasticity of human adipose stem cells to perform adipogenic and endothelial differentiation", *Differentiation; research in biological diversity*, vol. 75, no. 1, pp. 12-23.
- Xiao, G., Jiang, D., Thomas, P., Benson, M.D., Guan, K., Karsenty, G. & Franceschi, R.T. 2000, "MAPK pathways activate and phosphorylate the osteoblast-specific transcription factor, Cbfa1", *The Journal of biological chemistry*, vol. 275, no. 6, pp. 4453-4459.
- Xu, B., Ju, Y. & Song, G. 2014, "Role of p38, ERK1/2, focal adhesion kinase, RhoA/ROCK and cytoskeleton in the adipogenesis of human mesenchymal stem cells", *Journal of bioscience and bioengineering*, vol. 117, no. 5, pp. 624-631.
- Yamanaka, S. 2009, "A fresh look at iPS cells", *Cell*, vol. 137, no. 1, pp. 13-17.
- Yim, E.K. & Sheetz, M.P. 2012, "Force-dependent cell signaling in stem cell differentiation", *Stem cell research & therapy*, vol. 3, no. 5, pp. 41-53.
- Zhang, X., Guo, J., Zhou, Y. & Wu, G. 2014, "The roles of bone morphogenetic proteins and their signaling in the osteogenesis of adipose-derived stem cells", *Tissue Engineering Part B-Reviews*, vol. 20, no. 1, pp. 84-92.

- Zhang, L., Valdez, J.M., Zhang, B., Wei, L., Chang, J. & Xin, L. 2011, "ROCK inhibitor Y-27632 suppresses dissociation-induced apoptosis of murine prostate stem/progenitor cells and increases their cloning efficiency", *PloS one*, vol. 6, no. 3.
- Zhao, Y., Song, T., Wang, W., Wang, J., He, J., Wu, N., Tang, M., He, B. & Luo, J. 2012, "P38 and ERK1/2 MAPKs act in opposition to regulate BMP9-induced osteogenic differentiation of mesenchymal progenitor cells.", *PloS one*, vol. 7, no. 8.
- Zuk, P.A., Zhu, M., Ashjian, P., De Ugarte, D.A., Huang, J.I., Mizuno, H., Alfonso, Z.C., Fraser, J.K., Benhaim, P. & Hedrick, M.H. 2002, "Human adipose tissue is a source of multipotent stem cells", *Molecular biology of the cell*, vol. 13, no. 12, pp. 4279-4295.
- Zuk, P.A., Zhu, M., Mizuno, H., Huang, J., Futrell, J.W., Katz, A.J., Benhaim, P., Lorenz, H.P. & Hedrick, M.H. 2001, "Multilineage cells from human adipose tissue: implications for cell-based therapies", *Tissue engineering*, vol. 7, no. 2, pp. 211-228.

9. APPENDICES



Appendix 1. LIVE/DEAD[®] analysis of hASCs (HFSC 1/13 and 1/14 cell lines) in osteogenic medium condition. The effect of ROCK, FAK and MEK-ERK inhibitors on the cell viability. 500 cells/well were plated and cultured 7 days in BM supplemented with ROCK, FAK and MEK-ERK inhibitors. The cell viability was assessed with LIVE/DEAD[®] staining. The Green fluorescence indicates living cells while red fluorescence dead cells. The wells were imaged with fluorescence microscope, 4X magnification. Scale bar 1,0 mm (the same scale in every image).



Appendix 2. LIVE/DEAD[®] analysis of hASCs (HFSC 1/13 and 1/14 cell lines) in adipogenic medium condition. The effect of ROCK, FAK and MEK-ERK inhibitors on the cell viability. 500 cells/well were plated and cultured 7 days in BM supplemented with ROCK, FAK and MEK-ERK inhibitors. The cell viability was assessed with LIVE/DEAD[®] staining. The Green fluorescence indicates living cells while red fluorescence dead cells. The wells were imaged with fluorescence microscope, 4X magnification. Scale bar 1,0 mm (the same scale in every image).

Appendix 3. P values of the non-parametric Mann-Whitney analysis of the combined CyQUANT® results.

Statistical difference	P value (exact)	P value summary
BM vs. BM + ROCK 10µM	0,0009	***
BM vs. BM + ROCK 15µM	0,0005	***
BM vs. BM + ROCK 25µM	< 0,0001	****
OM vs. OM + ROCK 10µM	0,0386	*
OM vs. OM + ROCK 15µM	0,0083	**
OM vs. OM + ROCK 25µM	0,0009	***
AM vs. AM + ROCK 10µM	0,0881	ns
AM vs. AM + ROCK 15µM	0,0283	*
AM vs. AM + ROCK 25µM	0,0002	***

Statistical difference	P value (exact)	P value summary
BM vs. BM + FAK 0,5µM	0,0029	**
BM vs. BM + FAK 2µM	< 0,0001	****
BM vs. BM + FAK 5µM	< 0,0001	****
OM vs. OM + FAK 0,5µM	0,0083	**
OM vs. OM + FAK 2µM	< 0,0001	****
OM vs. OM + FAK 5µM	< 0,0001	****
AM vs. AM + FAK 0,5µM	0,0011	**
AM vs. AM + FAK 2µM	< 0,0001	****
AM vs. AM + FAK 5µM	< 0,0001	****

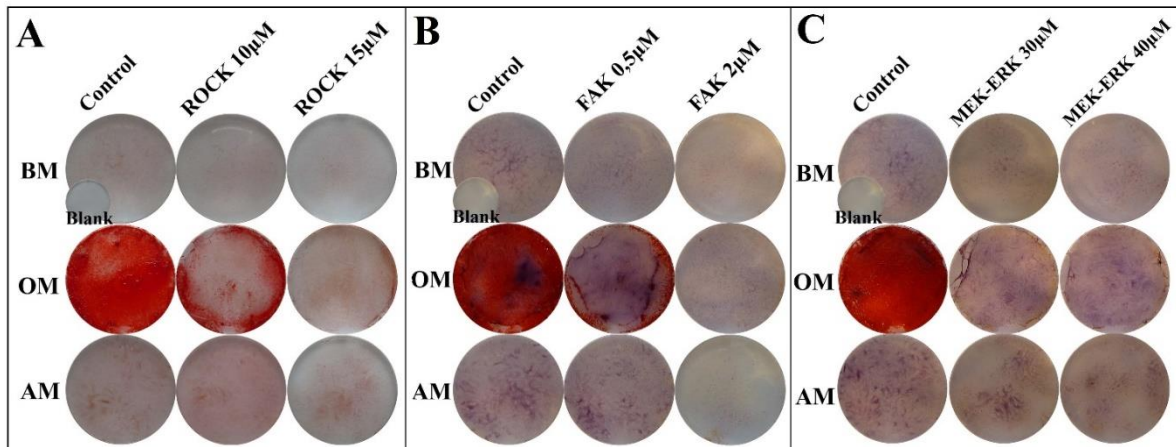
Statistical difference	P value (exact)	P value summary
BM vs. BM + MEK-ERK 30µM	0,0056	**
BM vs. BM + MEK-ERK 40µM	< 0,0001	****
BM vs. BM + MEK-ERK 60µM	< 0,0001	****
OM vs. OM + MEK-ERK 30µM	0,0001	***
OM vs. OM + MEK-ERK 40µM	< 0,0001	****
OM vs. OM + MEK-ERK 60µM	< 0,0001	****
AM vs. AM + MEK-ERK 30µM	< 0,0001	****
AM vs. AM + MEK-ERK 40µM	< 0,0001	****
AM vs. AM + MEK-ERK 60µM	< 0,0001	****

Appendix 4. P values of the non-parametric Mann-Whitney analysis of the combined ALP activity results.

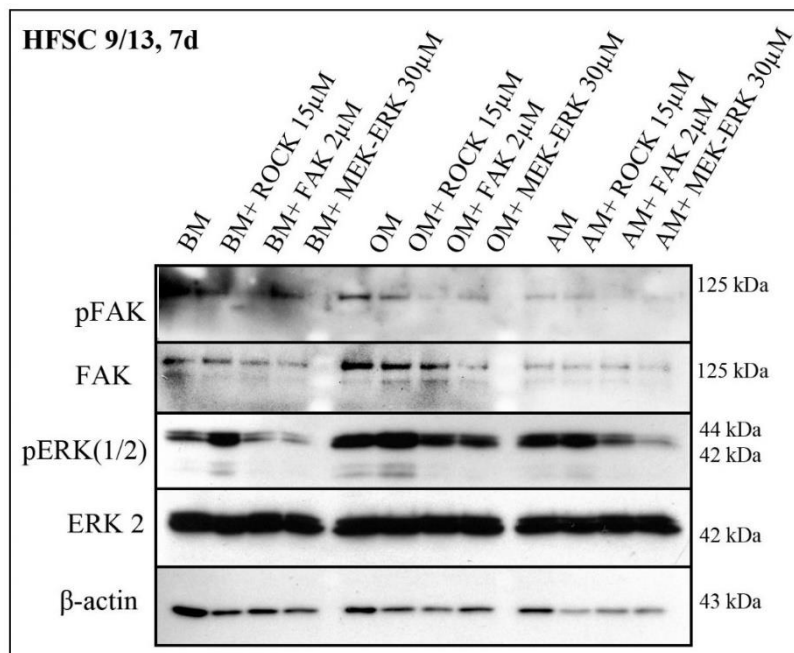
Statistical difference	P value (exact)	P value summary
BM vs. BM + ROCK 10 μ M	0,0121	*
BM vs. BM + ROCK 15 μ M	0,0036	**
BM vs. BM + ROCK 25 μ M	< 0,0001	****
OM vs. OM + ROCK 10 μ M	0,3724	ns
OM vs. OM + ROCK 15 μ M	0,0386	*
OM vs. OM + ROCK 25 μ M	0,0283	*
AM vs. AM + ROCK 10 μ M	0,1126	ns
AM vs. AM + ROCK 15 μ M	0,0447	*
AM vs. AM + ROCK 25 μ M	0,0083	**

Statistical difference	P value (exact)	P value summary
BM vs. BM + FAK 0,5 μ M	0,0283	*
BM vs. BM + FAK 2 μ M	0,0083	**
BM vs. BM + FAK 5 μ M	< 0,0001	****
OM vs. OM + FAK 0,5 μ M	0,1126	ns
OM vs. OM + FAK 2 μ M	0,0018	**
OM vs. OM + FAK 5 μ M	< 0,0001	****
AM vs. AM + FAK 0,5 μ M	0,0083	**
AM vs. AM + FAK 2 μ M	0,0003	***
AM vs. AM + FAK 5 μ M	< 0,0001	****

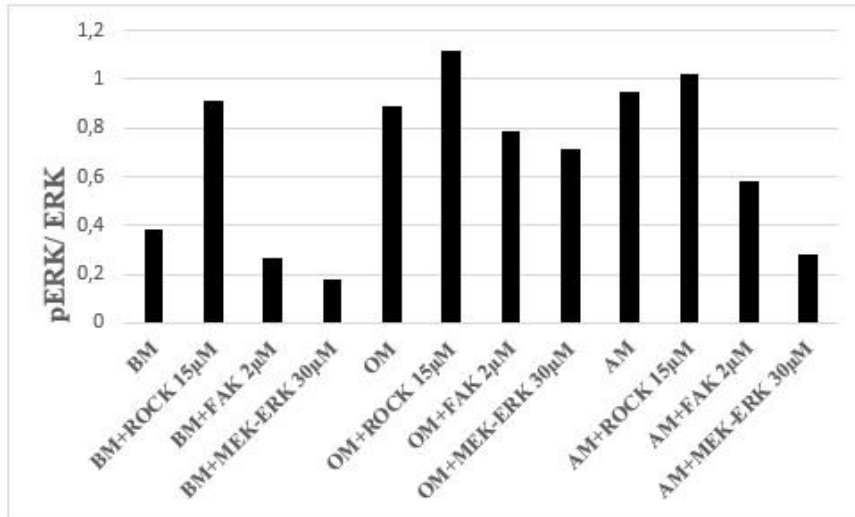
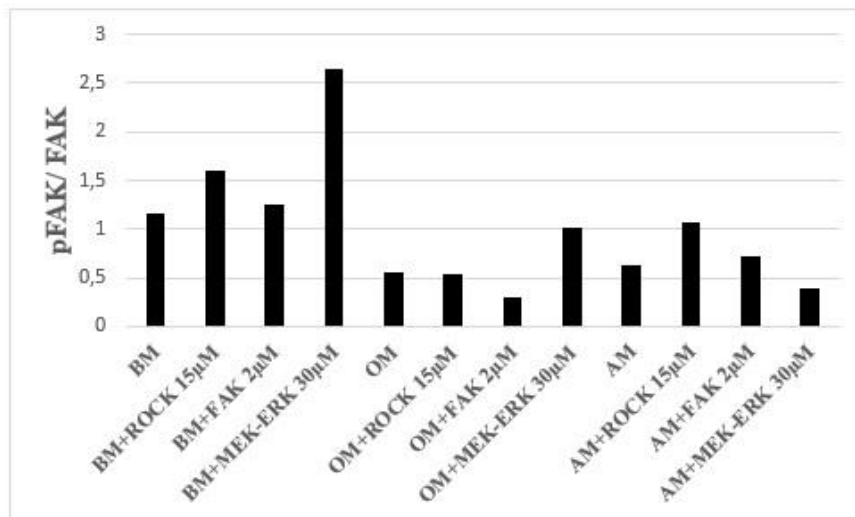
Statistical difference	P value (exact)	P value summary
BM vs. BM + MEK-ERK 30 μ M	0,0056	**
BM vs. BM + MEK-ERK 40 μ M	0,0005	***
BM vs. BM + MEK-ERK 60 μ M	< 0,0001	****
OM vs. OM + MEK-ERK 30 μ M	< 0,0001	****
OM vs. OM + MEK-ERK 40 μ M	< 0,0001	****
OM vs. OM + MEK-ERK 60 μ M	< 0,0001	****
AM vs. AM + MEK-ERK 30 μ M	0,0007	***
AM vs. AM + MEK-ERK 40 μ M	0,0004	***
AM vs. AM + MEK-ERK 60 μ M	0,0065	**



Appendix 5. Qualitative Alizarin Red staining of cell line HFSC 9/13 (21 d). hASCs were cultured three weeks in BM, OM and AM conditions supplemented with ROCK, FAK and MEK-ERK inhibitors. Qualitative mineral deposition was analyzed with Alizarin Red staining. The inhibitor effect on matrix mineralization is presented in the figure: A) ROCK inhibitor, B) FAK-inhibitor and C) MEK-ERK inhibitor. Mineralization is visualized by the bright red color of the well. The spherical images represent the surface area of the 24-well plates.



Appendix 6. Western blot of 7 day HFSC 9/13 sample lysates. 30 000 cells/well were plated and cultured in 1% starvation BM, OM or AM; all culture media were supplemented with 15µM ROCK, 2µM FAK or 30µM MEK-ERK inhibitor. Cells were lysed in 2X LAEMMLI sample buffer (100µl/well) and 15µl sample lysates were run in electrophoresis. Signaling molecules pFAK, FAK, pERK(1/2), ERK2 and β-actin were analyzed. For β-actin analysis, only 3,5µl of each lysates was run.

A**B**

Appendix 7. Semiquantification of the activation of signaling molecules. The band intensities were measured with Image J software. **A)** pFAK intensities were divided with corresponding FAK intensities. **B)** Similarly, pERK(1/2) intensities were divided with the intensities of ERK bands.